

# Quantifying Loss-Of-Control of Quadrotors

S.J.K. Kersbergen



# Quantifying Loss-Of-Control of Quadrotors

by

S.J.K. Kersbergen

to obtain the degree of Master of Science  
at the Delft University of Technology,  
to be defended publicly on Friday October 26, 2018 at 2:00 PM.

Student number:	4212223
Project duration:	December 7, 2017 – October 26, 2018
Thesis committee:	Dr. ir. C.C. de Visser, TU Delft, supervisor
	Dr. ir. Q.P. Chu, TU Delft
	Dr. ir. E. Mooij, TU Delft
	S. Sun, TU Delft

*This thesis is confidential and cannot be made public until October 26, 2021.*

An electronic version of this thesis is available at <http://repository.tudelft.nl/>.



# Preface

The report that you are about to read is the result of nine months and is my final assignment of the master of Control & Simulation at the faculty of Aerospace Engineering in Delft. The research I did into the quantification of Loss-Of-Control (LOC) for quadrotors is part of a bigger body of research. This body is part of the Control & Simulation department and focusses on the improvement of aviation safety, which with increasing aviation traffic is very important. Topics studied are for example Safe Flight Envelopes (SFEs), flight envelope prediction and the prediction and identification of stall models. I would like to thank all the staff from the department who helped me.

I wrote this report with the intention that one without any prior knowledge on the topic of LOC would be able to read and understand it. If one does have prior knowledge on quadrotors and/or LOC one could skip the problem description section (Chapters 3 and 4).

I could not have completed this assignment without the assistance and support of a few individuals: Firstly I owe my deepest thanks to my supervisor Coen de Visser, who suggested this topic to me. His guidance, suggestions and feedback have been invaluable in completing my research. I would also like to extend my heartfelt thanks to Sihao Sun for his optimism, enthusiasm and support for which this research would not have been completed. The countless discussions we had on various topics, the irreplaceable help with regards to flying the quadrotors in my experiment and for having the patience to sit through thrust experiments, which might have been the most boring experiments ever, the results however, were not! I would also like to thank my girlfriend Alissa and my friends, who made sure to keep me from working too hard, through 'just one more coffee break', or an extended lunch break and a few more beers of course! Finally, my big thanks to my fervent supporters, my parents, Khim and Hans who have been my core element and my sister, Caithlin who makes me laugh. They are always ready for me, to greet me and feed me with a world class dinner whenever I did show my face at home.

I am grateful to all of you for making this happen.

*S.J.K. Kersbergen  
Delft, October 2018*



# Summary

Due to a rise in popularity of Unmanned Aircraft System (UAS), of which quadrotors are part of, the need for robust UAS also increased. To achieve this robustness, researchers defined a general control systems for quadrotors known in literature as a Fault Tolerant Control System (FTCS) of which the flexible configuration is called the Active Fault Tolerant Control System (AFTCS). Research into the AFTCS led to the realization that current research focusses on singular challenges, as these usually contain complex dynamics, which do not apply to multiple challenges. Though recent research has shown some progression towards more general solutions, a larger effort needs to be made if the expected growth of the UAS market wants to be sustained.

In contrast to the unmanned aviation, Loss-Of-Control (LOC) in manned aviation has been extensively studied, since it was designated as one of the three major areas of concern in commercial aviation, in 1997. A research group consistent of various experts was set-up to do qualitative research into a set of suspected LOC cases, to find the primary causes and possible interventions. This research led to the invention of five envelopes related to aircraft flight dynamics, structural integrity, flight control and aerodynamics. To date these envelopes are still used as the basis for research into LOC prevention for commercial aircraft.

Like the Commercial Air Transport (CAT), helicopters have seen extensive research into emergencies and hazards. As the quadrotor is similar to the helicopter in dynamics it is not surprising that the emergency cases and hazards have been applied to the quadrotor. Examples of those cases are Vortex Ring State (VRS) and blade flapping. As research into those cases for quadrotors has seen a significant effect on the flight capabilities, and thus on LOC cases, it is surprising to see that in literature these effect are often not taken into account or even neglected.

To show the importance of modelling hazards such as the VRS and blade flapping and to broaden the approach on finding solutions to challenges regarding quadrotors, a quantitative description for LOC of quadrotors has been developed. Thus making it possible to indicate whether a quadrotor is in, or showing indication of entering, a LOC state.

Through the adaptation of LOC characteristics of CAT to quadrotors, characteristics of LOC of quadrotors were created. These characteristics were then used in a comparative data analysis of flight tests, flown up to 16 m/s in the Open Jet Facility (OJF) (wind tunnel) of the TU Delft, where abnormal dynamics and vehicle upsets were observed, categorized and related to LOC. The categories were then delimited and combined with observations, into a theory on the primary causes and precursors of dynamic LOC events of quadrotors. To validate this theory, an experiment on the thrust output of a single actuator and rotor in various flight conditions was performed. The output of this experiment was then fit with multivariate simplex splines, where the dynamics of the thrust model were validated with flight data. The model was then used to validate the theory on primary causes and precursors of dynamic LOC events of quadrotors.

A Quantitative Loss-Of-Control Definition (QLD) was then created for the identification of quadrotor LOC events through complementation of the characteristics of LOC of quadrotors, with the validated theory on primary causes and precursors of dynamic LOC events of quadrotors.



# Contents

<b>Summary</b>	<b>v</b>
<b>List of Symbols</b>	<b>ix</b>
<b>List of Acronyms</b>	<b>xi</b>
<b>List of Figures</b>	<b>xiii</b>
<b>1 Introduction</b>	<b>1</b>
<b>2 Thesis Project</b>	<b>3</b>
2.1 Research Motivation . . . . .	3
2.2 Research Questions . . . . .	3
<b>I Draft Paper</b>	<b>5</b>
<b>II Problem Description</b>	<b>21</b>
<b>3 The Quadrotor</b>	<b>23</b>
3.1 The Reduced Model . . . . .	24
3.2 Model Limitations . . . . .	25
3.3 Control Limitations . . . . .	25
<b>4 Background</b>	<b>27</b>
4.1 Active Fault Tolerant Control . . . . .	27
4.1.1 Fault Tolerant Control . . . . .	28
4.1.2 Fault Detection and Diagnosis . . . . .	28
4.1.3 Conclusions . . . . .	29
4.2 Loss-Of-Control for Manned Aviation . . . . .	29
4.2.1 Aeroplanes . . . . .	29
4.2.2 Helicopters . . . . .	31
4.3 Envelope Protection . . . . .	32
4.3.1 The Flight Envelope . . . . .	32
4.3.2 Safe Flight Envelope . . . . .	32
<b>III A Comparative Approach</b>	<b>35</b>
<b>5 Data Analysis</b>	<b>37</b>
5.1 Loss-Of-Control Characteristics of Quadrotors . . . . .	37
5.2 Quantitative Analysis . . . . .	38
5.3 Qualitative Analysis . . . . .	38
5.3.1 Exploration of Data . . . . .	38
5.3.2 Categories & Properties . . . . .	38
5.3.3 Category Integration and Delimitation . . . . .	39
5.4 Discussion . . . . .	41
5.4.1 (Double) Blade Flapping . . . . .	41
5.4.2 Aerodynamic Interaction of the Rotors . . . . .	42
5.4.3 Removed/Idle Rotors . . . . .	43
<b>6 Theory Generation</b>	<b>45</b>
6.1 Primary Causes of Loss-Of-Control . . . . .	45
6.2 Precursor Events . . . . .	46
6.2.1 Vortex Ring State . . . . .	46
6.2.2 Blade Flapping . . . . .	46
6.2.3 Aerodynamic Interaction of the Rotors . . . . .	46

6.2.4	Equipment Failure . . . . .	47
<b>IV</b>	<b>Validation Through Experimentation</b>	<b>49</b>
<b>7</b>	<b>Rotor Thrust Experiment</b>	<b>51</b>
7.1	The Experiment . . . . .	51
7.1.1	Measured Variables . . . . .	51
7.1.2	Data Acquisition Systems . . . . .	52
7.2	Rotor Thrust Model . . . . .	52
7.2.1	Measurement Influences. . . . .	52
7.2.2	Fitting Data . . . . .	53
7.2.3	Validation of Data Fit. . . . .	54
7.2.4	Validation of the Model . . . . .	54
7.3	Discussion . . . . .	55
<b>8</b>	<b>Theory Validation</b>	<b>57</b>
8.1	Vortex Ring State . . . . .	57
8.1.1	Thrust Variation . . . . .	57
8.1.2	A Flight in the Vortex Ring State . . . . .	58
8.2	Blade Flapping . . . . .	59
8.3	Rotor Saturation . . . . .	60
8.3.1	Nominal Quadrotor Rotor Saturation . . . . .	60
8.3.2	SRF Quadrotor Rotor Saturation . . . . .	61
<b>V</b>	<b>A Quantitative Description for Loss-Of-Control</b>	<b>63</b>
<b>9</b>	<b>Defining Loss-Of-Control of Quadrotor Quantitatively</b>	<b>65</b>
9.1	The Quantitative Loss-Of-Control Definition for Quadrotors . . . . .	65
9.2	Variable-Pitch Rotors for Increased Reliability . . . . .	66
<b>10</b>	<b>Conclusions &amp; Recommendations</b>	<b>67</b>
10.1	Conclusions. . . . .	67
10.2	Recommendations . . . . .	68
	<b>Bibliography</b>	<b>69</b>
<b>A</b>	<b>Loss-Of-Control of Aircraft</b>	<b>73</b>
A.1	Airplanes . . . . .	73
A.2	Helicopters . . . . .	74
<b>B</b>	<b>The Grounded Theory Approach</b>	<b>77</b>
B.1	Comparative Analysis. . . . .	77
B.2	The Constant Comparative Method of Qualitative Analysis . . . . .	78
<b>C</b>	<b>Quadrotor Flights</b>	<b>79</b>
C.1	Nominal Quadrotor Flights . . . . .	79
C.2	Single Rotor Failure Quadrotor Flights . . . . .	80

# List of Symbols

$A$	Area of the Rotor Disk, m <sup>2</sup>
$a_0$	Lift Curve per Radian
$A_b$	Area of the Rotor Surface Covered by Rotor Blades, m <sup>2</sup>
$B_{var}$	B-coefficient Variance
$c$	Chord Length of the Blade, m
$C_t$	Thrust Coefficient
$D$	Diameter, m
$\vec{F}_a$	Aerodynamic Forces Related to Translational Motion
$\vec{F}$	Resultant Force Vector
$\vec{F}_r$	Reduced Model of Forces
$\vec{G}$	Gravity Vector
$I_{r,z}$	z Direction Moment of Inertia of an Actuator, kg/m <sup>2</sup>
$I_v$	Moment of Inertia of the Quadrotor, kg/m <sup>2</sup>
$J$	Advance Ratio
$m$	Mass, kg
$\vec{M}_a$	Aerodynamic Moments Related to Translational Motion
$\vec{M}$	Resultant Moment Vector
$\vec{M}_r$	Reduced Model Moment
$n$	Rotation Rate, RPS
$p$	Angular Roll Acceleration, deg/s <sup>2</sup>
$\dot{p}$	Angular Roll Velocity, deg/s
$q$	Angular Pitch Velocity, deg/s
$\dot{q}$	Angular Pitch Acceleration, deg/s <sup>2</sup>
$r$	Angular Yaw Velocity, deg/s
$R$	Radius, m
$\dot{r}$	Angular Yaw Acceleration, deg/s <sup>2</sup>
$\vec{r}_i$	Location of Rotor i w.r.t. c.g.
$T$	Thrust, N
$T_h$	Rotor Thrust in Hovering Flight, N
$T_{loss}$	Thrust Loss, %
$T_{meas}$	Thrust Measured, N
$u$	Speed in x Direction, m/s
$v$	Speed in y Direction, m/s
$\vec{V}$	Total Velocity Vector, m/s
$\vec{V}_i$	Local Velocity Vector of Rotor i, m/s
$w$	Speed in z Direction, m/s
$\alpha$	Angle of attack, deg
$\alpha_{fl}$	Flapping Angle
$\hat{c}$	Ordinary Least Squares Estimator of the B-coefficients
$\epsilon$	Error
$\gamma$	Non-Dimensional Lock Number
$\kappa_0$	Rotor Coefficient
$\mu_{lon}$	Longitudinal Velocity to Tip Speed Ratio
$\omega$	Rotation Speed, rpm
$\vec{\Omega}$	Rotation Velocity Vector
$\rho$	Air Density, kg/m <sup>3</sup>

$\sigma$	Solidity Ratio
$\tau_0$	Drag Moment Coefficient

# List of Acronyms

AFTCS	Active Fault Tolerant Control System
CAST	Commercial Aviation Safety Team
CAT	Commercial Air Transport
DBF	Double Blade Flapping
F/M	Failure / Malfunction
FAA	Federal Aviation Administration
FDA	Fault Detection and Accomodation
FDD	Fault Detection and Diagnosis
FDI	Fault Detection and Isolation
FTC	Fault Tolerant Control
FTCS	Fault Tolerant Control System
INDI	Incremental Nonlinear Dynamics Inversion
JSAT	Joint Safety Analysis Team
LOC	Loss-Of-Control
LPV	Linear Parameter Varying
MPC	Model Predictive Control
NASA	National Aeronautics and Space Administration
OJF	Open Jet Facility
OLS	Ordinary Least Squares
PFTCS	Passive Fault Tolerant Control System
PIO	Pilot Induced Oscillation
QLD	Quantitative Loss-Of-Control Definition
RMS	Root Mean Square
RPAS	Remotely Piloted Aircraft System
rpm	Rotations Per Minute
SFE	Safe Flight Envelope
SRF	Single-Rotor Failure
UAS	Unmanned Aircraft System
UTM	Unmanned aircraft system Traffic Management
VRS	Vortex Ring State
VTOL	Vertical Take-Off and Landing



# List of Figures

3.1 Parrot Bebop 2: Body Axis Definition . . . . .	23
4.1 General AFTCS [9] . . . . .	27
4.2 Loss-Of-Control Envelopes with Simulator Validation Flight Data [30] . . . . .	30
4.3 The LOC Characteristics of Aeroplanes, the Primary Causes and the Causal and Contributing Factors [31] . . . . .	30
4.4 Height Velocity Diagram: Bell 204B [44] . . . . .	31
4.5 CS 23.333 Flight Envelope [45] . . . . .	32
4.6 Safe Flight Envelope [49] . . . . .	33
5.1 Loss-Of-Control Characteristics of Quadrotors, Adapted from [31] . . . . .	37
5.2 Visualisation of a Nominal Quadrotor Actuator Saturation Incident . . . . .	38
5.3 Distribution of Categories over flights (32 in Nominal Configuration & 27 in SRF Configuration)	40
5.4 Blade Flapping in the Nominal Case . . . . .	41
5.5 Double Blade Flapping . . . . .	42
5.6 Possible Rotation Configurations for Quadrotors . . . . .	43
7.1 The Angle of Attack . . . . .	52
7.2 Dynamometer Series 1580 [65] . . . . .	52
7.3 Assumptions for the Influence of the Thrust Stand at 90 Degrees . . . . .	53
7.4 Multivariate Splines Triangulation and Thrust Model . . . . .	53
7.5 Z-Normalised Nominal Configuration Flight Data & Model Data, $V = 8 \text{ m/s}$ . . . . .	55
8.1 Thrust Model, Maximum $C_t$ Fluctuation . . . . .	57
8.2 Thrust Fluctuation on Thrust Model . . . . .	57
8.3 A Flight in the Vortex Ring State . . . . .	58
8.4 Percentage Thrust Reference Error, Rotor One . . . . .	58
8.5 Flapping Angle (in deg) . . . . .	59
8.6 Thrust Loss due to Blade Flapping (in percent) . . . . .	59
8.7 Advance Ratio Distribution . . . . .	60
8.8 Vertical Flights of Quadrotors in SRF Configuration (All Rotors, Right Back (3) Removed) . . . . .	61
9.1 Quantitative LOC Definition (QLD) for quadrotors, Primary Causes and Precursors, Adapted from CAT LOC [31] . . . . .	65
A.1 Rotor Flight States in Vertical Flight [66] . . . . .	74
C.1 Vertical/Longitudinal Flights, Nominal Configuration . . . . .	79
C.2 Longitudinal Flights, Nominal Configuration . . . . .	79
C.3 Longitudinal Movement, SRF Configuration . . . . .	80
C.4 Vertical Movement, SRF Configuration . . . . .	80





# Introduction

Loss-Of-Control (LOC) in aviation has received considerable attention in recent years [1], especially in manned aviation. This is not unexpected as a recent study from Boeing [2] shows that LOC has been and still is the main cause of fatalities in commercial jet airplane accidents world wide. 25.8 % (16) of all accidents that occurred between 2007 and 2016 were caused by in flight LOC incidents. These incidents caused 45.8 % of all the fatalities. For small Unmanned Aircraft System (UAS) (under 55 lbs, approx. 25 kg), 35 % of the (reported) UAS crashes were due to LOC [3]. Note though that the total study group was only a 100 UAS cases, due to voluntary, inconsistent and non-standard mishap reporting.

The unmanned aviation market is an industry, which has prospects of significant growth in the coming years. The Federal Aviation Administration (FAA) estimates that by 2021 1.6 million small UAS will be in commercial use [4]. With a significant amount of UAS expected to be flying around urban areas. Thus, like currently is the case in manned aviation, LOC is expected to become an issue. Recently the National Aeronautics and Space Administration (NASA) has announced a proposal for a Unmanned aircraft system Traffic Management (UTM) [5], which borrows fundamental ideas from the manned air traffic system. This proposal acknowledges the expected growth in UAS, therefore prioritisation of their safety , and with that the individual, is a must. A well known UAS is the quadrotor. It is part of the class of multicopters and obtains flight through lift generation of four rotors. With its small size and mechanically simple design, making it easy to maintain, it is a cheap tool to evaluate for example flight control theory.

Most research regarding the safety of multicopters or quadrotors has been geared towards specific challenges e.g. loss of rotors or sensor failure, but what is not seen is a more general solution. As in manned aviation it is expected that when a definition can be given to LOC in quadrotors, research can be aimed more towards a holistic solution. A definition for LOC of quadrotors however, has not been actively pursued in research, until recently [3]. It is mentioned however that finding significant statistical data to back ideas for indicators of LOC is near impossible, as databases are currently not standardized and entries are voluntary.

Through the adaptation of LOC characteristics of Commercial Air Transport (CAT) to quadrotors, characteristics of LOC of quadrotors were created. These characteristics were then used in combination with a comparative data analysis of flight tests, flown up to 16 m/s in the Open Jet Facility (OJF) (wind tunnel), to create a theory on the primary causes and precursors of dynamic LOC events of quadrotors. This theory was then validated through the analysis of the thrust performance of an actuator and its rotor. With a Quantitative Loss-Of-Control Definition (QLD) for quadrotors, a more holistic approach to finding interventions for LOC should be possible. Furthermore the importance of modelling individual events will also become more apparent.

The report of this research is split into five parts and is introduced in Chapter 2. In part I, the draft paper of this thesis is shown. Then, in part II, the quadrotor is presented in Chapter 3, followed by background information on LOC in Chapter 4. In part III, the data analysis and theory generation are discussed in Chapters 5 and 6. Part IV, contains the experiment performed to validate the generated theory in Chapter 7, followed by the validation of the generated theory, in Chapter 8. Finally in part V, the quantitative description of LOC of quadrotors is presented in Chapter 9 , which is then followed by the conclusions and recommendations of this report in Chapter 10.



# 2

## Thesis Project

This thesis project works towards the development of a Quantitative Loss-Of-Control Definition (QLD) of quadrotor Loss-Of-Control (LOC) events. By being able to define what LOC is, it should be possible to anticipate and design systems to improve the safety of quadrotors. This research lays its focus on defining LOC through the analysis of data sets flown, in nominal and Single-Rotor Failure (SRF) configurations under varying flight conditions. The motivation for this research is presented in Section 2.1 followed by the research questions in Section 2.2.

### 2.1. Research Motivation

With most of the current research in quadrotor LOC being focussed on specific failure cases e.g. actuator faults, SRF, etc. the growth that is expected in the drone industry will not be able to be sustained, in regards to the safety of individuals in urban areas. Without an assurance of reliability regarding the safety of drones it is just not feasible. With the National Aeronautics and Space Administration (NASA) outlining flight traffic rules for drones it seems to be just a matter of time until it will be normal to see such vehicles flying around. Therefore it is of the utmost importance to improve the overall resilience of quadrotors.

In manned aviation this scenario has also been seen. Due to a considerable amount of accidents regarding LOC cases, a research group was formed to research the phenomenon. Through that research various methods have been developed to deal with such cases. As little is known about LOC cases of quadrotors it is very important that this phenomenon is studied and quantified, such that a more holistic approach to the development of interventions can be taken.

### 2.2. Research Questions

From literature it was found that current research into challenging situations for quadrotors, such as loss of rotor(s), mostly focusses on singular cases. Furthermore research on LOC of quadrotors was sparse. In contrast the LOC research for manned aviation has been actively pursued in the past decades. Therefore to improve the overall resilience of quadrotors and to work towards a more holistic solution for quadrotor failure, the same strategy, that was used to define LOC in manned aviation, will be used for this research. To find a quantitative description for LOC of quadrotors, the following research objective has been defined as the main focus of this research:

*"The research objective is to develop a quantitative loss-of-control definition for quadrotors by analysing suspected loss-of-control data sets and testing the boundaries of the flight envelopes of nominal and off-nominal quadrotors through flight tests."*

To find a complete answer to the problem at hand the following research questions and sub-questions have been set-up:

1. *"How should loss-of-control be characterized to facilitate the quantification of loss-of-control of quadrotors in nominal configuration?"*
  - 1.1. *"What are the primary causes of loss-of-control of quadrotors in nominal configuration?"*
  - 1.2. *"What states are involved in loss-of-control of quadrotors in nominal configuration?"*
  - 1.3. *"What is the relationship between these states, with regard to loss-of-control of quadrotors in nominal configuration?"*
2. *"How should loss-of-control be characterized to facilitate the quantification of loss-of-control of quadrotors in single rotor failure configuration?"*
  - 2.1. *"What are the primary causes of loss-of-control of quadrotors in single rotor failure configuration?"*
  - 2.2. *"What states are involved in loss-of-control of quadrotors in single rotor failure configuration?"*
  - 2.3. *"What is the relationship between these states, in regard to loss-of-control of quadrotors in single rotor failure configuration?"*
3. *"What is the relationship between loss-of-control of quadrotors in nominal and single rotor failure configuration?"*

I  
Draft Paper

# QUANTIFYING LOSS-OF-CONTROL OF QUADROTORS

S.J.K. KERSBERGEN<sup>1</sup>, S. SUN<sup>2</sup> AND C.C. DE VISSER<sup>3</sup>

Control and Simulation, Delft University of Technology, 2629 HS Delft, The Netherlands

## ABSTRACT

With most of the current research in quadrotor Loss-Of-Control (LOC) being focussed on specific failure cases e.g. sensor faults and Single-Rotor Failure (SRF), the growth that is expected in the drone industry will not be able to be sustained, in regards to the safety of individuals in urban areas. Without an assurance of reliability regarding the safety of drones this is just not feasible. With the National Aeronautics and Space Administration (NASA) outlining flight traffic rules for drones it seems to be just a matter of time until it will be normal to see such vehicles flying around. Therefore it is of the utmost importance to improve the overall resilience of quadrotors. This work seeks to show the importance of modelling hazards such as the Vortex Ring State (VRS) and blade flapping to broaden the approach on solving LOC of quadrotors. Through the adaptation of the definition of LOC of aircraft to quadrotors and a comparative analysis of quadrotor flights, of both the nominal and SRF configuration, a Quantitative LOC Definition (QLD) for quadrotors is created. This definition is then validated through the analysis of thrust stand measurements and quadrotor flights. Resulting in a measure for the identification of LOC events.

**Keywords:** Loss-Of-Control, Quadrotor, Thrust, Modelling, QLD

## NOMENCLATURE

$\alpha$	Angle of Attack	[deg]
$\alpha_{fl}$	Flapping Angle	[deg]
$\gamma$	Non-Dimensional Lock Number	[-]
$\mu_{lon}$	Longitudinal Velocity to Tip Speed Ratio	[-]
$\omega$	Rotation Speed	[rpm]
$\vec{\Omega}$	Rotation Velocity Vector (p,q,r)	[rad/s]
$\vec{r}_i$	Location of Rotor $i$ w.r.t. c.g.	[m]
$\vec{V}_i$	Local Velocity Vector of Rotor $i$	[m/s]
$\vec{V}_{tot}$	Total Velocity Vector of Quadrotor	[m/s]
$\rho$	Air Density	[kg/m <sup>3</sup> ]
$\sigma$	Solidity Ratio	[-]
$A$	Area of the Rotor Disk	[m <sup>2</sup> ]
$a_0$	Lift Curve per Radian	[-]
$A_b$	Area Covered by Rotor Blades	[m <sup>2</sup> ]
$c$	Chord Length	[m]
$C_t$	Thrust Coefficient	[-]
$D, R$	Diameter and Radius	[m]
$I_B$	MOI of the Blade about the Hinge	[kg/m <sup>2</sup> ]
$J$	Advance Ratio	[-]
$m$	Mass	[kg]
$n$	Rotation Rate	[rps]
$T$	Thrust	[N]

## I. INTRODUCTION

Loss-Of-Control (LOC) in aviation has received considerable attention in recent years [1], especially in manned aviation. This is not unexpected as a recent study from Boeing [2] shows that LOC has been and still is the main cause of fatalities in Commercial Air Transport (CAT) accidents world wide. 25.8 % (16) of all accidents that occurred between 2007 and 2016 are caused by in flight LOC incidents. These incidents caused 45.8 % of all the fatalities. For small Unmanned Aircraft System (UAS) (under 55 lbs, approx. 25 kg), 35 % of the (reported) UAS crashes are due to LOC [3]. Note though that the total study group consisted of a 100 cases, due to voluntary, inconsistent and non-standard mishap reporting.

The unmanned aviation market is an industry, which has prospects of significant growth in the coming years. With a significant amount of UAS expected to be flying around urban areas, like currently is the case in manned aviation, LOC is expected to become an issue. Recently NASA has announced a proposal for an Unmanned aircraft system Traffic Management (UTM) [4], which borrows fundamental ideas from the manned air traffic system. This proposal acknowledges the expected growth in UAS, therefore prioritisation of their safety, and with that the individual, is a must. A well known UAS is the quadrotor. It is part of the class of multicopters and obtains flight through lift generation of four rotors. With its small size and mechanically simple design, making it easy to maintain, it is a cheap tool to evaluate for example flight control theory.

Most research regarding the safety of multicopters or quadrotors has been geared towards specific challenges e.g. loss of rotors or sensor failure, but what is not seen is a more general solution. As in manned aviation, it is expected that when a definition can be given to LOC in quadrotors, research can be aimed more towards a holistic solution. A definition for LOC of quadrotors however,

<sup>1</sup> Graduate student, Control and Simulation Division, Faculty of Aerospace Engineering; kieran.kersbergen@gmail.com

<sup>2</sup> Ph.D. student, Control and Simulation Division, Faculty of Aerospace Engineering; s.sun-4@tudelft.nl

<sup>3</sup> Assistant professor, Control and Simulation Division, Faculty of Aerospace; AIAA Member

has not been actively pursued in research, until recently [3]. It is mentioned however that finding significant statistical data to back ideas for indicators of LOC is near impossible, as databases are currently not standardized and entries are voluntary.

Through the adaptation of the LOC definition of CAT to quadrotors and a comparative analysis of quadrotor flights, of both the nominal and Single-Rotor Failure (SRF) configuration, a Quantitative LOC Definition (QLD) for quadrotors is created. This definition is then validated through the analysis of thrust stand measurements and quadrotor test flights.

With a Quantitative LOC Definition (QLD) for quadrotors, a more holistic approach to finding prevention methods for LOC should be possible. Furthermore the importance of modelling individual events will also become more apparent.

The paper is arranged into sections as follows: Section II provides the current state of the art of LOC of quadrotors. Section III then introduces the performed data analysis. The rotor experiment is then discussed in Section IV, followed by the validation of the model and the generated theory in Section V. Finally the Quantitative Loss-Of-Control Definition (QLD) for quadrotors is introduced in Section VI.

## II. BACKGROUND

Currently most of the research regarding quadrotor failure is geared towards the various parts of Active Fault Tolerant Control Systems (AFTCS) [5], which has as a main objective to keep normal steady-state performance under nominal and off-nominal conditions. A general structure of an AFTCS can be seen in Fig. 1.

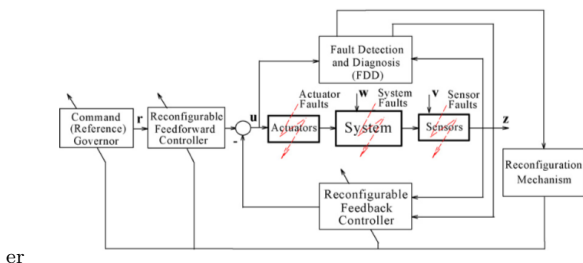


Figure 1. General AFTCS [5]

An AFTCS system has four different sub-systems: a reconfigurable controller or Fault Tolerant Controller (FTC), a mechanism that reconfigures the controller, a Fault Detection and Diagnosis (FDD) system and a command/reference governor. The difficulties in designing a good AFTCS system are the design of: a flexible FTC, a fast and accurate FDD system and a reconfigurable mechanism. Where the first two are discussed most, in literature. Faults considered in most FTC and FDD research are sensor, actuator and structural/component failure damage [6]. However the effects of structural damage e.g. a broken arm, have not been researched yet.

There are various solutions in research for FTC systems that deal with tracking and attitude stabilization of quadrotors under off-nominal conditions e.g. adaptive INDI [7]. Furthermore in literature solutions for challenging tasks such as single, double and triple-rotor fail-

ure [8] can also be found. Though for rotor failure cases, the control systems are usually tested in a simulation environment or under low speed flight conditions. Except for a recently published multi-loop hybrid nonlinear controller that is able to control a SRF configuration under high speed flight conditions (up to 9 m/s) [9]. With some exceptions, these control strategies are usually very specific due to the dynamics involved and authors generally assume that faults have already been detected and leave the FDD system to the recommendations.

What is essential in FDD is the speed at which faults are detected and second, the accuracy the detection. If a FTC system needs to react and reconfigure, it is crucial that it has enough time. In literature the observer-based FDD are most common e.g. Tau's observer [10]. With the exception of a few systems, the majority of FDD systems are however evaluated through simulations [6]. Though recently two researchers presented a FDD with experimental results [11] [12], where sensor bias faults and actuator faults are detected through a bank of nonlinear adaptive estimators. The output is then used for the adjustment of the controller output for fault accommodation. Unification of the two is recommended as future work.

What can be concluded from the current research into AFTCS is that there are various solutions to individual challenging control tasks and fault detection problems. In both FTC and FDD most solutions are designed for singular problems. Furthermore, these sub-systems are supposed to work together to form the basis of an AFTCS system, but they are often researched separately, leaving other sub-systems as recommendation. Though recent research has been moving towards a more unified systems there is still considerably more research and experimentation needed for a fully functioning AFTCS.

In contrast to the specific solutions in quadrotors, manned aerospace has seen a major effort into finding a holistic solution for LOC [1]. This effort was a result of the Commercial Aviation Safety Team (CAST) designating LOC as one of the three major areas of concern in CAT, in 1997. A Joint Safety Analysis Team (JSAT) was created, which did research into 24 cases that were classified as LOC cases, by CAST [14]. Though LOC still did not have a definition, therefore a call for development of a quantitative definition for LOC was made. NASA and Boeing jointly developed a set of five envelopes related to aircraft flight dynamics, structural integrity, flight control and aerodynamics. Using the generally accepted characteristics of LOC, see Fig. 2, they found the primary causes for LOC, from the research of the JSAT [14], and derived the most important variables related to these causes. These variables were then used to derive the five envelopes giving a quantitative description to LOC, which addressed 95% of the CAST LOC cases. With this tool investigators are able to consistently define LOC cases and find viable solutions to reduce them. From this research, methods for the prevention of LOC of CAT have been designed. These methods have been consistently reviewed and summarized by NASA [1] [13].

In quadrotor research this kind of effort has not been seen. Recently however, a preliminary risk assessment and hazard identification analysis for UAS has been conducted by the same group that publishes reviews on LOC of CAT [3] [15]. A key finding in their research is that a

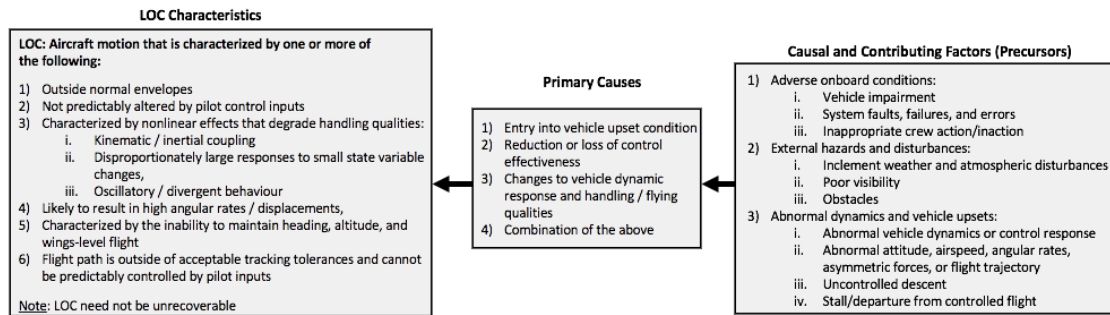


Figure 2. CAT LOC Characteristics, Primary Causes and Causal and Contributing Factors [13]

lack of standardized reporting of incidents leads to situations in which meaningful analyses of data is challenging. Furthermore an increase in amateur induced incidents is noticed, LOC is found to be a key hazard in UAS as well and research into the modelling of off-nominal flight dynamics for multicopters is sparse. Also hazards identified for aircraft are found to not necessarily be translatable to UAS. The general consensus is that there is just not enough qualitative data for hazard identification, this is backed by the lack of literature about statistics on quadrotor failure, like [16].

The helicopter, has also not seen a quantification for LOC. Though emergencies and hazards have been defined [17], which could be compared to LOC. Examples of such cases are: (1) autorotation, (2) the height/velocity diagram, (3) dynamic roll over, (4) settling with power, also known as the Vortex Ring State (VRS), and (5) retreating blade stall. As the quadrotor is a simplified helicopter with four rotors, the failures and the dynamics that govern the helicopter state can also be partly applied to quadrotors. The simple design of the quadrotor gives it some advantages and disadvantages over the helicopter with respect to rotorcraft LOC, but autorotation is in theory not applicable for quadrotors as rotors are usually fixed pitch. The height/velocity diagram or flight envelope is definitely applicable to quadrotors. Furthermore the dynamic roll over is directly countered by having multiple rotors. The last two examples are also applicable to quadrotors and have also been thoroughly discussed in literature [18].

The flight envelope is a term used loosely in literature as a means to indicate limitations of aircraft. In manned aviation it commonly refers to a region of velocity and load factor or altitude in which an aircraft can be flown safely. When an aircraft leaves this region, it reaches a state from which returning to a stable state is difficult. As these flight envelopes only take into account quasi-stationary states, e.g. symmetrical manoeuvres and level flight, they do not assure safety for dynamic manoeuvres. Therefore in the search for a safety assurance region, research into flight envelopes has transitioned towards Safe Flight Envelopes (SFE). The SFE defines a region where safety is guaranteed and in which externally posed constraints will not be violated [19], it is however computationally expensive, especially for nonlinear systems such as aircraft and quadrotors.

The envelope estimation problem can also be seen as a reachability problem [20]. Starting from a initial target set, the forward reachable and backwards reachable sets are computed for a given time horizon. Where, the for-

ward reachable set contains all states that can be reached from the initial conditions, within the given time horizon, and the backwards reachable set contains all states that can be steered towards from the initial target set, for the given time horizon. The intersection of these sets gives the SFE. An example of which can be seen in Fig. 3.

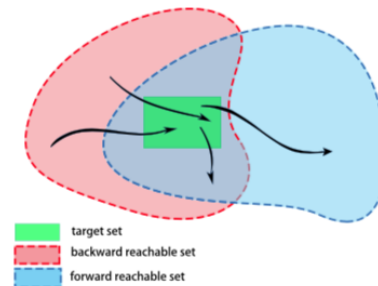


Figure 3. Safe Flight Envelope [21]

The SFE sounds applicable to finding a quantitative definition for quadrotor LOC. Though enough challenges still exist for the application of online SFE estimation for quadrotors, as they only have the essentials on board for high performance flight. A method to lower the computational complexity of the SFE is the database-driven safe flight envelope prediction system, suggested in [22]. Where the local aircraft model is updated through a system identification model, supported by an offline database which contains SFE for various damage cases.

The reachability analysis has also recently been applied to the UTM concept, where an efficient and flexible method for UAS highway placement is designed for UTM [23]. Thus one can safely assume that reachability analysis will be part of the future of quadrotors. For now it seems that reachability analysis is too computationally expensive for online application. Offline it could be applied as a verification/validation method for theories/algorithms against Loss-Of-Control.

### III. DATA ANALYSIS

To find a QLD for quadrotors, characteristics of LOC of quadrotors were defined. As the description of the characteristics of LOC of CAT is widely applicable to other vehicles, with minor changes, the following description of LOC characteristics of quadrotors was created through its adaptation to quadrotors:

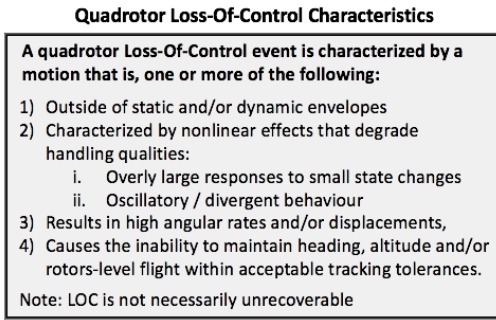


**Figure 4.** LOC Characteristics of Quadrotors, Adapted from [24]

### A. Categories & Properties

The characteristics were used in the comparative data analysis performed on test flights flown with a Parrot Bebop 2 in the Open Jet Facility (OJF) (wind tunnel), where preliminary categories and groups were created through grouping of similar flights. From the 110 flights that were flown up to wind speeds of 16 m/s, 62 flights crashed, three of which did however not have sufficient data for analysis. The two main groups, that were created from the 59 left over datasets, were the nominal (32) and SRF (27) groups, these groups were then split into translational and vertical flights and finally the SRF groups were further divided based on the rotor state e.g. Left-Back (LB) removed, Right-Back (RB) removed or Idle Rotor (IR).

The preliminary categories provided a good basis for incident comparison. Each preliminary category was separately analysed, where time histories of all on-board variables and wind speeds were explored per incident, compared to other incidents in the same category and grouped if similarities occurred. After all the preliminary categories were analysed, cross-category similarities were sought for and grouped when found. Through the analysis of the preliminary categories and the grouping of similar incidents the most frequent events became evident. These are discussed and listed below:

- **Failure/Malfunction During Descent (DD)**  
This category was seen the most in SRF configuration flights and never during the flights in nominal configuration. This category is suspected to be caused by the VRS, as that state occurs in descent.  
**Properties:** Negative vertical speed, forward speed, angle of attack
- **F/M During Ascent (DA)**  
The opposite of the previous category. This category was seen sparsely, though mostly during the flights in SRF configuration, it is also suspected to be caused by the VRS, but after recovery.  
**Properties:** Positive vertical speed, forward speed, angle of attack
- **Phi Spike (PS)**  
A spike in the roll angle was seen at the end of a few flights. This is probably caused by the control system trying to recover from an unrecoverable situation and spiking the roll angle.  
**Properties:** Near crash, high roll rate reference

- **Theta Spike (TS)**

A spike in the pitch angle was seen close to the end of a few flights. Like the phi spike it was probably caused by the control system trying to recover from an unrecoverable situation. In some cases this spike seemed to be what caused the quadrotor to crash, increasing the angle of attack and thus exposing a greater surface area to the wind.

**Properties:** Near crash, high pitch rate reference

- **Increasing Oscillation of Acceleration (IO)**

The increased oscillation of translational, vertical and angular accelerations was seen in translational flight of SRF configuration flights. As the angle of attack in forward flight is effected by the forward velocity, an increasing wind speed is seen as the main reason for the increase in oscillations.

**Properties:** Increasing velocity, increasing wobble angle, increasing angle of attack

- **Actuator Saturation (AS)**

As derived from the reduced model, actuator saturation seems to be one of the major reasons for failures. Furthermore as expected it is positively correlated to the velocity and thus to the angle attack.

**Properties:** Increasing velocity, angle of attack, rotation speeds

- **High Velocity (HV)**

High velocity, or high wind speeds caused an increase in rotor speeds. This usually led to actuator saturation and thus ultimately to failure.

**Properties:** Increased angle of attack, actuator saturation, slow descent

- **Slow Descent (SD)**

Seen at high velocities, probably caused by the fact that the velocity is too much for the quadrotor to handle. Thus the thrust vector is angled more into the wind and height is lost in the process.

**Properties:** High velocity, angle of attack, close to crash

- **Equipment Failure (EF)**

Failures due to equipment e.g. actuator failure, battery voltage low, bad tracking and screws loose.

**Properties:** Equipment not optimal

Note that the VRS was not added to the categories as it was not apparent that the state was active or not. Its indicators were however added to the categories i.e. F/M During Descent, F/M During Ascent and the Phi/Theta Spikes. The distribution of the categories over the flights can be seen in Fig. 5.

As the categories had overlapping features, they were integrated and delimited, to create a more concise theory. Through experimentation and data analysis, the categories which were most important, which were not needed anymore and which could be combined were identified.

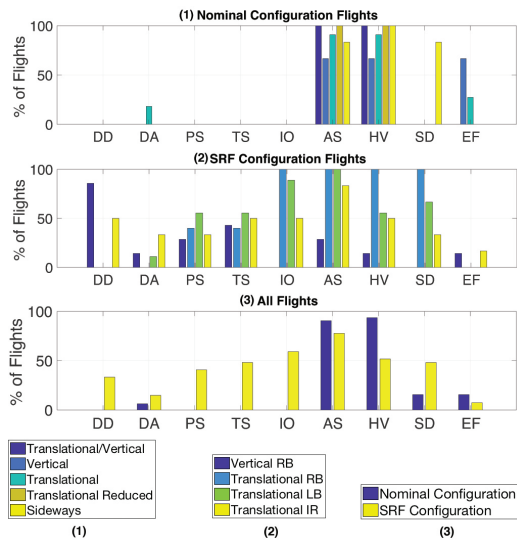


Figure 5. Distribution of Categories over the Flights

The first four categories, DD, DA, PS and TS are the indicators of the VRS. They were exclusively seen in the SRF configuration flights, see Fig. 5. The expectation was that these categories would also be seen in vertical nominal configuration flights, but none of the flights crashed during descent or ascent, though one flight without wind showed some instabilities during descent. Furthermore the DD category happened more often than the DA category, which was expected as VRS happens due to descent into one's own turbulence, note that the DA category usually occurred right after descent. As these categories are connected through theory and were mostly seen in combination with each other they were combined into the "Vortex Ring State" category.

The IO category was also only seen in the SRF configurations, where an increase in wind speed caused an increase in oscillations of the accelerations. As this was not seen in the nominal configuration this oscillation is expected to be caused by the control strategy for quadrotors in SRF configuration [9]. This strategy led to a new aerodynamic phenomenon: Double Blade Flapping (DBF), that was observed during test flights (see Sub-Section B.i.). The phenomenon causes the control system to command different rotor speeds for each rotor based on their location w.r.t. the centre of gravity and is seen as the cause of the oscillations. Thus the IO category is combined with the HV category into the "Blade Flapping" category.

AS and HV are the categories that were seen the most, thus they are seen as the main causes for quadrotor failures in both the nominal and SRF configuration. Furthermore, the SD category was seen frequently in combination with the two. What was observed is that due to the high wind speeds the quadrotor needed more thrust, in both the nominal and SRF configurations, to hold position. Thus with higher speeds, higher rotor speeds and more actuator saturation cases are observed. Also slow descents were observed due to the quadrotor needing to tilt its thrust vector into the wind to keep its position. As the HV category can be seen as a cause of other categories it is combined with the AS and SD categories into the "Actuator Saturation" category.

The final category EF, although not seen that frequently, always causes dangerous situations. From empty/broken batteries causing random landing sequences or thrust spikes to actuators breaking causing uncontrolled crashes. Thus the "Equipment Failure" category remains unchanged.

## B. Discussion

The discussion contains phenomena seen and comparisons made in the analysis.

### B.i. (Double) Blade Flapping

Blade flapping is a phenomena which is seen in helicopter operations during translational flight, where the advancing side of the rotor disk sees a higher effective velocity with respect to the air, whereas the retreating side of the rotor disk sees a lower effective velocity. This difference creates a change in the lift distribution between the two halves and thus effectively flaps the blades up and down once per revolution [25]. Helicopters counter this effect by changing the angle of attack of their blades with the position in the rotor cycle, though this eventually leads to retreating blade stall [17]. Quadrotors do not have variable pitch propellers.

As the quadrotor uses more than one rotor it has advantages over helicopters with respect to blade flapping. Due to the symmetry of the quadrotor, the lateral effects of blade flapping are cancelled, but in longitudinal direction the plane of the rotor disk is tilted away from the direction of motion, see Fig. 6, where the movement is into the wind. Due to the tilt of the rotor disk the translational movement is damped and the effective upwards thrust is lowered. In [18] a decrease in hover thrust of a few percent and a decrease in attitude tracking of a few degrees due to torque is observed as a direct cause of blade flapping.

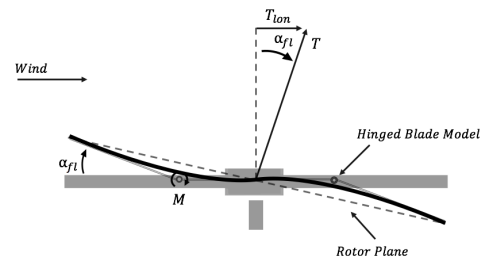


Figure 6. Blade Flapping: Hinged Blade Model

As the flapping angle was not measured during flight, the influence on the thrust remains unknown. However in the SRF configuration flights an interesting phenomenon was seen. The commanded and observed rotor speeds of the quadrotor were oscillating with the location of the rotor in the yaw plane. It was observed that a second flapping plane was created due to the quadrotor spinning around its own axis, see Fig. 7, where the plots show the rotor speeds of each respective rotor over a single flight. Note that the rotors are numbered as in Fig. 8. The red and blue half circles indicate the phase of the yaw of the quadrotor in which the respective rotor is in the advancing side (red) and retreating side (blue)

respectfully. Finally the black lines show the direction of the incoming wind.

A rotor in the right half of the rotation plane experiences a higher effective velocity due to the quadrotor spinning about the primary-axis. Consequently, a rotor in the left half plane experiences a less effective velocity, thus causing a rolling moment due to the offset in thrust produced. This rolling tendency was not observed in the experiments, this lack of observation is theorized to be caused by the control system changing the rotation speeds of each individual rotor based on their location within the rotation plane, which can be seen in the Fig. 7. The figure shows that the rotor opposite to the removed rotor, where the minimum rotation speed was hardcoded to be 3000 rpm, is commanded to counter the rolling moment through increasing the rotation speed of the rotor in the retreating side and decreasing the rotation speed of the rotor in the advancing side. This phenomenon, named Double Blade Flapping, was observed in multiple flights where it was always the rotor opposite to the removed rotor that showed the behaviour described above.

The behaviour seen in the two (working) rotors opposite of each other also showed similar behaviours in multiple flights, where the rotor speeds would be observed to be identical. This difference in expected behaviour could have multiple sources e.g. wobbling angle, symmetry, translational velocity and the aerodynamic moments due to the different planes of the rotors and the centre of gravity. Thus this phenomenon should be further investigated by for example examining the rotor speeds of the rotors in a double-rotor failure case.

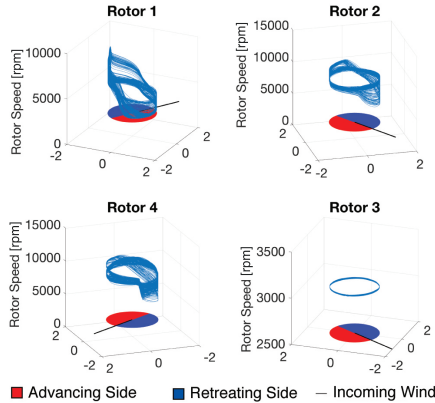


**Figure 7.** Double Blade Flapping ( $3^{rd}$  rotor Removed)

### B.ii. Aerodynamic Interaction of the Rotors

What was observed from the nominal configuration flights flown in the OJF is that the back rotors on average had higher rotation rates than the front two rotors. This observation was confirmed by a recent study regarding the aerodynamics of quadrotors [26]. The two possible configurations, with respect to rotor turning direction, were compared using a higher-order potential flow method. The two configurations can be seen in Fig. 8, where the 'bear hug' (a) has front rotors which envelope the wind in a 'hug' and the 'breast stroke' (b) has front

rotors which rotate in a motion such as a swimmer doing breaststroke. Furthermore a diamond flying configuration was also tested, where instead of flying with two rotors in front the quadrotor would fly with one rotor in front. Thus creating a different downstream turbulence pattern.

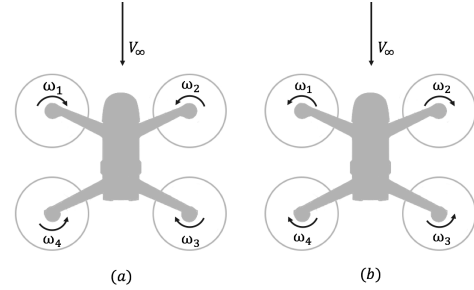


**Figure 8.** Possible Rotation Configurations for Quadrotors

Results show that the front rotors in both configurations provided equal thrust and that the back rotors produced less thrust than the front. There was however a difference in thrust produced by the back rotors due to the configuration. The 'bear hug' had a higher induced velocity on the advancing side of the rear rotors due to cross-rotor interactions, where the 'breaststroke' configuration had a higher induced velocity on the retreating side of the rear rotors. Therefore the 'breaststroke' configuration had less of a tendency to pitch up, thus less need for trim. With less trim, less power is needed for stability, thus the conclusion was made that the 'breaststroke' configuration was preferable. A quadrotor could also be flown with a different side forward to preserve energy, though this could have mixed effects due to drag effects of the main body.

Flying in diamond configuration showed similar but mirrored results for clockwise and counter-clockwise rotating rotors in front. The clockwise rotor had an increased vorticity density in the wake of the second rotor, assuming the configuration in Fig. 8 (a) with rotor one in front. Consequently the second rotor produced a higher thrust thus a tendency to roll in the positive direction. With the counter-clockwise rotating rotor in front the exact opposite happened. Thus flying in an asymmetrical rotating rotor configuration causes a tendency for instability, though this could also have been caused by blade flapping. Furthermore the effect on the rear rotor was not discussed, as it is directly in the wakes of all the other rotors it would be expected that it would perform badly.

This interaction between rotors was more apparent in the flights with reduced rotors. In all flights with (front/back) reduced rotors the first rotors to saturate were the reduced ones. Where the average rotor speeds of the other rotors, just before crashing, were higher in the case where the front rotors were reduced. As such the conclusion is made that damaged rotors are less efficient than nominal rotors and thus need a higher rotation speed to produce the same amount of thrust. Furthermore the rotors in the front perform better, as they are in laminar flow. Thus, in case rotors are damaged during flight, it is best to place those in the laminar flow by rotating the quadrotor.

### B.iii. Removed/Idle Rotors

Different configurations of the SRF quadrotor were tested e.g. right-back rotor removed, left-back rotor removed and idle rotors. The difference observed between these configurations was that the idle rotors were forced to rotate at 3000 rpm due to a hardcoded minimum limit. Thus creating thrust in idle mode, where the removed rotors did not produce any thrust. This thrust, though minimal, caused different thrust patterns in the rotors adjacent to the 'failed' rotor, in comparison to the thrust patterns of the removed rotors. The difference between removing the right back and left back rotor is that the rotor thrust patterns of the two front rotors flipped. The rotor opposite to the removed rotor showed the exact DBF pattern, where the rotor speed of that rotor was sped up in the retreating side of the rotation and vice versa.

## IV. THRUST EXPERIMENT

To validate the primary causes and precursors to quadrotor LOC a thrust experiment was designed to measure the thrust produced by the Parrot Bebop 2 actuator and accompanying rotor under all possible flight circumstances.

### A. Measurement Variables

- **The Angle of Attack (AoA),  $\alpha$ :**  
Defined as seen in Fig. 9, where the angle of attack is always defined positive for both positive (upwards) and negative (downwards) velocities.
- **The Advance Ratio,  $J$ :**  
A ratio used for propellers in aeronautics and hydrodynamics to show the ratio between the free stream fluid speed and the propeller. Where the velocity is defined positive in upwards motion and negative in downwards motion.

$$J = \frac{V}{n \cdot D} \quad (1)$$

Where  $V$  is the total velocity vector,  $n$  is defined as the rotation rate of the rotors in rotations per second and  $D$  is the rotor diameter in meters.

- **The Thrust Coefficient,  $C_t$ :**  
The dimensionless coefficient of the thrust produced by the rotor.

$$C_t = \frac{T}{\rho n^2 D^4} \quad (2)$$

Where  $T$  is defined as the thrust,  $\rho$  is defined as the density of air, assumed to be  $1.225 \text{ kg/m}^3$ , and  $n$  and  $D$  are defined as in Eq. 1.

For the acquisition of the data, the dynamometer series 1580 of RcBenchmark was used. Using the accompanying software the thrust and the rotation speed were measured with a frequency of 10 Hz. Finally the wind was extracted from the computer system of the OJF.

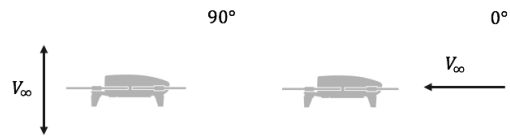


**Figure 9.** Angle of Attack Definition

For each test run, the angle of attack and the velocity were kept constant, while the rotor was varied over rotational values of 3,000 to 12,000 rpm in increments of 1000 rpm. For each rotational value 50 data points were acquired, leading to 500 data points per run. The angle of attack was then varied from 0 to 90 degrees in increments of 10 degrees and the velocity was varied from 0 to 14 m/s in increments of 2 m/s. To do measurements on descending flight without influence of the dynamometer, the rotation direction and the rotor were both flipped to measure the thrust produced in descending flight.

### B. Rotor Thrust Model

The actuator and rotor were tested for 1600 points, where each point had 50 thrust measurements. The thrust at that data point was then taken to be the average of the 50 measurements. By taking 50 measurements per point the expected thrust fluctuations could be identified per point [27], thus indicating certain areas of the flight regime to be less stable than others.

#### B.i. Measurement Influences

As the thrust stand was close to the rotor itself, and would also be effected by the incoming wind, a slight influence was to be expected. Therefore all the measurements were taken after setting all values to zero on the device (tare), this however would also remove the influence of the rotor itself, therefore extra measurements were made without setting the values to zero on the device. Furthermore the thrust stand was tested separately to test its influence. Following those measurements, the following assumptions were made:

$$F_{notare} = F_{tare} + F_{static} \quad (3)$$

$$F_{real} = -F_{notare} + F_{testbench} \quad (4)$$

Where  $F_{notare}$  in Eq. 4 has flipped signs for the descending tests and  $F_{static}$  equals all the static forces:

$$F_{static} = F_{testbench} + F_{rotor} \quad (5)$$

For zero degrees, perpendicular to the wind tunnel, there was hardly any difference between the non-tared approximate (Eq. 3) or the actual non-tared measurement, but the higher the angle of attack the bigger the difference became, where the non-calibrated measurement showed higher values of thrust. As preliminary results showed lower thrust values than the flight data, the decision was made to use the non-tared measurement.

#### B.ii. Data Fitting

To fit the obtained data multivariate splines were used. As the density of data points along the angles of attack was lower than the density of the data points

along the advance ratio, the data along constant advance ratio values were fitted with 1<sup>st</sup> order polynomials to counter the behaviour of multivariate splines along low data density points. As the centre of the dataset had more dynamics, different triangulation densities were tested. The final triangulation was made with 1-simplices on a constant field of 10 points along the angle of attack, each corresponding to 10 degrees. Along J a different triangulation was used where the advance ratio was split into three sections, with two, eight and two simplices each. Thus in total creating 216 simplices. In Fig. 10 the triangulation can be seen, with the final thrust model, which used 5<sup>th</sup> order polynomials over each simplex with 0<sup>th</sup> order continuity ( $S_0^5$ ).

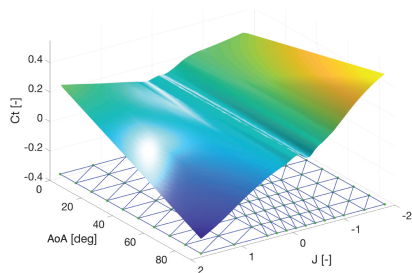


**Figure 10.** Triangulation and Thrust Model

To validate the fit of the thrust model the variance of the B-coefficients was examined, furthermore a residual quality analysis was performed. Firstly the dataset was split in two separate data sets: the identification dataset and the validation dataset. The identification dataset was then used to identify the model and the validation dataset was then used to validate it.

The final model had an average B-coefficient variance of 0.0011, a Root Mean Square (RMS) error of 0.0004 and a relative RMS error of 0.19%, where the relative RMS error is defined as the RMS of the error over the RMS of the validation model.

#### B.iii. Model Validation

To validate the model, it was compared to flight data. An external motion capture system (Optitrack), was used to obtain the velocity of the quadrotor. The velocity per rotor was determined through Eq. 6, where  $\vec{\Omega}$  is the rotation velocity vector consistent of p, q and r,  $\vec{r}_i$  indicates the location of the  $i^{th}$  rotor w.r.t. the centre of gravity and  $\vec{V}_{tot}$  is the total velocity of the quadrotor.

$$\vec{V}_i = \vec{\Omega} \times \vec{r}_i + \vec{V}_{tot} \quad (6)$$

The thrust coefficient, advance ratio and angle of attack were determined through their definitions given in Sub-Section A (Eqs. 1 and 2). Where the thrust was determined through Newton's first law and the local velocity and rotor speeds were used to determine the  $C_t$  values per rotor.

In Fig. 11 the comparison between the flight data and the model data can be seen, where the dataset is split up in four manoeuvres: (1) vertical manoeuvre, (2) transverse manoeuvre, (3) longitudinal manoeuvre and

(4) yaw changes while holding position. Where manoeuvres (1) & (2) were performed at yaw angles of 0 to 90 degrees. To compare the  $C_t$  value of the whole quadrotor to the data obtained from the model both sets were z-normalised, thus the datasets indicate the standard deviations with respect to the mean of the respective set. Note that the model data was multiplied by 1.3.

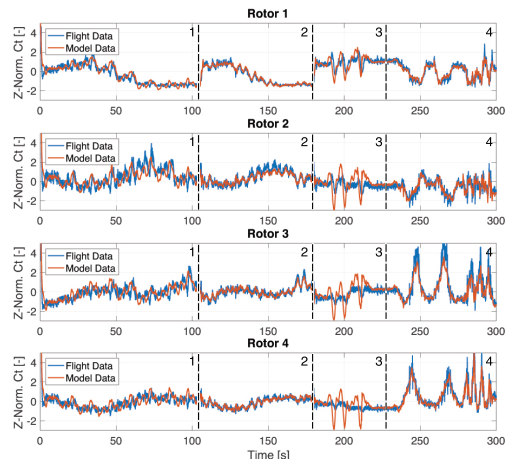


**Figure 11.** Z-Normalised Nominal Configuration Flight Data & Model Data,  $V = 8$  m/s

#### B.iv. Discussion

From the model quality results the  $S_0^5$  model was chosen because of its lowest average B-coefficient variance. From the comparison, Fig. 11, it can be seen that the dynamics of the model are similar to those of the flight data, except for dynamics in the longitudinal manoeuvre. This difference is theorized to be caused by rotor speed and velocity inaccuracies during forward flight. Furthermore the thrust magnitude is not similar as the model data was multiplied by 1.3. This thrust difference is theorized to come from several factors:

- The lift produced from the body of the quadrotor, which was not taken into account in the model.
- The actuator being directly attached to the thrust stand and consequently the small rotor being in close proximity to the thrust stand.
- The quality of the rotor. New rotors from the same batch, produced different thrust values for the same commands and flight conditions.
- A possible bias in the accelerometer data of the quadrotor.

As the thrust model was meant to be used as an indication for LOC areas in the flight regime of a quadrotor, validation of the dynamics of the model is considered to be sufficient. The validation results indicated that the dynamics of the model showed similarities to those of the quadrotor, therefore the model is considered to be validated. With the dynamics validated the model can be used to find and validate the (un)stable areas in the flight regime of the quadrotor.

To be able to use the thrust model in for example SFEs or simulations, the thrust difference should be identified. Thus more experiments should be performed to quantify this difference. One could for example design an experiment to measure the forces and moments of a rotor in the same flight regime as the experiments that were performed. This data could also be used to quantify the effect of blade flapping and the aerodynamics caused by the offset of the rotor plane and the centre of gravity plane.

## V. VALIDATION

The validated thrust model was used to validate the categories and observations that were found through the data analysis, Section III. Where actuator saturation is seen as the primary cause to LOC events of quadrotors and the other categories and observations are seen as precursors. As the model was created for a single rotor, the aerodynamic influences of rotors on each other will not be discussed.

### A. Vortex Ring State

From multiple sources the VRS is seen as a regime where the momentum theory fails, as it is essentially the state in the flight regime where the wind flow is reversed in direction. In this unstable flight regime, the thrust produced is expected to be fluctuating [27].

#### A.i. Thrust Variation

To find the thrust variation over the flight regime of the actuator the 50 measurements per data point were used. The minimum and maximum values per data point were obtained and their difference was taken as variation. The variation was obtained for all the data points of the thrust model and can be seen in Fig. 10.

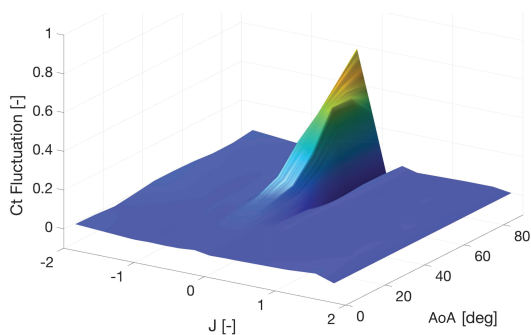


Figure 12. Thrust Model  $C_t$  Fluctuation

One can see that the thrust only fluctuates in a single area in the flight regime. The thrust fluctuations experienced in that area are in the range of  $\pm 20\%$  of the average thrust experienced in the model. Furthermore it can be seen that for higher angles of attack the fluctuation is highest. When the area is plotted over the thrust model, see Fig. 13, one can see that this area actually corresponds to the dip in thrust coefficient that is observed around an advance ratio of  $-0.3$ , see Fig. 10. Note that the indicated area shows thrust fluctuations of more than 3%.

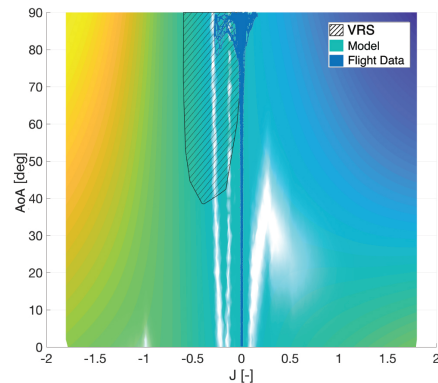


Figure 13. Thrust Fluctuation and VRS Flight on Thrust Model

As the location of the dip in thrust, with respect to the thrust model, and the observed fluctuation of thrust values were what was expected from literature, this area is seen as the area of the flight regime where one encounters the VRS. Thus one can conclude from the Fig. 13, that when descending it is best to have some translational velocity, to minimize thrust fluctuation. In amateur flight, translational movement is also known as a way to counter the "Wobble of Death".

#### A.ii. A Flight in the Vortex Ring State

One flight, in nominal configuration, was flown with the intention to maximize descent velocity with minimum forward speed. The only indication of the expected instability that was seen, was a slight wobble when stabilizing after dropping from maximum height. Therefore the assumption was made that the descent velocity was not high enough to reach the VRS.

The flight is projected over the thrust model in Fig. 13. One can see that according to the model the VRS was reached. Contrary to the assumption made, the descent velocity was high enough. The area with the highest thrust fluctuation was even reached, which corresponds to  $\pm 20\%$ . However, the time history of the manoeuvre only showed a thrust reference error of 1.5 %, where overall in the flight the reference error fluctuated between  $\pm 0.25\%$ . This could be caused by various factors such as time in descent, influence of the control system and sudden side winds, which are frequently discussed in the amateur scene. For further validation, more experiments should be performed in the heart of the VRS area, possibly from higher heights.

### B. Blade Flapping

As the experiment only produced vertical thrust, it was not possible to directly extract the flapping angles. In order to investigate the effect of blade flapping on the quadrotor performance, the hinged blade model suggested in [28] was used to estimate the blade flapping angle:

$$\alpha_{fl} = \frac{1}{1 + \frac{\mu_{lon}^2}{2}} \frac{4}{3} \left( \frac{C_t}{\sigma} \frac{2 \mu_{lon} \gamma}{3 a_0} + \mu_{lon} \right) \quad (7)$$

Where  $a_0$  is the lift curve per radian, which is approximately 6.0 for conventional airfoils at low Mach numbers [25].  $\mu_{lon}$  is defined as the longitudinal velocity to tip

speed ratio, see Eq. 8,  $\sigma$  is defined as the solidity ratio, which is the area of the rotor surface covered by rotor blades, see Eq. 9 and  $\gamma$  is the non-dimensional Lock number, which gives the ratio between aerodynamic and centrifugal forces, see Eq. 10, where  $I_b$  is the moment of inertia of the blade about the hinge and  $c$  is the chord of a blade.

$$\mu_{lon} = \frac{v_{lon}}{v_t} \quad (8)$$

$$\sigma = \frac{A_b}{A} \quad (9)$$

$$\gamma = \frac{\rho a_0 c R^4}{I_b} \quad (10)$$

The flapping angle is then used to determine the percentage of lost thrust due to flapping, see Eq. 11 and Fig. 6, where  $F_{meas}$  is the force perpendicular to the original blade:

$$T_{loss} = \left(1 - \frac{T_{meas}}{T}\right) \cdot 100 = (1 - \cos \alpha_{fl}) \cdot 100 \quad (11)$$

The results of the hinged blade model can be seen in Fig. 14, where one can see the flapping angle with respect to the angle of attack and the advance ratio and the percentage of thrust lost due to blade flapping. The flapping angle goes up to a max/min of  $\pm 40$  degrees and the percentage of thrust loss reaches a maximum of 25 %. Though the maximum values only occur for the high values of  $J$ , which only occur at high velocities with low rotor rotation rates. Normal flights occur between  $\pm 0.8J$  (App. B), in which more plausible values are seen. To make up for such a big loss of thrust, the rotor speeds need to be increased, thus causing a higher probability of rotor saturation. As the results are from a model and very sensitive to the estimation of the moment of inertia of the blade about the hinge, it is recommended that an experiment be performed to validate the results of the model.

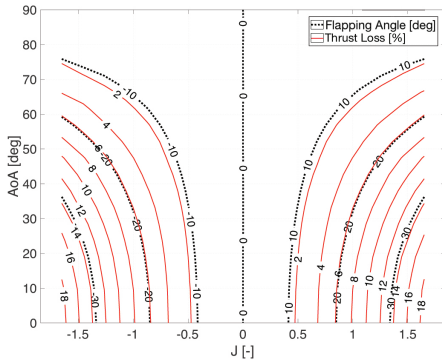


**Figure 14.** Flapping Angle [deg] and Thrust Loss [%]

### C. Rotor Saturation

The limitations of the actuators of the Bebop 2 are 3000 and  $\pm 11000$  rpm. Where the minimum limit is caused by the inbuilt hardware, and the maximum limit was found through experiments. Through analysis of the advance ratio it was found that rotor saturation is not

immediately visible, like the VRS, or expected to be omnipresent, like the loss in thrust due to blade flapping. In Fig. 15 one can see the distribution of the advance ratio with the minimum and maximum limits saturation limits and the advance ratio indicated in steps of  $0.1J$ , where the red lines indicate steps of  $0.5J$ .

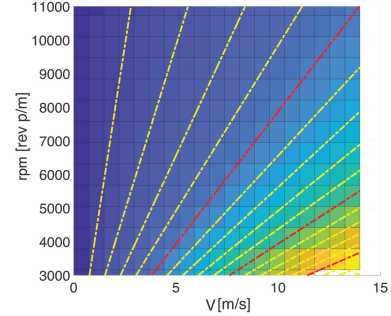


**Figure 15.** Advance Ratio Distribution

One can see what advance ratios can be expected at which velocities and vice versa. Take for example a flight at 14 m/s, through the maximum actuator saturation one can see that the advance ratio range is from  $0.5J$  till  $1.8J$ . However the advance ratio was determined through an equation, thus trying to reach a theoretical advance ratio of  $1.8J$  at 14 m/s would be implausible as the rotors would not produce enough thrust to remain stable.

To show the the limiting factor of the quadrotor that is rotor saturation, flights in both the nominal and SRF configuration are projected over the flight regime that was tested in the thrust experiment. They will be discussed in respective order in the following sub-sections.

#### C.i. Nominal Quadrotor Rotor Saturation

In App. B data of the flights that were flown in both the nominal and SRF configuration are projected on the flight regime, that was used for the thrust model, to give an indication of the range the quadrotor can reach in different configurations and under various circumstances. Note that these projections are the data sets of the first rotor, where in the nominal case the other rotors show similar behaviour. Also note that the advance ratio per rotor was determined through the same method as in the Model Validation (Sub-Section B.iii.).

From the nominal configuration flights it can be seen that the advance ratio varied between  $\pm 0.8J$ , where, in combination with Fig. 15, it can be seen that the limit of  $0.8J$  at 14 m/s is a lower limit of 7000 rpm. From the advance ratio ranges observed for the other velocities in Fig. 18, it can be seen that the maximum advance ratio flown in each flight speed is limited by the minimum rpm and thus consequently the minimum advance ratio is limited by the maximum rpm. Thus the maximum attainable advance ratio for nominal quadrotors is dependent on the minimum rpm that can stabilize the quadrotor at a given velocity. This minimum value increases with the velocity, which in turn also increases the angle of attack and the flapping angle. This eventually leads to the minimum rpm exceeding the maximum rpm, thus one can conclude that the nominal configuration is indeed limited by rotor saturation.

### C.ii. Single-Rotor Failure Quadrotor Rotor Saturation

The quadrotor flights in SRF configuration can be found in App. B.2. As with the nominal configuration flights only the first rotor datasets were projected on the flight regime used for the thrust model. However, contrary to the rotors of the nominal configuration, the rotors of the SRF configuration did not show similar behaviour, see Fig. 16. As the SRF configuration uses high-speed spinning relaxed hovering solutions [29], this was to be expected. Note that the flights in the SRF configuration do not include a legend, as the pattern of the SRF configuration flights is more dependent on the wobbling angle than the wind speed.

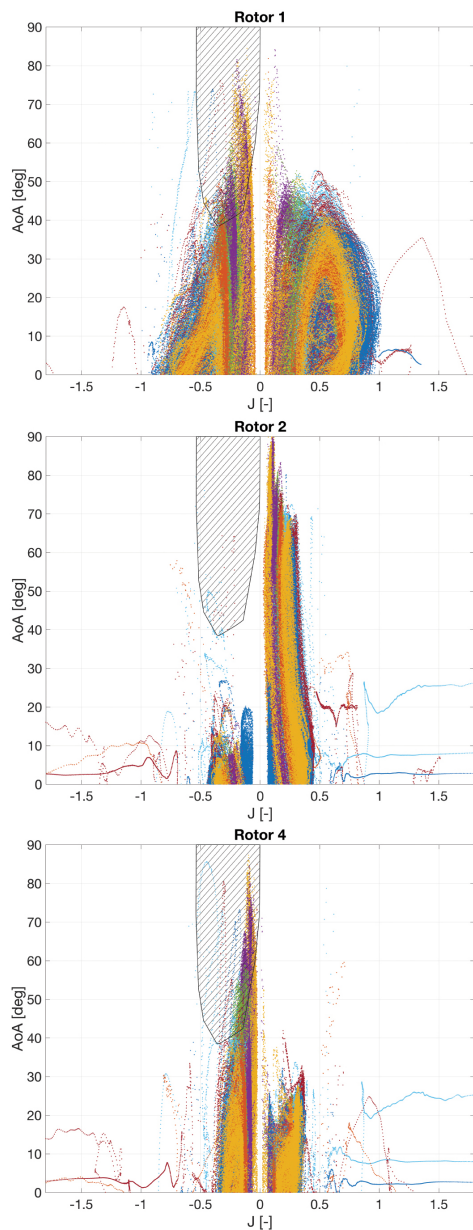


**Figure 16.** Vertical Flights of Quadrotors in SRF Configuration (3<sup>rd</sup> Rotor Removed)

In comparison to the nominal configuration the SRF configuration reaches higher angles of attack and higher advance ratio values in the rotor opposite to the failed rotor. This increase is caused by the wobbling angle that increases with the tilt of the primary-axis. Increasing the tilt of the primary-axis in the direction of the rotor opposite to the failed rotor also lowers the energy needed to keep wobbling and thus the rpm of the remaining rotors (two and four) are lowered. Note that there is an optimum in trading rpm speeds between the rotors.

It can be observed that the higher advance ratio values seen in the SRF configuration all occur in the rotor opposite to the failed rotor. Furthermore the remaining rotors have similar, but mirrored patterns. This pattern is also seen in the discussion on the DBF phenomenon. Due to the increased effective velocity on the advancing side and the lowered effective velocity on the retreating side the rotor opposite to the failed rotor sees a greater fluctuation in rotor rpm, where the minimum rpm is the cause of the increased advance ratio. Thus as with the nominal configuration, the maximum advance ratio of the SRF configuration is determined by the minimum rpm needed to stabilize at a given velocity and therefore it is also limited by rotor saturation.

Finally the vertical flights in the SRF configuration also touched upon the VRS domain. As 80% of the SRF configuration test flights showed crashes during descending vertical flight, this could likely be due to the thrust variation in the VRS. Where the prime suspects for rotor saturation is the first rotor as it sees higher rotation speeds than the other rotors (second & fourth). Note that this assumption changes when the quadrotor rotates in the opposite direction and/or a different rotor fails.

## VI. A QUANTITATIVE DESCRIPTION FOR LOSS-OF-CONTROL

The Quantitative Loss-Of-Control Definition (QLD) for quadrotors is similar to the definition given to LOC of CAT, but where the CAT have multiple upset conditions, the quadrotor only has one: actuator saturation. Furthermore a difference is seen in the dynamic and equipment failure precursors. The definition of the QLD can be found in Fig. 17, where the precursors are further specified in App. A. Hazards, which are currently unlikely to occur, such as the hazards under the "Atmospheric Disturbances", were also added as they are likely to occur when quadrotors will eventually be used for longer flights over greater distances.

As the two major sub-systems of the AFTCS, the FTC and FDD, are often researched separately in literature and have not been successfully unified, actuator failure has not been added to the primary causes. Once the AFTCS has been completed and actuator failures have become survivable, it should be added. In case the QLD is adapted to multicopters it could be immediately added, as multicopters, that have more rotors than the quadrotor, have inbuilt redundancy and are therefore resistant to actuator failure.

With the QLD for quadrotors defined, investigators of LOC events of quadrotors have a valuable tool to be able to label and group events and thus are able to systematically seek viable safety intervention strategies to reduce the occurrence of LOC.

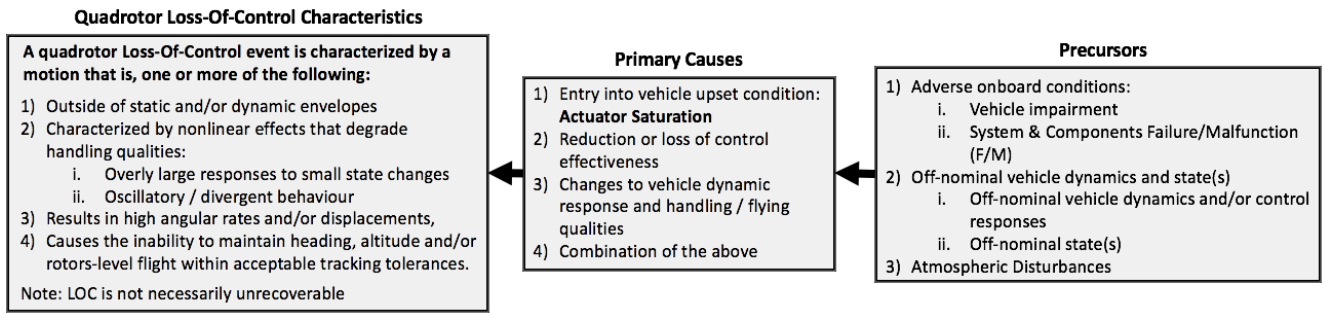


**Figure 17.** Quantitative LOC Definition (QLD) for quadrotors, Primary Causes and Precursors, Adapted from CAT LOC [24]

## VII. CONCLUSIONS

To push for a holistic view on preventing LOC of quadrotors and to give insight on such situations, the QLD for quadrotors has been defined through a comparative data analysis. Quadrotor LOC characteristics were defined through the application of CAT LOC characteristics to quadrotors. These characteristics were used in the comparative data analysis of test flights, flown under real life conditions, which resulted in categories of failures, which were related to LOC. Through delimitation and in combination with observations a theory on the primary causes and precursors of LOC was created.

The theory was then validated through comparison to a rotor thrust experiment, where a single actuator and rotor were tested over the expected flight range. Where, for both the nominal and SRF configuration, actuator saturation was seen as the only primary cause of the quadrotor LOC events and the VRS, blade flapping, aerodynamic interaction of the rotors and equipment failure were seen as the precursors to LOC events, where in the SRF case the DBF phenomenon, observed in flight tests, was also added as a precursor. With the QLD for quadrotors defined, investigators of LOC events of quadrotors have a valuable tool to be able to label and group events and thus are able to systematically seek viable safety intervention strategies to reduce the occurrence of LOC.

The authors are grateful to the Open Jet Facility, MAVlab and the TU Delft for their support.

## REFERENCES

- [1]Belcastro, C., Foster, J., Shah, G., Gregory, I., Cox, D., Crider, D., Groff, L., Newman, R., and Klyde, D., "Aircraft Loss of Control Problem Analysis and Research Toward a Holistic Solution," *Journal of Guidance, Control, and Dynamics*, Vol. 40, 2017.
- [2]Boeing, "Statistical Summary of Commercial Jet Airplane Accidents Worldwide Operations 1959-2016," Technical report, Aviation Safety Boeing Commercial Airplanes, Seattle, Washington, USA, 2017.
- [3]Belcastro, C., Newman, R., Evans, J., Klyde, D., Barr, L., and Ancel, E., "Hazards Identification and Analysis for Unmanned Aircraft System Operations," *17th AIAA Aviation Technology, Integration, and Operations Conference*, Denver, Colorado, USA, 2017.
- [4]Jiang, T., Geller, J., Ni, D., and Collura, J., "Unmanned Aircraft System Traffic Management: Concept of Operation and System Architecture," *International Journal of Transportation Science and Technology*, Vol. 5, 2016.
- [5]Zhang, Y. and Jiang, J., "Bibliographical Review on Reconfigurable Fault-Tolerant Control Systems," *Annual Reviews in Control*, Vol. 32, 2008, pp. 229–252.
- [6]Zhang, Y., Chamseddine, A., Rabbath, C., Gordon, B., Su, C., Rakheja, S., Fulford, C., Apkarian, J., and Gosselin, P., "Development of Advanced FDD and FTC Techniques with Application to an Unmanned Quadrotor Helicopter Testbed," *Journal of the Franklin Institute*, Vol. 350, 2013, pp. 2396–2422.
- [7]Smear, E. J., Chu, Q., and de Croon, G., "Adaptive Incremental Nonlinear Dynamic Inversion for Attitude Control of Micro Air Vehicles," *Journal of Guidance, Control, and Dynamics*, Vol. 38, 2015.
- [8]Mueller, M. and D'Andrea, R., "Stability and Control of a Quadcopter Despite the Complete Loss of One, Two, or Three Propellers," *IEEE International Conference on Robotics and Automation (ICRA)*, Hong Kong, China, 2014.
- [9]Sun, S., Sijbers, L., Wang, X., and de Visser, C., "High-Speed Flight of Quadrotor Despite Loss of Single Rotor," *IEEE Robotics and Automation Letters*, Vol. 3, No. 4, 2018.
- [10]Freddi, A., Longhi, S., and Monteriu, A., "A Model-Based Fault Diagnosis System for a Mini-Quadrotor," *Workshop on Advanced Control and Diagnosis*, Zielona Gora, Poland, 2009.
- [11]Avram, R., Zhang, X., and Muse, J., "Quadrotor Sensor Fault Diagnosis with Experimental Results," *Journal of Intelligent and Robotic Systems*, Vol. 86, No. 1, 2017, pp. 115–137.
- [12]R.C.Avrar, Zhang, X., and Muse, J., "Quadrotor Actuator Fault Diagnosis and Accommodation Using Nonlinear Adaptive Estimators," *IEEE Transactions on Control Systems Technology*, Vol. 25, No. 6, 2017.
- [13]Belcastro, C., "Loss of Control Prevention and Recovery Onboard Guidance, Control, and Systems Technologies," *AIAA Guidance, Navigation, and Control Conference*, Minneapolis, Minnesota, USA, 2012.
- [14]Pardee, J. and Russell, P., "Final Report - Loss of Control JSAT: Results and Analysis," Technical report, Federal Aviation Administration (FAA), Washington D.C., USA, 2000.
- [15]Barr, L., Newman, R., Ancel, E., Belcastro, C., Foster, J., Evans, J., and Klyde, D., "Preliminary Risk Assessment for Small Unmanned Aircraft Systems," *AIAA Aviation Technology, Integration, and Operations conference*, Denver, Colorado, USA, 2017.
- [16]Wild, G., Murray, J., and Baxter, G., "Exploring Civil Drone Accidents and Incidents to Help Prevent Potential Air Disasters," *Aerospace*, Vol. 3, No. 3, 2016.
- [17]Federal Aviation Administration, *Helicopter Flying Handbook*, chap. Helicopter Emergencies and Hazards, Oklahoma City, USA, 2012, pp. 11–1 – 11–24.
- [18]Huang, H., Hoffmann, G., Waslander, S., and Tomlin, C., "Quadrotor Helicopter Flight Dynamics and Control: Theory and Experiment," *AIAA Guidance, Navigation and Control Conference and Exhibit*, South Carolina, USA, 2007.
- [19]Oort, E. V., *Adaptive Backstepping Control and Safety Analysis for Modern Fighter Aircraft*, Dissertation, Delft University of Technology, 2011.
- [20]Stapel, J., de Visser, C., Kampen, E.-J. V., and Chu, Q., "Efficient Methods for Flight Envelope Estimation through Reachability Analysis," *AIAA Guidance, Navigation, and Control Conference*, 2016.
- [21]Zhang, Y., de Visser, C., and Chu, Q., "Database Building and Interpolation for a Safe Flight Envelope Prediction System," *2018 AIAA Information Systems-AIAA Infotech @ Aerospace*, Kissimmee, Florida, USA, 2018.

- [22]Zhang, Y., de Visser, C., and Chu, Q., “Online Safe Flight Envelope Prediction for Damaged Aircraft: A Database-driven Approach,” *AIAA Modeling and Simulation Technologies Conference*, San Diego, California, USA, 2016.
- [23]Chen, M., Hu, Q., Fisac, J., Akametalu, K., Mackin, C., and Tomlin, C., “Reachability-based Safety and Goal Satisfaction of Unmanned Aerial Platoons on Air Highways,” *Journal of Guidance, Control, and Dynamics*, Vol. 40, No. 6, 2017.
- [24]Belcastro, C., Newman, R., Crider, D., Klyde, D., Foster, J., and Groff, L., “Aircraft Loss of Control: Problem Analysis for the Development and Validation of Technology Solutions,” *AIAA Guidance, Navigation, and Control Conference*, San Diego, California, USA, 2016.
- [25]Prouty, R., *Helicopter Performance, Stability, and Control*, Prindle, Weber and Schmidt (PWS Publishers), 1986.
- [26]Barcelos, D., Kolaei, A., and Bramesfeld, G., “Performance Predictions of Multirotor Vehicles Using A Higher-Order Potential Flow Method,” *2018 AIAA Aerospace Sciences Meeting*, Kissimmee, Florida, 2018.
- [27]Shetty, O. R. and Selig, M. S., “Small-Scale Propellers Operating in the Vortex Ring State,” *49th AIAA Aerospace Sciences Meeting AIAA*, 2011.
- [28]Pounds, P., Mahony, R., and Corke, P., “Modelling and Control of a Quad-Rotor Robot,” *Proceedings of the Australasian Conference on Robotics and Automation*, 2006.
- [29]Mueller, M. and D’Andrea, R., “Relaxed Hover Solutions for Multicopters: Application to Algorithmic Redundancy and Novel Vehicles,” *The International Journal of Robotics Research*, 2015.

## APPENDIX

## MULTICOPTER LOC

In this appendix the precursors of the Quantitative Loss-Of-Control Description (QLD) are further defined in sub-categories and hazards. These can be found in Tab. 1.

Precursors	Sub-Categories	Hazards
Adverse Onboard Conditions	Vehicle Impairment	Improper Maintenance Improper Loading: Weight/Balance CG Airframe, Actuator and/or Rotor Damage
	System & Components Failure/Malfunction (F/M)	Control Component Failure/Inadequacy System Software Failure/Inadequacy <sup>1</sup>
Off-Nominal Vehicle Dynamics & State(s)	Off-Nominal Vehicle Dynamics and/or Control Responses	Aerodynamic Interaction of Rotors Vortex Ring State (VRS) (Double) Blade Flapping (DBF) <sup>2</sup> Oscillatory Response Asymmetric Vehicle
	Off-Nominal State(s)	Off-Nominal Attitude, Angular Rates and/or Wind Speed Abrupt Disproportionate Response Flight Trajectory Not Within Tolerances
Atmospheric Disturbances	Atmospheric Disturbances	Wake Vortex Wind/Turbulence Thunderstorms/Rain <sup>1</sup>

<sup>1</sup> To be investigated, but is expected to be a precursor

<sup>2</sup> DBF will only occur in rotor failure flights that use the primary axis control scheme

**Table 1**  
Quadrotor LOC Precursors and Accompanying Hazards, Adapted From Aircraft LOC Precursors [24]

## QUADROTOR FLIGHTS

In this appendix datasets of flown flights are projected over the thrust model to give an indication of the flight regime that the quadrotor operates in, note that the data of the first rotor is used in all cases. The flights have been split in two main sections: the flights in nominal configuration, which can be found in Section B.1 and the flights in SRF configuration, which can be found in Section B.2.

*Nominal Quadrotor Flights*

The flights in nominal configuration are split into two different sets: the flights which covered the movements in vertical and longitudinal directions under all wind conditions, which can be seen in Fig. 18 and flights in which only longitudinal movements were flown, in Fig. 19.

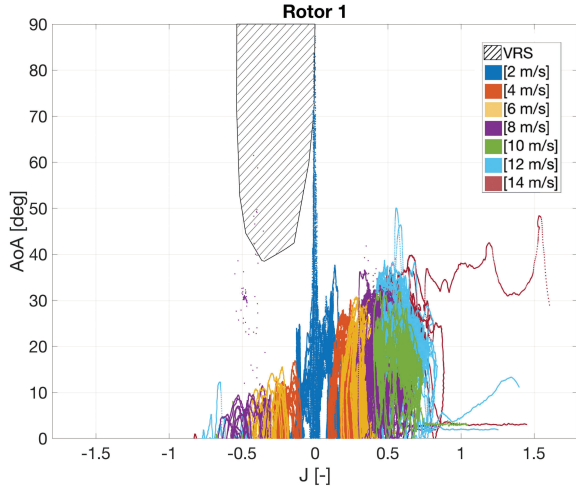


**Figure 18.** Vertical/Longitudinal Flights, Nominal Configuration

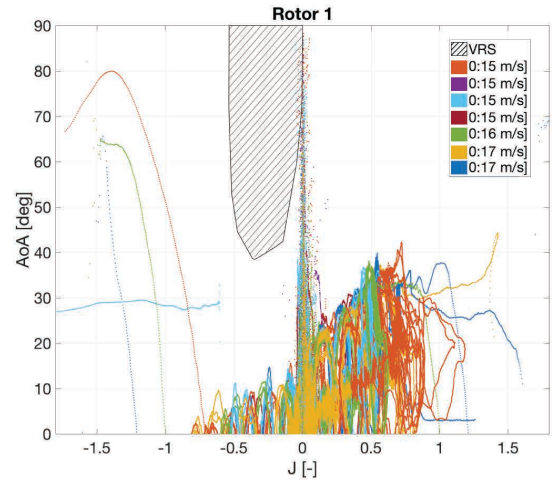


**Figure 19.** Longitudinal Flights, Nominal Configuration

*Single Rotor Failure Quadrotor Flights*

The flights in SRF configuration were flown in two different sets: the longitudinal flights, seen in Fig. 20 and the vertical flights, which can be seen in Fig. 21.

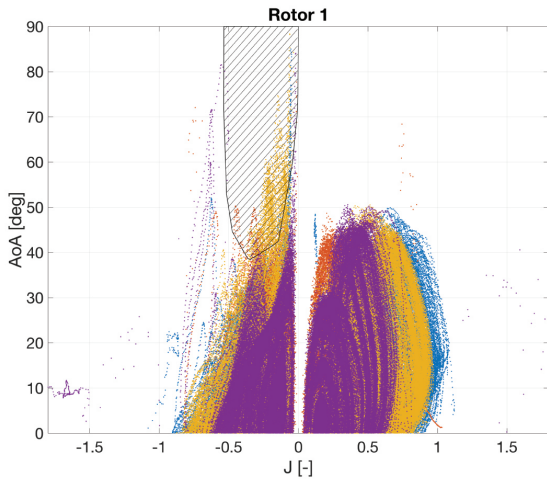


**Figure 20.** Longitudinal Movement, SRF Configuration

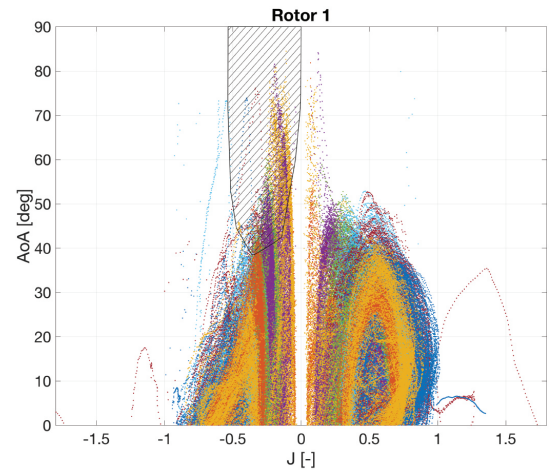


**Figure 21.** Vertical Movement, SRF Configuration



# III

## Problem Description



# 3

## The Quadrotor

The quadrotor is one of the smaller family members of the multicopters, which, unlike helicopters, use multiple rotors with fixed pitch blades to generate lift. This gives them Vertical Take-Off and Landing (VTOL) and hovering capabilities. By using their rotors as main lifting devices the need for larger area lifting devices, such as wings, is removed. This ability also gives them substantially more agility and freedom than classic aircraft. A quadrotor is equipped with four brushless motors with fixed pitch blades, in most newer quadrotors a camera is also included. Furthermore the sensors on board usually include a 3-axis magnetometer, gyroscope and accelerometer.

In Figure 3.1 one can see the Parrot Bebop 2, which was the quadrotor that was used in all the experiments that were performed for this research. Degradation of the hardware is seen as the main reason for quadrotor failure, as failure in sensors or rotors will lead to bad tracking and stability of the system. Also unlike bigger multicopters the quadrotor does not have redundancy in rotors and will therefore likely crash in the case that a rotor fails, assuming the control system has not been designed for such a case.

The rest of this chapter is structured as follows: Firstly the reduced model of a quadrotor and its definitions will be shown in Section 3.1, then the general limitations of the quadrotor are explored through analysis of the model in Section 3.2 and finally the control limitations are discussed with regards to Loss-Of-Control (LOC) of quadrotors in Section 3.3.

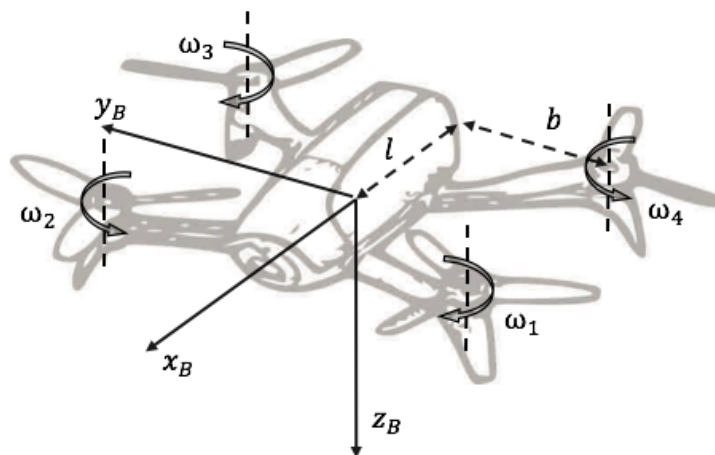


Figure 3.1: Parrot Bebop 2: Body Axis Definition

### 3.1. The Reduced Model

To analyse the quadrotor for possible failures, the reduced model, which is widely used in controllers for hovering flight, was analysed. The assumption is made that the quadrotor is a rigid body. Therefore the Newton-Euler equations can be used to define the translational and rotational dynamics of the quadrotor. Starting from the body axis definition in Figure 3.1, where the x-axis is defined positive in forward direction and the z-axis is defined as positive in the downwards direction, the translational and rotational dynamics are defined as in [6]:

$$m \begin{bmatrix} \dot{u} \\ \dot{v} \\ \dot{w} \end{bmatrix} = m \begin{bmatrix} p \\ q \\ r \end{bmatrix} \times \begin{bmatrix} u \\ v \\ w \end{bmatrix} + \vec{G} + \vec{F} \quad (3.1)$$

$$I_v \begin{bmatrix} \dot{p} \\ \dot{q} \\ \dot{r} \end{bmatrix} = \begin{bmatrix} p \\ q \\ r \end{bmatrix} \times I_v \begin{bmatrix} p \\ q \\ r \end{bmatrix} + \vec{M} \quad (3.2)$$

Where  $u, v, w$  are defined as the velocities in their respective axes and  $p, q, r$  are defined as the rotational velocities around the three axes. The mass and inertia matrices of the quadrotor are defined as  $m$  and  $I_v$ , and finally  $\vec{G}$ ,  $\vec{F}$  and  $\vec{M}$  are defined as: the gravity vector, the resultant force vector (excluding gravity) and the resultant moment on the quadrotor respectively.

As these equations do not hold well for any other flight states than hovering, Sun et. al suggest aerodynamic terms in the resultant force and moment vectors [6] for translational motion. Thus defining them as:

$$\vec{F} = \vec{F}_r + \vec{F}_a \quad (3.3)$$

$$\vec{M} = \vec{M}_r + \vec{M}_a \quad (3.4)$$

Where  $\vec{F}_r$  is defined as the reduced model of forces, which only holds in the hover condition and  $\vec{M}_r$  is defined as the reduced model moment, which does not include aerodynamic effects:

$$\vec{F}_r = \begin{bmatrix} 0 \\ 0 \\ -T_h \end{bmatrix} = \begin{bmatrix} 0 \\ 0 \\ -\kappa_0 \sum \omega_i^2 \end{bmatrix} \quad (3.5)$$

$$\vec{M}_r = \begin{bmatrix} b\kappa_0(\omega_1^2 - \omega_2^2 - \omega_3^2 + \omega_4^2) + qI_{r,z}(-\omega_1 + \omega_2 - \omega_3 + \omega_4) \\ l\kappa_0(\omega_1^2 + \omega_2^2 - \omega_3^2 - \omega_4^2) + pI_{r,z}(\omega_1 - \omega_2 + \omega_3 - \omega_4) \\ \tau_0(\omega_1^2 - \omega_2^2 + \omega_3^2 - \omega_4^2) + I_{r,z}(-\omega_1 + \omega_2 - \omega_3 + \omega_4) \end{bmatrix} \quad (3.6)$$

In Equation 3.5,  $T_h$  is defined as the rotor thrust in hovering flight,  $\omega_i$  indicates the rotor speed of the  $i^{th}$  rotor and  $\kappa_0$  is a coefficient that relates rotor properties and air density and is seen as a constant for each actuator. In Equation 3.6,  $b$  and  $l$  are defined as the distances between the centre of gravity and the rotors in x and y direction, see Figure 3.1,  $\tau_0$  is defined as a coefficient for drag moment which is considered to be constant and finally  $I_{r,z}$  is the z-direction moment of inertia of a single actuator.

The rotor speed combinations in the left term of  $\vec{M}_r$  are the combinations needed for roll, pitch and yaw respectively. Furthermore the total left term represents the rotor thrust and drag, and the total right term represents the rotor inertia effects, the gyroscopic affect and inertia torque.

Finally  $\vec{F}_a$  and  $\vec{M}_a$  are defined, as the aerodynamic forces and the moments related to translational motion, which are unique to each quadrotor and were identified for the Bebop 1 through high speed flight data in [6].

## 3.2. Model Limitations

Quadrotor movement in space is defined by the reduced model in Equations 3.1 and 3.2. Both equations are fully dependent on rotor speeds  $\omega_1, \omega_2, \omega_3$  and  $\omega_4$ . Therefore the expectation is that the health and capabilities of a quadrotor are fully dependent on the health and limitations of its rotors. With actuators having saturation limits and therefore rotor speed limits the capabilities of the quadrotor are limited to the saturation limit of the actuator. Note however that the body of the quadrotor itself is able to produce lift in certain conditions, though not enough to hover or slow down descent.

In rotorcraft the state known as autorotation is used in case the engine of the rotorcraft fails, the engine is disengaged from the rotor and the upward flow from descending is used to, in most cases, land safely, see Appendix A.2 for further details on autorotation. As most quadrotors work with fixed pitch rotors, which are used for their simplicity, it is not possible for them to achieve control in the state of autorotation. One should note though that currently research is being done on a prototype variable pitch quadrotor [7], thus in the future it might be possible to use autorotation in case of actuator failure.

## 3.3. Control Limitations

As the thesis project is limited in time, the decision was made to use the control system that was readily available on the quadrotor. This holds for both the nominal configuration and the Single-Rotor Failure (SRF) case. For the nominal case an Incremental Nonlinear Dynamics Inversion (INDI) control scheme was used. For the SRF configuration an INDI control scheme applied to a primary-axis based attitude loop controller [8] was used.

One could argue that the performance of quadrotors with regards to LOC is affected by the controller and therefore multiple control systems should be tested against each other to see if there is a difference. One could also argue that, the control system does indeed have an effect on how the quadrotor is 'controlled', but that does not affect the stable or unstable states. A quadrotor, in nominal configuration, flying in constant wind of 14 m/s has an optimal angle of attack combined with an optimal thrust to stabilize around a certain trim point. How the quadrotor reaches this state is indeed effected by the controller, but the stable state is not affected by the controller. Thus the controller limits the ability to fly safely to stable states, but not the range in which the quadrotor should theoretically be safe.



# 4

## Background

Loss-Of-Control (LOC) is the biggest contributor to manned aviation fatalities over all classes of aircraft. Especially in Commercial Air Transport (CAT) operations, where, between 2007 and 2016, LOC was the main cause for 16 accidents, which attributed to 45.8 % of all the casualties [2]. This is also the reason why LOC is one of the most researched topics within the aerospace community. With LOC being a prominent culprit of accidents within aerospace it is surprising that little research has been done into LOC of quadrotors. In this chapter background information is given on current research into LOC for quadrotors and research that is applicable to the topic at hand.

This chapter is structured as follows: Firstly the current solutions to challenging situations of quadrotors will be shown in Section 4.1. Then LOC for other manned aviation classes are discussed in Section 4.2. Finally envelope protection is explained in Section 4.3.

### 4.1. Active Fault Tolerant Control

Currently most of the research regarding quadrotor failure is geared towards the various parts of Active Fault Tolerant Control System (AFTCS) [9], which has as a main objective to keep normal steady-state performance under nominal and off-nominal conditions. Where under nominal condition the emphasis of the performance should be on the quality of the systems performance and in off-nominal conditions the emphasis should be on the survival of the system. A general structure of an AFTCS can be seen in Figure 4.1. The other configuration of Fault Tolerant Control System (FTCS) is the Passive Fault Tolerant Control System (PFTCS), which is designed to be robust against a set of presumed faults [9]. As this research is looking into possibly actively quantifying LOC, PFTCS was not further researched.

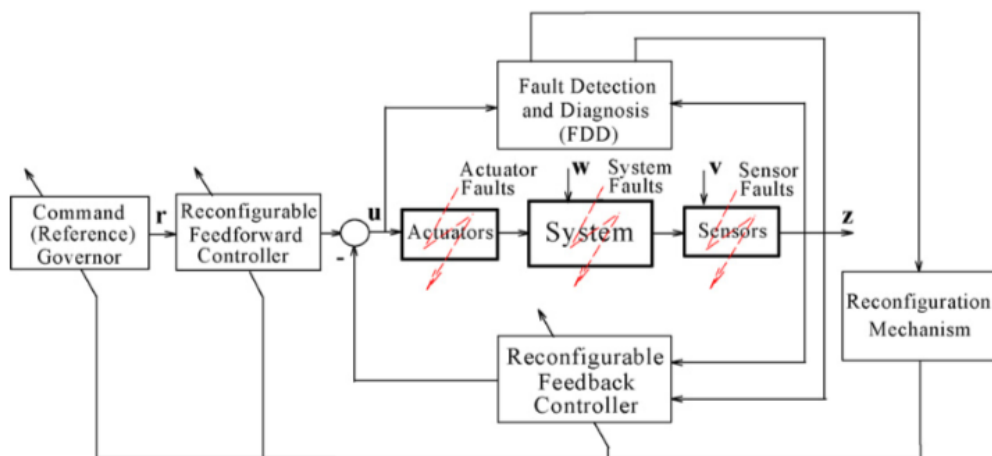


Figure 4.1: General AFTCS [9]

In general an AFTCS system has four different sub-systems: a reconfigurable controller, a mechanism that reconfigures the controller, a Fault Detection and Diagnosis (FDD) system and a command/reference governor. The FDD system and the reconfigurable controller are the features that set a AFTCS apart from a PFTCS [9]. The major difficulties in designing a good AFTCS system are therefore: the design of a control system that can be reconfigured for the problem at hand, the design of a fast and accurate FDD system and the design of the reconfigurable mechanism. What is seen in literature is that the first two are discussed the most and that the latter is seen as part of the control system. Though the reconfigurable controller is often referred to as a Fault Tolerant Control (FTC) and the FDD system is often also referred to as Fault Detection and Isolation (FDI) system. Faults considered in most FTC and FDD research are sensor, actuator and structural/component failure damage [10]. However the effects of major structural damage e.g. a broken arm, have not been researched yet.

#### 4.1.1. Fault Tolerant Control

There are various solutions in research for FTC systems that deal with tracking and attitude stabilization of quadrotors under off-nominal conditions. Take for example the adaptive Incremental Nonlinear Dynamics Inversion (INDI) [11], which is a control strategy that uses sensors for high performance nonlinear control, it uses a control effectiveness model, which is part of the vehicle model [12] and essentially replaces the model with angular accelerations. Or a FTC system based on sliding mode theory [13], which essentially constrains a systems motion such that the dynamics have a lower order than the original system and makes the system more robust against disturbances. Another example is a FTC system based on Model Predictive Control (MPC) [14], which uses the dynamic model of the quadrotor to predict where the state of the model is going in the future and in doing so compares that future state to the desired state to find an appropriate control command. There are many other control systems in literature [10]. There are also various systems that are a combination of FTC techniques e.g. a combination of MPC and  $H_\infty$  [15], where the MPC is used to track the reference trajectory and the  $H_\infty$  is used to stabilize the rotational movements.

Furthermore in literature solutions for challenging tasks have been shown, though usually these control strategies were specific due to the dynamics involved [16]. Take for example the case of rotor failure, in [17], control strategies are discussed for quadrotors with single, double and triple rotor failures, which revolves around relinquishing yaw control and spinning around a primary axis that is fixed with respect to the quadrotor. Translational control is then achieved through tilting this primary axis. In [18] a separate complementary FDD system is also suggested for the detection of rotor failure, though not validated through experiment. For the specific case of rotor failure, the developed control systems are usually tested in a simulation environment or under low speed flight conditions. Except for a recently published multi-loop hybrid nonlinear controller that was able to control a SRF configuration under high speed flight conditions (up to 9 m/s) [19]. Other examples of solutions for challenging tasks are [20], where feasible aggressive maneuvers are designed for driving a quadrotor to a desired state in state space, and [21], where thrown poles are caught and balanced on quadrotors and also transferred to other quadrotors. In both the last examples experiments were used for validation. In [16], a control system is presented that was able to handle two different tasks. Unified motion control, uses a more generalized approach with an iterative optimal control algorithm. It was used to tackle both a slung load problem and a rotor failure problem, though this was not validated through experiments.

#### 4.1.2. Fault Detection and Diagnosis

What is most important in FDD systems is the speed at which faults are detected and second, the accuracy of those detected faults. If a FTC system needs to react and reconfigure based on a fault, it needs to have enough time to do that. Regarding FDD systems in literature, the observer-based are the most common [10]. Take for example Tau's observer, in [22], it is used for the generation of residuals that are then used for FDD of accelerometer and inclinometer faults. In [23] it is used for the detection and diagnosis of actuator faults, [24] does the same but using a Linear Parameter Varying (LPV) sliding mode observer. Other techniques used for FDD include: a differential flatness technique [25] which capitalizes on nonlinear systems, which have difference flat discrete dynamics, to diagnose sensor faults, and a two stage Kalman Filter [26] that models faults in rotors as losses of control effectiveness and estimates and isolates possible faults at the same time. With the exception of a few systems, such as the last mentioned, the majority of FDD systems are evaluated through simulations [10].

Recently however two researches were published regarding FDD with experimental results. The first, was the fault detection and diagnosis of sensor bias faults in gyro and accelerometer measurements [27]. Where a sliding mode observer was used for the estimation of accelerometer measurements in roll and pitch, using the inherent robustness of the sliding mode observer against gyro bias faults. The sensors were modeled as virtual actuator faults in the quadrotor state equation, such that multiple simultaneous sensor faults could be detected. Furthermore adaptive thresholds were designed for the enhancement of the FDD algorithms. The second was one of the first researches with an AFTCS, or Fault Detection and Accomodation (FDA) as the authors called it, with experimental results [28]. Actuator faults were detected with a bank of nonlinear adaptive estimators. As with their research in FDD in sensor bias faults in gyro and accelerometer measurements, nonlinear adaptive thresholds were designed for the enhancement of their FDD algorithms. The FDD output is then used for adjusting the controller output for fault accommodation. Recommendations for further research was a unification of both researches, for the detection of both sensor and actuator faults.

### 4.1.3. Conclusions

What can be concluded from the current research into AFTCS for quadrotors, or FTC and FDD as the sub-systems of the AFTCS are usually called in literature, is that there are various solutions to individual challenging control tasks and fault detection problems. In both FTC and FDD most solutions are designed for singular problems. Furthermore, these sub-systems are supposed to work together to form the basis of an AFTCS system, but they are often researched separately in literature, leaving the other sub-system as recommendation. Though recent research has been moving towards a more unified system, such as the control system that is able to deal with two challenging tasks [16], and the FDA system with experimental research [28], there is still considerably more research and experimentation needed for a fully functioning AFTCS.

## 4.2. Loss-Of-Control for Manned Aviation

Within manned aviation there are three major types of aircraft, (1) the aeroplane, (2) the helicopters and (3) the lighter than air vehicles. Other vehicles include hybrids of the main types such as Vertical Take-Off and Landing (VTOL) airplanes. As the first two are more comparable to quadrotors they will be discussed below.

### 4.2.1. Aeroplanes

In contrast to the solutions for specific challenges in quadrotors, manned aerospace has seen a major effort into finding a holistic solution for LOC [1]. This effort was a result of the Commercial Aviation Safety Team (CAST) designating LOC as one of the three major areas of concern in the safety of commercial aviation, in 1997. A Joint Safety Analysis Team (JSAT) was created, which did research into 24 cases that were classified as LOC cases by CAST [29]. Though the problem still existed that LOC was not defined, therefore a call for development of a quantitative way to define LOC was made. National Aeronautics and Space Administration (NASA) Langley Research Center and Boeing jointly developed a set of five envelopes related to aircraft flight dynamics, structural integrity, flight control and aerodynamics. Using the generally accepted description of LOC [30], LOC is a motion that is: (1) outside the normal operating flight envelopes, (2) not predictably altered by pilot control inputs, (3) characterized by nonlinear effect, such as kinematic/inertial coupling, disproportionately large responses to small state variable changes, or oscillatory/divergent behaviour, (4) likely to result in high angular rates and displacements and (5) characterized by the inability to maintain heading, altitude, and wings-level flight. They found the primary causes for LOC, from the research of the JSAT [29], and derived the most important variables related to these causes. These variables were then used to derive the five envelopes giving a quantitative description to LOC, which addressed 95% of the CAST LOC cases. It was found that when an aircraft passed the boundaries of three or more envelopes one could speak of a LOC situation [30]. In Figure 4.2 flight test data that was flown for the validation of crew training simulators is shown in the envelopes quantifying LOC. The data from the given LOC cases were also evaluated with the envelopes, with most showing three or more envelope excursions, thus indicating LOC. Note however that a LOC situation does not always lead to an accident, it is meant as an indicator of a dangerous situation.

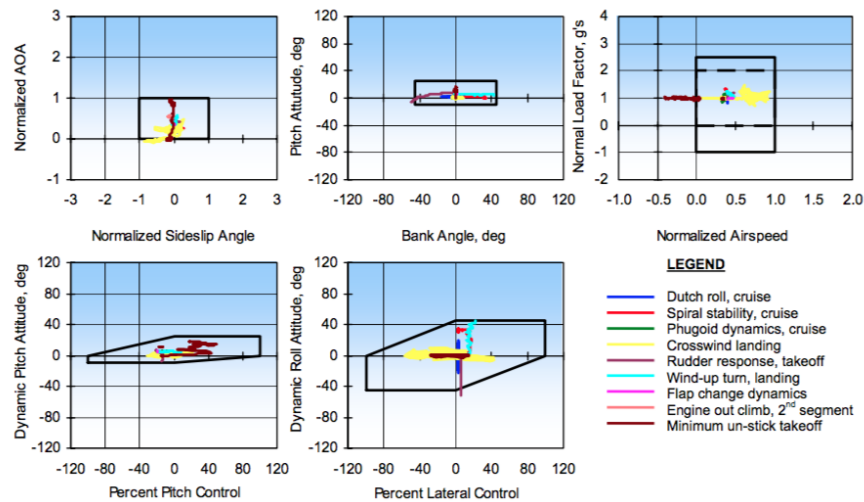


Figure 4.2: Loss-Of-Control Envelopes with Simulator Validation Flight Data [30]

With this tool investigators were able to consistently define LOC cases and find viable solutions to reduce them. From this research various methods for the mitigation of LOC in commercial aircraft have been designed. These methods have consistently been reviewed and summarized by NASA [31] [1] [32] [33] [34], where a more complete description of LOC of aeroplanes was created, see Figure 4.3. Recent interesting publications amongst those, which could possibly be related to LOC of quadrotor are: a command-limiting architecture for commercial aircraft [35], which is based on the quantitative definition of LOC [30], a new quantitative permissible flight envelope proposal based on closed loop tracking performance [36], a real-time rapid trim envelope estimation and system identification method for LOC prevention [37] and an autonomous flight envelope estimation system for LOC protection [37], which uses nonlinear dynamics and system identification for the determination of the safe flight envelope.

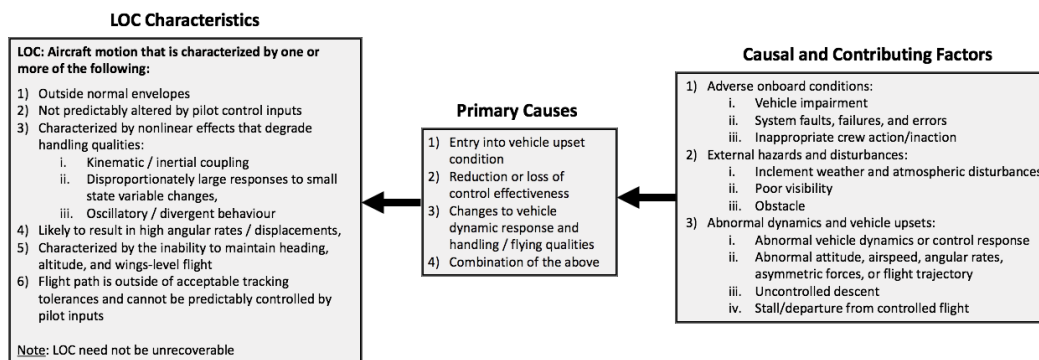


Figure 4.3: The LOC Characteristics of Aeroplanes, the Primary Causes and the Causal and Contributing Factors [31]

In quadrotor research this kind of effort has not been seen, except for possibly more recent publications, which explore systems for multiple separate challenges [16] [28]. Recently however, a preliminary risk assessment and hazard identification analysis for Unmanned Aircraft System (UAS) was done by the same group that had been publishing reviews on LOC of aircraft [3] [38]. A key finding in their research was that a lack of standardized reporting of incidents led to situations in which meaningful analyses of data was hard, which might be the reason for the lack of a search for a general solution. Furthermore an increase in hobbyist and amateur induced incidents was noticed, LOC was found to be a key hazard in UAS as well and it was observed that research into the modelling of off-nominal flight dynamics for multicopters had been sparsely conducted, therefore simulation models are being developed [39]. It was also noted that hazards identified for aircraft were not necessarily translatable to UAS. The general consensus seems to be that there is just not enough qualitative data that can be used to identify hazards, this was backed by the lack of literature about statistics on the failures of quadrotors, such as [40].

In [41] a statistical approach was taken to compare CAT incidents to Remotely Piloted Aircraft System (RPAS). Again it was seen that LOC was the biggest contributor to incidents with RPAS. Furthermore RPAS operations were concluded to have more LOC cases in flight, incidents during the take-off and cruise phase and equipment problems. Finally robustness of systems were concluded to be the key contributor to RPAS incidents, not human factors which seemed the most logical reason for failure following the CAT LOC cases. This is however opposed by Tvarynas et al. [42] who attribute the low human factor involvement in RPAS to the relatively low involvement needed in the operation of RPAS. Furthermore they argue that RPAS are in their infancy and thus have yet to be perfected and therefore have more technical failures, in contrast to for example the triple redundant systems in current CAT systems. G. Wild et al. [41] conclude that in trying to reduce RPAS incidents one should definitely look at the human factors involved, though one should not forget that these incidents could also be reduced through improved airworthiness requirements and improved robustness of RPAS.

### 4.2.2. Helicopters

Like the quadrotor, the helicopter, has also not seen a quantification for LOC. Though a significant effort has been put into understanding helicopter emergencies and hazards [43], which is similar to LOC, though differently phrased. Examples of such cases which are interesting with respect to quadrotors are: (1) autorotation, where the engine is essentially disengaged from the main rotor and the blades are driven by the upward flow, (2) the height/velocity diagram, which indicates the (un)safe sections of the flight regime for specific helicopters, see Figure 4.4, comparable to the flight envelopes for CAT, (3) dynamic roll over, which is caused by a lateral rolling tendency due to contact with the ground during take-off, (4) settling with power, also known as the Vortex Ring State (VRS), which is experienced while descending into the downwash of the rotor, enlarging tip vortices and causing loss of thrust and random thrust vectors, and (5) retreating blade stall, which is caused by blade flapping counter measures, by twisting the blade against blade flapping the retreating blade reaches certain angles of attack where there the blade starts to stall at the tips.

In essence the quadrotor is a simplified helicopter with four rotors, therefore the failures and the dynamics that govern the helicopter state can also be partly applied to quadrotors. Though the simple design of the quadrotor gives it some advantages and disadvantages over the helicopter with respect to rotorcraft LOC. Autorotation is in theory not applicable for quadrotors as rotors are fixed pitch and control is dependent on rotor speeds, with some changes to the standard design this might be possible. The height/velocity diagram or flight envelope is definitely applicable to quadrotors. Furthermore the dynamic roll over is directly countered by having multiple rotors. The last two examples mentioned above are also applicable to quadrotors and have also been thoroughly discussed in literature. More in-depth explanations on LOC cases of helicopters and airplanes can be found in Appendix A

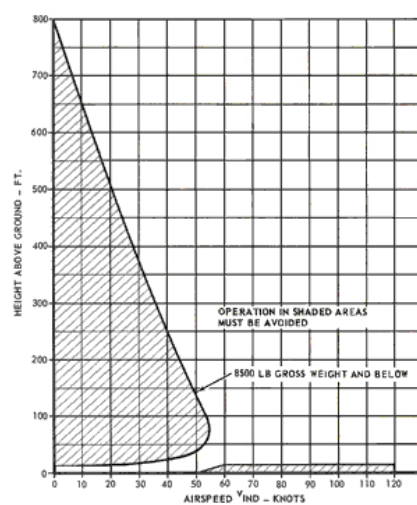


Figure 4.4: Height Velocity Diagram: Bell 204B [44]

### 4.3. Envelope Protection

Following the quantification of LOC in aircraft [30], research was done into the determination of flight envelopes. Where one can make a distinction between basic flight envelopes for static states and safe flight envelopes for dynamic states.

#### 4.3.1. The Flight Envelope

The term flight envelope is used loosely in literature as a means to indicate limitations of aircraft. In manned aviation it commonly refers to a region of velocity and load factor or altitude in which an aircraft can be flown safely, see Figure 4.5. When an aircraft leaves this region, one speaks of an excursion. The aircraft then reaches a state from which returning to a stable state from such a state is difficult. The envelopes which are defined in this region are the manoeuvre and gust envelope, which define the load factors for symmetrical manoeuvres and for symmetrical vertical gusts during level flight respectively [45]. Note the similarities with the quantitative LOC envelopes defined for aircraft [30].

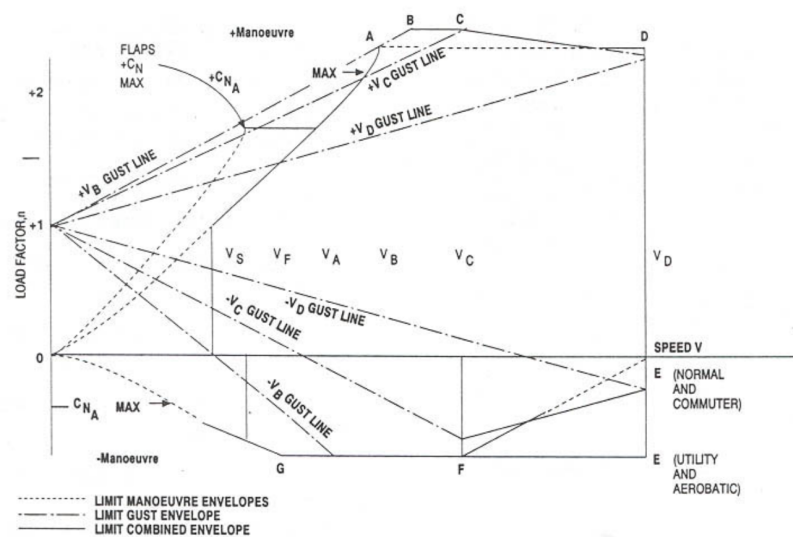


Figure 4.5: CS 23.333 Flight Envelope [45]

#### 4.3.2. Safe Flight Envelope

As general flight envelopes only take into account quasi-stationary states, such as symmetrical manoeuvres and level flight, they do not provide a safe area for dynamic manoeuvres. Therefore in the search for a bigger safety assurance region, research into flight envelopes has transitioned towards Safe Flight Envelope (SFE). The difference between the standard flight envelope and the SFE is that the SFE defines a region in which safety can be guaranteed and in which externally posed constraints will not be violated [46]. Thus it can be used as an indication of health and as LOC prevention system [37]. This envelope does have a major downside: it is computationally expensive, especially for dynamics of nonlinear systems, which tend to have higher dimension systems e.g. aircraft, quadrotors.

The envelope estimation problem can also be seen as a reachability problem [47]. Starting from an initial target set the forward reachable and backwards reachable sets are computed for a given time horizon. Where, the forward reachable set contains all states that can be reached from the initial conditions within the given time horizon and the backwards reachable set contains all states that can be steered towards from the initial target set for the given time horizon [48]. The intersection of these sets gives the SFE. An example of which can be seen in Figure 4.6. Take for example an aircraft that enters a deep stall from an initial target set, this deep stall is then part of the forward reachable set. If it is possible to return from this state to the original target set it is also part of the backwards reachable set. So theoretically the total SFE is computable, though one should understand that the scale of possible scenarios for higher dimension systems is very big, which therefore causes the theory to be computationally expensive.

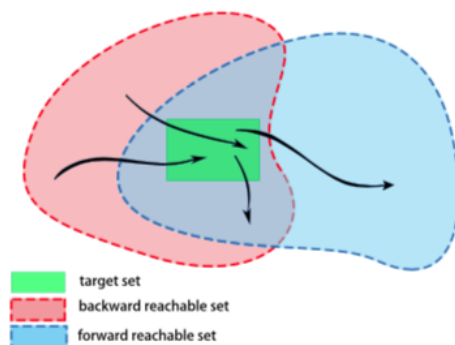


Figure 4.6: Safe Flight Envelope [49]

In [37], the SFE was used as well. It was proven that a low resolution version of the SFE for pilot displays was available within a few seconds, furthermore a fast trim state algorithm was shown to be capable of computing a part of the SFE and used for the assessment of the reliability of the envelope estimation based on the system identification system. In [50], a framework for constrained flight control is presented that uses fast computable recoverable sets to link together trim states for safe recovery trajectories from LOC cases. Recoverable sets are defined as sets that contain all states for which a control sequence exists, that have a response that is guaranteed to adhere to imposed constraints and are therefore only subsets of the complete safe envelope. Though if one can safely recover with a partial safe envelope, why would one need to compute the full envelope?

The SFE sounds applicable to the problem at hand: finding a quantitative definition for quadrotor failure. Though enough challenges still exist for the application of online SFE estimation for quadrotors. Firstly aircraft have access to more computational power onboard than quadrotors, which usually have the bare bones on board that is needed for high performance flight. Furthermore, quadrotors fly at relatively low altitudes, thus not giving much time for recovering, this also emphasizes the importance of speed in FDD. Finally quadrotors are relatively fast and nimble, leading again to a need for a fast solution. Despite the possible incompatibility of this method, it was applied to quadrotors recently [51], a capture basin was computed offline, through level set methods, for a linear model and an input from a pilot was then tested against it online. Where necessary the control signals were modified for safety. The model was however only able to handle a bit of nonlinearity through a worst-case analysis [51].

A way to work around the computational complexity of the SFE is the database-driven safe flight envelope prediction system, which is suggested in [52]. The onboard system is supported by an offline database which contains SFE for various damage cases. In case an off-nominal event happens the local aircraft model is updated through a system identification model. The FDD system evaluates the actuator/engine failure and gives the position of the error, type of damage and assess the damage severity. In case the error is more severe e.g. structural damage, the updated local model of the aircraft is used to obtain the global damaged model offline instead of having to perform a global model identification. This model is then used as retrieval index for the offline database. In case of multiple failures it is difficult to correctly isolate the problems by using only the local model, therefore immediate comparison to the offline database is applied. This database contains 60 LOC cases developed by NASA through past accident analysis. By looking up the most similar case a SFE can be found relatively fast. As sifting through the whole database might take up too much time, the comparison to the global nominal model can be used to get a general idea of what might be wrong with the aircraft, thus cutting down on the search in the offline database. Recent updates to this system include: research into an improved damage assessment method by comparing two nonlinear classification methods: neural networks and support vector machines, where the support vector machines outperform the neural networks [53] and a method to mitigate the limitations of a database: an online interpolation of envelopes taken from the database to improve accuracy and safety [49]. Finally proof of feasibility is given through three damage case simulations in [54]. Once the limitations of quadrotors become more apparent through LOC research, this database-drive SFE prediction system could also be applied.

Recently new methods for solving Hamilton Jacobi problems have been presented in [55]. An interesting publication is [56] where the computational load of computing a SFE is significantly alleviated, through time-scale separation. A backwards reachable set that used to be impossible to compute or very expensive, was proven to be quickly and exactly computable by using lower-dimensional subspaces. This technique was applied to a 6D quadrotor model, though in practice the computed SFE may not be feasible. In [57] it was shown that exploiting the time-scale separation method as a way to alleviate the curse of dimensionality does work, but in practice the faster dynamics showed a theoretically reachable SFE which was impossible to reach due to limitations on rate and pilot bandwidth. As the dynamics of quadrotors are very fast, the suggested method to alleviate the curse of dimensionality may be limited in its applicability.

The reachability analysis was also recently applied to the Unmanned aircraft system Traffic Management (UTM) concept. An efficient and flexible method for UAS highway placement was designed for the use in UTM [58]. Thus one can safely assume that reachability analysis will be part of the future of quadrotors, though not just yet. For now it seems that reachability analysis is still too computationally expensive for on-line application. However the potential exists for it to be used offline, for example as verification/validation method for theories/algorithms against loss-of-control.

# III

A Comparative Approach



# 5

## Data Analysis

To find a Quantitative Loss-Of-Control Definition (QLD) for quadrotors, a definition for Loss-Of-Control (LOC) characteristics of quadrotors was realised by adapting the LOC characteristics of Commercial Air Transport (CAT) to quadrotors. These characteristics were then used in the comparative data analysis that was performed on the datasets of test flights that were obtained from the Open Jet Facility (OJF) (wind tunnel). The results of the comparative data analysis, that was based on the grounded theory approach see Appendix B, were then used to create a theory on what the primary causes and precursors of LOC of quadrotors are, see Chapter 6.

In this chapter firstly the LOC characteristics of quadrotors are presented in Section 5.1. Followed by the data analysis which is split into two parts: The quantitative and qualitative part of the data analysis, which are discussed in Section 5.2 and 5.3 respectively. Finally, in Section 5.4, a discussion on comparisons and phenomena seen in the analysis is presented.

### 5.1. Loss-Of-Control Characteristics of Quadrotors

As the description of the characteristics of LOC of aeroplanes is widely applicable to other vehicles with minor changes, the following description of LOC characteristics of quadrotors was created through its adaptation to quadrotors:

#### Quadrotor Loss-Of-Control Characteristics

**A quadrotor Loss-Of-Control event is characterized by a motion that is, one or more of the following:**

- 1) Outside of static and/or dynamic envelopes
- 2) Characterized by nonlinear effects that degrade handling qualities:
  - i. Overly large responses to small state changes
  - ii. Oscillatory / divergent behaviour
- 3) Results in high angular rates and/or displacements,
- 4) Causes the inability to maintain heading, altitude and/or rotors-level flight within acceptable tracking tolerances.

**Note:** LOC is not necessarily unrecoverable

Figure 5.1: Loss-Of-Control Characteristics of Quadrotors, Adapted from [31]

## 5.2. Quantitative Analysis

The characteristics were used in the comparative data analysis performed on test flights flown with in the Open Jet Facility (OJF), where preliminary categories and groups were created through grouping of similar flights. From the 110 flights that were flown up to wind speeds of 16 m/s, 62 flights crashed, three of which did however not have sufficient data for analysis. The two main groups, that were created from the 59 left over datasets, were the nominal (32) and SRF (27) groups, these groups were then split into translational and vertical flights and finally the SRF groups were further divided based on the rotor state e.g. Left-Back (LB) removed, Right-Back (RB) removed or Idle Rotor (IR).

## 5.3. Qualitative Analysis

Through exploration of the data categories of primary causes and precursors of LOC of quadrotors and their accompanying properties became apparent. Then through comparison of similar incidents, literature and experience categories were integrated and delimited into definite versions. To give an overview of the process of the qualitative data analysis this section was split into three sub-sections, starting out with the exploration of data in Sub-Section 5.3.1, followed by the categories and properties that were found in Sub-Section 5.3.2 and finally the category integration and delimitation in Sub-Section 5.3.3.

### 5.3.1. Exploration of Data

Various preliminary categories were created through exploration, see Sub-Section 5.3.2, these categories provided a good basis for incident comparison. Each preliminary category was taken separately and analysed. Time histories of all on-board variables and wind speeds were explored per incident, compared to other incidents in the same category and grouped if similarities occurred. After all the preliminary categories were analysed, cross-category similarities were sought for and grouped when found. Throughout this process, videos of the incidents and visualisations, such as Figure 5.2, helped in getting a general feel for sub-categories.

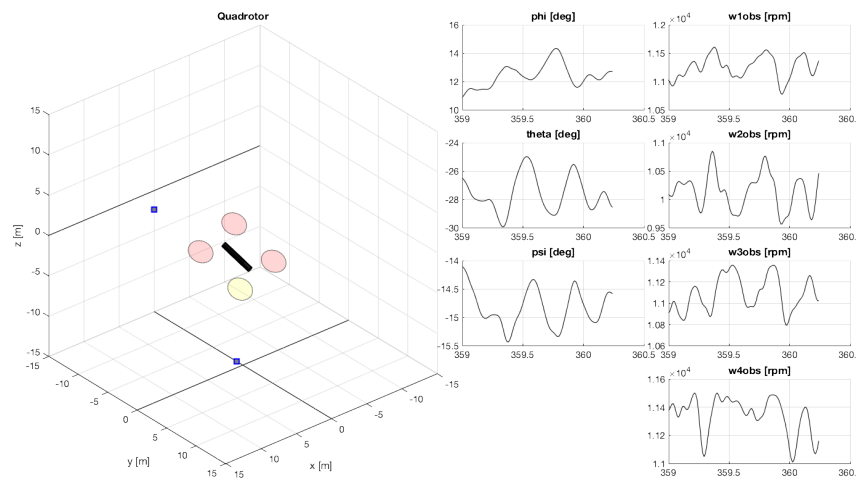


Figure 5.2: Visualisation of a Nominal Quadrotor Actuator Saturation Incident

### 5.3.2. Categories & Properties

The categories and properties were formed through the process of the exploration of the data. Through the analysis of the preliminary categories and the grouping of similar incidents the most frequent events became evident. These are discussed and listed below:

#### – Failure / Malfunction (F/M) During Descent (DD)

This category was seen most during flights in the Single-Rotor Failure (SRF) configuration and never during the flights in nominal configuration. This category is suspected to be caused by the Vortex Ring State (VRS), as that state occurs in descent.

**Properties:** Negative vertical speed, forward speed, angle of attack

- **F/M During Ascent (DA)**  
The opposite of the previous category. This category was sparsely seen, though mostly during the flights in SRF configuration. This category is also suspected to be caused by the VRS, but after recovery.  
*Properties:* Positive vertical speed, forward speed, angle of attack
- **Phi Spike (PS)**  
A spike in the roll angle was seen at the end of a few flights. This was probably caused by the control system trying to recover from an unrecoverable situation and spiking the roll angle.  
*Properties:* Near crash, high  $p$  reference
- **Theta Spike (TS)**  
A spike in the pitch angle was seen close to the end of a few flights. Like the phi spike it was probably caused by the control system trying to recover from an unrecoverable situation. In some cases this spike seemed to be what caused the quadrotor to crash, increasing the angle of attack and thus exposing a greater surface area to the wind.  
*Properties:* Near crash, high  $q$  reference
- **Increasing Oscillation of Acceleration (IO)**  
The increased oscillation of translational, vertical and angular accelerations was seen in translational flight of SRF configuration flights. As the angle of attack of the quadrotor in forward flight is effected by the forward velocity, an increasing wind speed is seen as the main reason for the increase in oscillations.  
*Properties:* Increasing velocity, increasing wobble angle, increasing angle of attack
- **Actuator Saturation (AS)**  
As derived from the reduced model, actuator saturation seems to be one of the major reasons for failures. Furthermore as expected it is positively correlated to the velocity and thus to the angle attack.  
*Properties:* Increasing velocity, angle of attack, rotation speeds
- **High Velocity (HV)**  
High forward velocity, or in the experiments case, high wind speed causes an increase in rotor speeds. This usually leads to actuator saturation and thus ultimately to failure.  
*Properties:* Increased angle of attack, actuator saturation, slow descent
- **Slow Descent (SD)**  
Seen at high velocities, probably caused by the fact that the velocity is too much for the quadrotor to handle. Thus the thrust vector is angled more into the wind and losing height in the process.  
*Properties:* High velocity, angle of attack, close to crash
- **Equipment Failure (EF)**  
Failures due to equipment e.g. battery low and screws loose.  
*Properties:* Equipment not optimal

Note that the VRS was not added to the categories as it was not apparent that the state was active or not. Its indicators were however added to the categories i.e. F/M During Descent, F/M During Ascent and the Phi/Theta Spikes.

### 5.3.3. Category Integration and Delimitation

The integration and delimitation of the categories and their properties started as soon as there were no more categories to be thought of. Furthermore doing experiments and looking at data gave a general feel for which categories were the most important, which were not needed anymore and which could be combined. The distribution of the categories over the flights can be seen in Figure 5.3, where in total 32 nominal configuration flights and 27 SRF configuration flights were examined for LOC events. The acronyms indicate the categories of Sub-Section 5.3.2

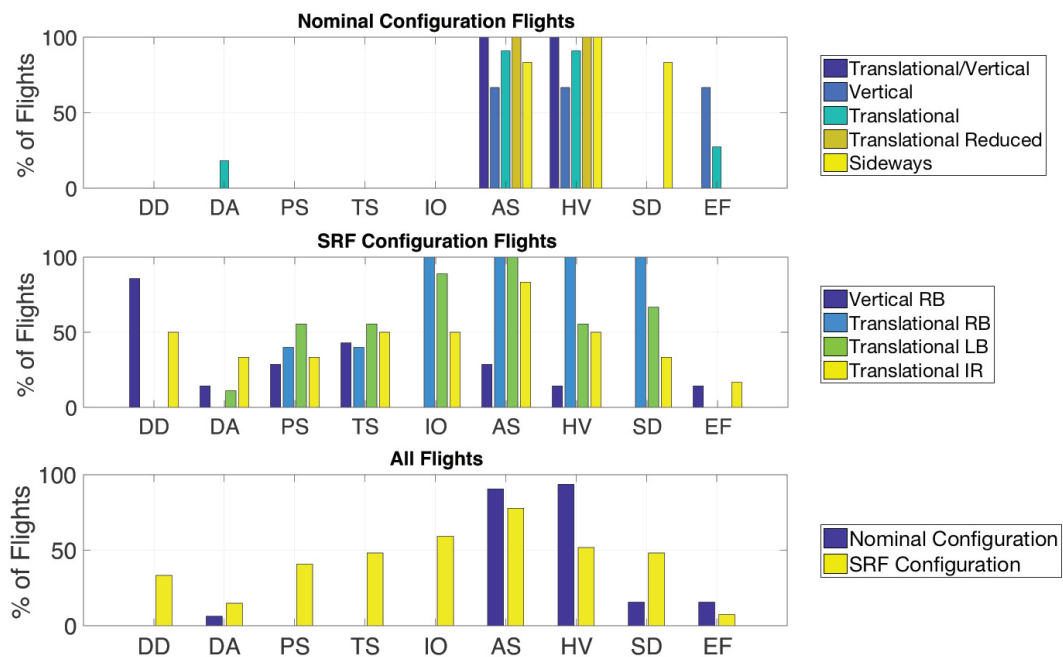


Figure 5.3: Distribution of Categories over flights (32 in Nominal Configuration & 27 in SRF Configuration)

The first four categories, F/M During Descent, F/M During Ascent, Phi Spike and Theta Spike are the indicators of the VRS. They were exclusively seen in the flights in SRF configuration. The expectation was that these categories would also be seen in vertical nominal configuration flights, but none of the flights actually crashed during descent or ascent, though one flight without wind showed some instabilities during descent.

Furthermore the DD category happened more often than the DA category, which should happen as VRS happens due to descent into ones own turbulence, note that the DA category usually occurred right after descent. As these categories are connected through theory and were mostly seen as in combination with each other they were combined into the "Vortex Ring State" category.

The Increasing Oscillation of Accelerations category was also only seen in the SRF configurations, where an increase in wind speed caused an increase in oscillations of the accelerations. As this was not seen in the nominal configuration this oscillation is expected to be caused by the control strategy for quadrotors in SRF configuration [19]. One should note that an increase in wind speed causes an increase in the angle of attack, which was seen in both main groups, however in the SRF configurations it was also seen that due to this increase in angle of attack the oscillation of accelerations increased.

Furthermore blade flapping is directly involved with the oscillations seen in the rotor speeds, this is further explained in Section 5.4. It was observed that due to the control strategy the quadrotor created a Double Blade Flapping (DBF) situation, which could be seen as the cause of the oscillation. Thus the IO category was combined with the HV category into the "Blade Flapping" category.

Actuator Saturation and High Velocity are the categories that were seen the most, thus they are seen as the main causes for quadrotor failures in both the nominal and SRF configurations. Furthermore, the Slow Descent category was seen frequently in combination with the two. What was observed is that due to the high wind speeds the quadrotor needed more thrust, in both the nominal and SRF configurations, to keep hovering in the same position. Thus with higher speeds, higher rotor speeds and more actuator saturation cases were observed. Also slow descents were observed due to the quadrotor needing to tilt its thrust vector into the wind to keep its position. As the HV category can be seen as a cause of other categories it was decided to combine it with the AS and SD categories into the "Actuator Saturation" category.

The final category, Equipment Failure, although not seen that frequently always causes dangerous situations. From empty/broken batteries causing random landing sequences or thrust spikes to actuators breaking causing uncontrolled crashes. Thus it was decided that the "Equipment Failure" category would remain unchanged.

## 5.4. Discussion

It became apparent that, as with the LOC characteristics of CAT, the primary causes and causal contributing factors of LOC of CAT, see Figure 4.3, were also partly applicable to the quadrotor. Except for the abnormal dynamics and vehicle upsets category of the causal and contributing factors, as these are vehicle dependent. Therefore all the comparisons made and phenomena seen, discussed in this section, are expected to be within the "abnormal dynamics and vehicle upsets" category. The section is structured as follows: Firstly the phenomenon of DBF is discussed in Sub-Section 5.4.1. Then the discussion on aerodynamic interaction of the rotors of the quadrotor is shown in Sub-Section 5.4.2. Finally the comparison between removed rotors and idle rotors is presented in Sub-Section 5.4.3.

### 5.4.1. (Double) Blade Flapping

Blade flapping is a phenomenon which is seen in helicopter operations during translational flight, where the advancing side of the rotor disk sees a higher effective velocity with respect to the air, whereas the retreating side of the rotor disk sees a lower effective velocity. This difference creates an offset in lift between the two halves and thus effectively flaps the blades up and down once per revolution [59]. Helicopters counter this effect by changing the angle of attack of their blades with the position in the rotor cycle, though this eventually leads to retreating blade stall [43]. Quadrotors in general do not have variable pitch propellers, though a prototype with such propellers is currently being studied [7].

As the quadrotor uses more than one rotor it has advantages over helicopters with respect to blade flapping. Due to the symmetry of the quadrotor, the lateral effects of blade flapping are cancelled, but in longitudinal direction the plane of the rotor disk is tilted away from the direction of motion, see Figure 5.4, where the movement is into the wind. Due to the tilt of the rotor disk the translational movement is damped and the effective upwards thrust is lowered. In [60] various models for blade flapping are suggested, with various outcomes. In Figure 5.4 a stiff blade modeled as hinged blade can be seen, this model [61] over predicted the experimental results shown, but does give a good visual representation of the phenomenon. Overall, the authors saw a decrease in hover thrust of a few percent and a decrease in attitude tracking of a few degrees due to torque resulting from blade flapping, which were seen as significant effects on the control of quadrotors.

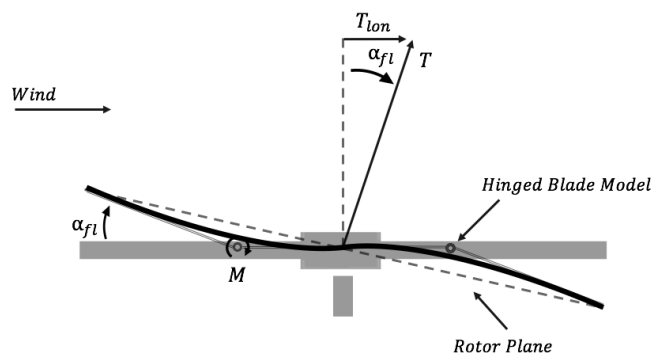


Figure 5.4: Blade Flapping in the Nominal Case

As the flapping angle was not measured during flight, the influence on the thrust remains unknown for the nominal configuration. However the flights in SRF configuration showed an interesting phenomenon. The commanded and observed rotor speeds of the quadrotor were oscillating with the location of the rotor in the yaw plane. It was observed that a second rotation plane was created due to the quadrotor spinning around its own axis, see Figure 5.5, where the plots show the rotor speeds of each respective rotor over a single flight. The red and blue half circles indicate the phase of the yaw of the quadrotor in which the respective rotor is in the advancing side (red) and retreating side (blue) respectfully. Finally the black lines show the direction of the incoming wind.

A rotor in the right half of the rotation plane would have more effective velocity than in the nominal configuration due to the quadrotor spinning about the primary axis. Consequently, a rotor in the left half plane would have less effective velocity, thus causing a rolling moment due to the offset in thrust produced. This rolling tendency was not observed in the experiments, this lack of observation was theorized to be caused by the control system changing the rotation speeds of each individual rotor based on their location within the rotation plane, which can be seen in the figures.

The figure shows that the rotor opposite to the removed rotor, where the minimum rotation speed was hard-coded to be 3000 Rotations Per Minute (rpm), is commanded to counter the rolling moment through increasing the rotation speed of the rotor in the retreating side and decreasing the rotation speed of the rotor in the advancing side. This phenomenon, named Double Blade Flapping, was observed in multiple flights where it was always the rotor opposite to the removed rotor that showed the behaviour described above.

The behaviour seen in the two (working) rotors opposite of each other also showed similar behaviours in multiple flights, where the rotor speeds would be observed to be identical. This difference in expected behaviour could have multiple sources e.g. wobbling angle, symmetry, translational velocity and the aerodynamic moments due to the different planes of the rotors and the centre of gravity. Thus this phenomenon should be further investigated by for example examining the rotor speeds of the rotors in a double rotor failure case.

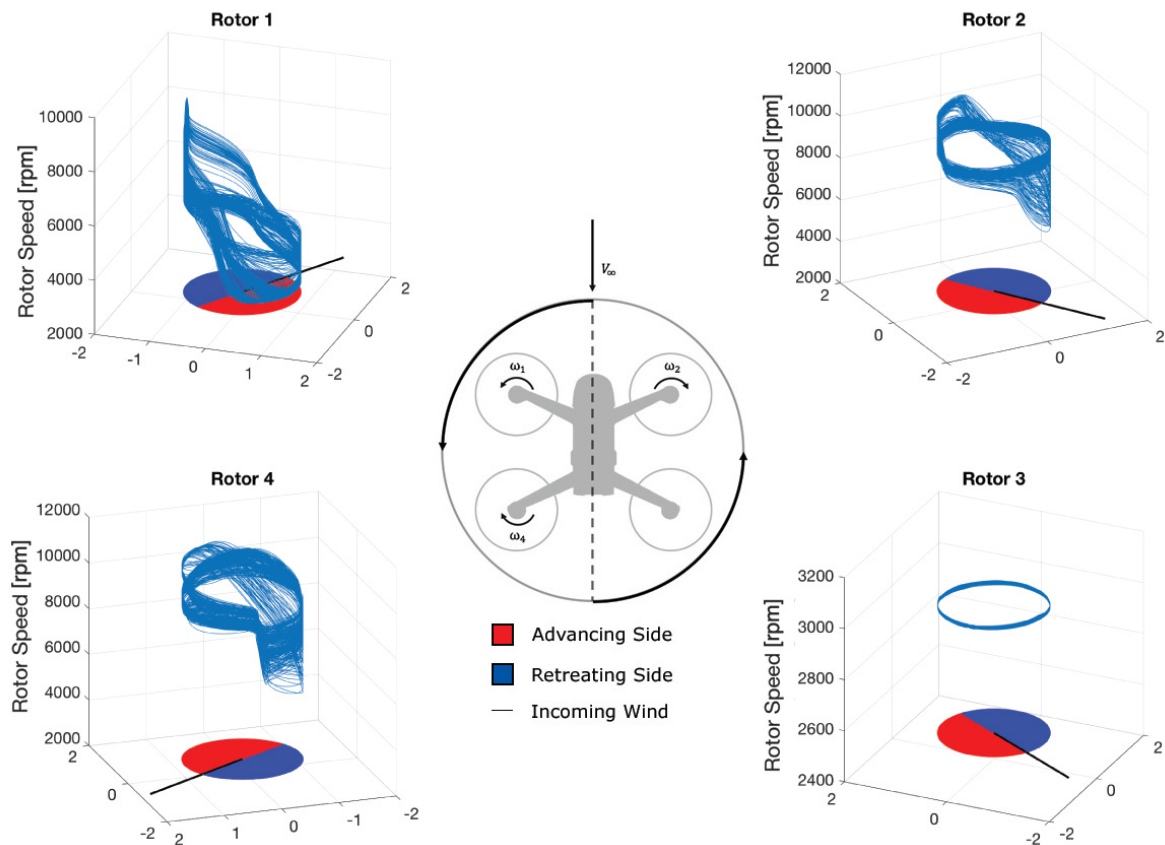


Figure 5.5: Double Blade Flapping

#### 5.4.2. Aerodynamic Interaction of the Rotors

What was observed from the flights in nominal configuration, flown in the OJF, is that the back rotors on average had higher rotation rates than the front two rotors. This observation was confirmed by a recent study regarding the aerodynamics of quadrotors [62]. The two possible configurations, with respect to rotor turning direction, were compared using a higher-order potential flow method. The two configurations can be seen in Figure 5.6, where the 'bear hug' (a) configuration has front rotors which envelope the wind in a 'hug' and the 'breast stroke' (b) configuration has front rotors which rotate in a motion such as a swimmer doing breaststroke. Furthermore a diamond flying configuration was also tested, where instead of flying with two rotors in front the quadrotor would fly with one rotor in front. Thus creating a different downstream turbulence pattern.

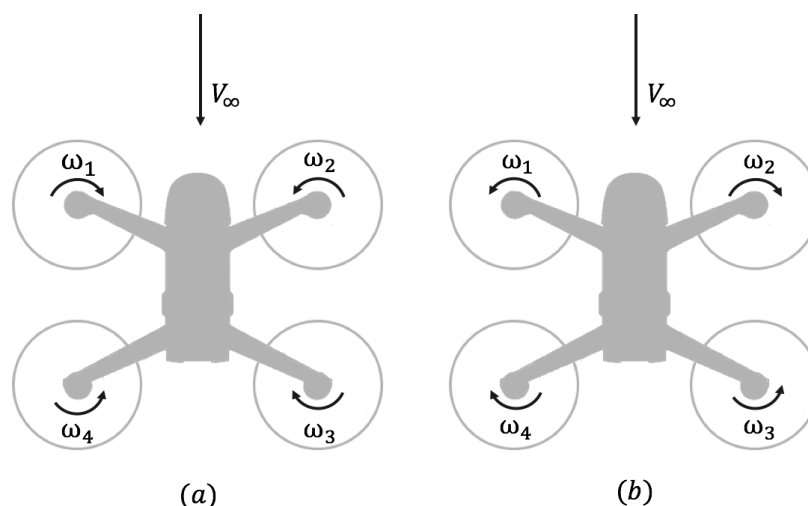


Figure 5.6: Possible Rotation Configurations for Quadrotors

Results show that the front rotors in both configurations provided equal thrust and that the back rotors produced less thrust than the front. There was however a difference in thrust produced by the back rotors due to the configuration. The 'breaststroke' rear rotors experienced higher upwash than the 'bear hug' rear rotors, though this seemed to not have a significant contribution to overall thrust. Due to the distribution of the induced velocity the 'bear hug' configuration actually had more effective thrust than the 'breaststroke'. The 'bear hug' had a higher induced velocity on the advancing side of the rear rotors due to cross-rotor interactions, where the 'breaststroke' configuration had a higher induced velocity on the retreating side of the rear rotors. Therefore the 'breaststroke' configuration had less of a tendency to pitch up, thus less need for trim. With less trim, less power in is needed for stability, thus the conclusion was made that the 'breaststroke' configuration was preferable. A quadrotor also be flown with a different side forward to preserve energy, though this could have mixed effects due to drag effects of the main body.

Flying in diamond configuration showed similar but mirrored results for clockwise and counter-clockwise rotating rotors in front. The clockwise rotor had an increased vorticity density in the wake of the second rotor, assuming the configuration in Figure 5.6 (a) with rotor one in front. Consequently the second rotor produced a higher thrust thus a tendency to roll in the positive direction. With the counter-clockwise rotating rotor in front the exact opposite happened. Thus flying in an asymmetrical rotating rotor configuration causes a tendency for instability, though this could also have been caused by blade flapping. Furthermore the effect on the rear rotor was not discussed, as it is directly in the wakes of all the other rotors it would be expected that it would perform badly.

This interaction between rotors was more apparent in the flights with reduced rotors. In all flights with (front/back) reduced rotors the first rotors to saturate were the reduced ones. Where the average rotor speeds of the other rotors, just before crashing, were higher in the case where the front rotors were reduced. As such the conclusion was made that damaged rotors are less efficient than nominal rotors and thus need a higher rotation speed to produce the same amount of thrust. Furthermore the rotors in the front are more efficient than the ones in the back, as they are in laminar flow. Thus, in case the rotors of a quadrotor are damaged during flight, it is best to make it fly with those rotors in front.

### 5.4.3. Removed/Idle Rotors

During the experiments different configurations of the quadrotor in SRF configuration were tested e.g. right back rotor removed, left back rotor removed and idle rotors. The difference observed between these configurations was that the idle rotors were forced to rotate at 3000 rpm due to a hardcoded minimum limit. Thus creating thrust in idle mode, where the removed rotors did not produce any thrust. This thrust, though minimal, caused different thrust patterns in the rotors adjacent to the 'failed' rotor, in comparison to the thrust patterns of the removed rotors. The difference between removing the right back and left back rotor was that the rotor thrust patterns of the two front rotors flipped. The rotor opposite to the removed rotor would show the exact DBF pattern, where the rotor speed of that rotor would be sped up in the retreating side of the rotation and vice versa.



# 6

## Theory Generation

This chapter contains the theory generated through the dynamic model limit analysis, qualitative analysis and the discussion of the analysis. With regards to the constant comparative method of qualitative analysis it can be compared to the final step [63]. The chapter is structured as follows: firstly the primary causes of Loss-Of-Control (LOC) events are discussed in Section 6.1, then events that are considered to be precursors to the primary causes are presented in Section 6.2.

### 6.1. Primary Causes of Loss-Of-Control

Through the adaptation of the LOC characteristics of Commercial Air Transport (CAT) [31] to the quadrotor, LOC characteristics for quadrotors were created, see Section 5.1. As the LOC characteristics of CAT were easily applicable to quadrotors, the primary causes and the causal and contributing factors to LOC of CAT were also adapted to the quadrotor. In this adaptation the difference between the two vehicles turned out to be the dynamics and the vehicle specific problems e.g. actuator failure. Through the dynamic model limit analysis, in Section 3.2, the qualitative data analysis in Section 5.2 and the phenomena seen and comparisons made in the discussion, Section 5.4, it became quite clear that the factor that had the most influence on quadrotor LOC events was the rotation speed limitations of the actuator. Thus in comparison with the multiple vehicle upset conditions of aircraft, the quadrotor only had one. The following theory was defined:

The primary causes to quadrotor LOC events are:

1. Entry into the vehicle upset condition: **actuator saturation**
2. Reduction or loss of control effectiveness
3. Changes to vehicle dynamic response and handling / flying qualities
4. A combination of the above

### Loss-Of-Control Variables

Traditionally the time history analysis has been used for the investigation of accidents and incidents, but more recent studies [30] [64] have shown that the parametric approach, where variables are mapped against each other can show interesting insights. Thus, the following parameters have been defined to be the most influential with regards to LOC of quadrotors:

$V$ , airspeed  
 $\alpha$ , angle of attack  
 $\omega_i$ , rotation rate of rotor  $i$

$D$ , diameter of rotor  
 $p$ , roll rate  
 $q$ , pitch rate

## 6.2. Precursor Events

Precursor events are seen as the events that lead to the primary causes of LOC events. All the precursors that will be discussed in this section were the cause for an increase in rotor Rotations Per Minute (rpm) and thus a direct cause to actuator saturation. Firstly the Vortex Ring State (VRS) is examined in Sub-Section 6.2.1, then blade flapping is discussed in Sub-Section 6.2.2, the aerodynamic interaction of the rotors with each other is then discussed in Sub-section 6.2.3 and finally the various cases of equipment failure are discussed in Sub-Section 6.2.4.

### 6.2.1. Vortex Ring State

The VRS causes not only a loss of thrust, but also a higher fluctuation in produced thrust [64]. From the flights performed in the Open Jet Facility (OJF) there were several suspected cases for the Single-Rotor Failure (SRF) configuration flights and a singular case for the nominal configuration flights. In both the SRF and the nominal configuration, the fluctuation in thrust and loss in thrust cause the control system to increase the commanded rotor speeds thus in some cases causing rotor saturations. Note that the speed of the controller in this case is important as different thrust fluctuations on the rotors might cause instabilities.

### 6.2.2. Blade Flapping

As blade flapping is different for nominal and SRF configurations, as seen in Sub-Section 5.4.1, they are seen as two different types of precursor events.

#### Nominal Case:

Blade flapping tilts the rotor plane, and thus the thrust vector, backwards in the opposite direction of the wind or flight direction. This makes flying in any translational direction less efficient than hovering. If a certain speed in a translational direction is commanded there are two options: (1) the thrust vector is tilted even more into the desired direction and (2) the thrust vector is increased to increase the horizontal vector. In both cases the thrust vector needs to be increased to prevent height loss, thus a higher rotation speed is needed, which finally results in actuator saturation.

#### Single-Rotor Failure:

As with the nominal configuration the rotor plane is tilted backwards, but as the control strategy is to spin around a primary axis [17] the induced velocity is different for each rotor based on the orientation of the quadrotor with respect to the wind.

Looking from behind the quadrotor, the right half plane of the rotation plane has an increased induced velocity and thus will have higher thrust for the same rotation rates. Therefore the rotation rates on that side of the quadrotor need to be decreased, or the rotation rates of the other side need to be increased to offset the roll angle that is otherwise created. Results (Sub-Section 5.4.1) show that this expected counter measure indeed happens for the rotor opposite to the failed rotor.

However the average rotor speeds of the remaining rotors are generally higher than that rotor, thus those rotors are expected to saturate first. Note that the primary-axis can be pointed in the direction of the single rotor, this increases the wobbling angle of the quadrotor and lowers the thrust needed from the pair of rotors thus lowering their rotor speeds. This does also influence the size of the surface of the quadrotor that is subjected to the incoming wind. Furthermore one should note that there is a limit to how much thrust can be 'offset' to the single rotor.

### 6.2.3. Aerodynamic Interaction of the Rotors

From experiment results and literature [62] it was observed that the back rotors of a quadrotor are effected by the turbulence of the front rotors, thus making them less efficient. This effect was even more pronounced in the flights where reduced rotors were used. In both cases the effectiveness of the rotors was lowered and thus a higher rotation velocity was observed for stable flight. These higher rotation velocities eventually, like the other precursor events, lead to actuator saturation and thus LOC events.

#### **6.2.4. Equipment Failure**

Unlike with CAT, an equipment failure during quadrotor flight results in a near immediate crash. As the dynamics of a quadrotor are much faster than traditional aircraft, low batteries, loose screws, failed actuators, etc, drastically change the control effectiveness and the dynamic responses of a quadrotor. Take for example a rotor failure experiment performed in the OJF, in which the goal was to see how fast a quadrotor would need to detect a fault and configure the system to accommodate for it, the delay between the switch of control systems was determined to be between 0.1 and 0.15 seconds for a recovery. Note however that this time could be increased by flying at a higher altitude. Thus equipment failure has, for now, not been classified as a primary cause to LOC events. Furthermore, it should be split up in different sub-categories as the range of equipment failures observed, was found to be diverse.

The special case of equipment failure: rotor failure, could potentially be added to the upset conditions of quadrotors, as research is headed towards the recovery of rotor failures during flight. As it has already been proven that it is perfectly possible to fly with one or two missing/broken rotors in [17], the rotor failure case should be added to the upset conditions as soon as the speed for the detection and configuration of the control system for actuator/rotor faults has been solved.



# IV

Validation Through  
Experimentation



# 7

## Rotor Thrust Experiment

From the data analysis, Chapter 5, and literature it has become clear that actuators in combination with their rotors are the limiting factor on capabilities of quadrotors. Therefore an experiment was performed in the Open Jet Facility (OJF) to create a model for a single Bebop 2 actuator with a rotor. This chapter describes the experiment and the obtained model, structured as follows: Firstly the experiment is discussed in Section 7.1, then the thrust model is presented in Section 7.2 and finally a discussion regarding the validation results is provided in Section 7.3.

### 7.1. The Experiment

The experiment was designed to measure the thrust produced by the actuator and accompanying rotor under all possible flight circumstances. The variables that were measured are discussed in Sub-Section 7.1.1 and the data acquisition systems are shown in Sub-Section 7.1.2.

#### 7.1.1. Measured Variables

The measured variables, in the experiment were the following:

- **The Angle of Attack,  $\alpha$ :**  
Defined as seen in Fig. 7.1. To measure all flight circumstances the thrust was measured over a range of 0 to 90 degrees for both positive (upwards) and negative (downwards) velocities.
- **The Advance Ratio,  $J$ :**  
A ratio used for propellers in aeronautics and hydrodynamics to show the ratio between the free stream fluid speed and the propeller. Where the velocity is defined positive in upwards motion and negative in downwards motion.

$$J = \frac{\vec{V}}{n \cdot D} \quad (7.1)$$

Where  $\vec{V}$  is the total velocity vector,  $n$  is defined as the rotation rate of the rotors in rotations per second and  $D$  is defined as the rotor diameter in meters.

- **The Thrust Coefficient,  $C_t$ :**  
The dimensionless coefficient of the thrust produced by the rotor.

$$C_t = \frac{T}{\rho n^2 D^4} \quad (7.2)$$

Where  $T$  is defined as the thrust,  $\rho$  is defined as the density of air, assumed to be  $1.225 \text{ kg/m}^3$  for this experiment, and  $n$  and  $D$  are defined as in Equation 7.1.

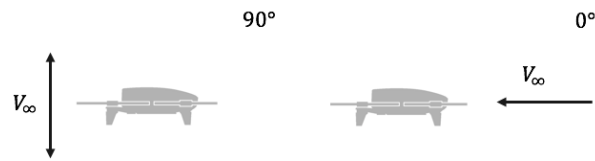


Figure 7.1: The Angle of Attack

### 7.1.2. Data Acquisition Systems

For the acquisition of the data, the dynamometer series 1580 of RcBenchmark was used, see Figure 7.2. Using the software of RcBenchmark.com the thrust and the rotation speeds were measured with a frequency of 10 Hz. Finally the wind was extracted from the computer system of the OJF.

For each test run the angle of attack and the velocity were kept constant, while the rotor was varied over rotational values of 3,000 to 12,000 Rotations Per Minute (rpm) in increments of 1000. For each rotational value 50 data points were acquired, leading to 500 data points per run. The angle of attack was then varied from 0 to 90 degrees in increments of 10 degrees and the velocity was varied from 0 to 14 m/s in increments of 2 m/s. Note that to achieve descending flight without influence of dynamometer, the rotation direction and the rotor were both flipped to measure the thrust produced in descending flight.

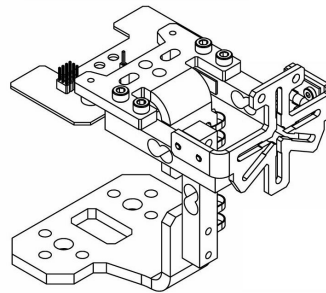


Figure 7.2: Dynamometer Series 1580 [65]

## 7.2. Rotor Thrust Model

The actuator and rotor were tested for 1600 points, where each point had 50 thrust measurements. For each point the thrust was then taken to be the average of the 50 points. By taking 50 measurements per point the expected thrust fluctuations could be identified per point [64], thus indicating certain areas of the flight regime to be less stable than others. This section will be structured as follows: firstly a discussion on influences on the measurements in Sub-section 7.2.1. Then an explanation of how the data points were fit is given in Sub-section 7.2.2, the multivariate spline fit is validated in Sub-Section 7.2.3 and finally the model is validated in Sub-Section 7.2.4.

### 7.2.1. Measurement Influences

As the thrust stand was close to the rotor itself, and would also be effected by the incoming wind, a slight influence was to be expected. Therefore all the measurements were taken after setting all values to zero on the device (tare), this however would also remove the influence of the rotor itself, therefore extra measurements were made without setting the values to zero on the device. Furthermore the thrust stand was tested separately to test its influence. Following those measurements, the following assumptions were made:

$$F_{notare} = F_{tare} + F_{static} \quad (7.3)$$

$$F_{real} = -F_{notare} + F_{testbench} \quad (7.4)$$

Where  $F_{static}$  equals all the static forces:

$$F_{static} = F_{testbench} + F_{rotor} \quad (7.5)$$

Furthermore, note that  $F_{notare}$  in Equation 7.4 has flipped signs for the descending tests. The comparison of the data with the above assumptions can be seen in Figure 7.3. Where the 'approx' indicates that the assumptions (equations) were used, and the 'Real notare' and 'Real tare' indicate the measured non-tared and tared data respectively. For zero degrees, perpendicular to the wind tunnel, there was hardly any difference between the non-tared approximate (Equation 7.3) or the actual non-tared measurement, but the higher the angle of attack the bigger the difference became, where the non-tared measurement showed higher values of thrust. From the figure one can see that 'Freal approx' and the 'Real nocali' were similar for higher angle of attack values. As preliminary results showed lower thrust values than the flight data, the decision was made to use the non-tared measurement.

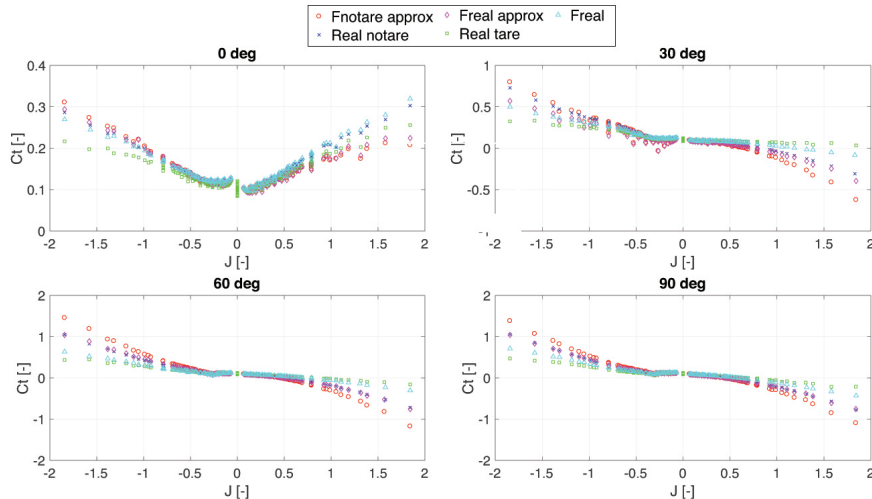


Figure 7.3: Assumptions for the Influence of the Thrust Stand at 90 Degrees

### 7.2.2. Fitting Data

To fit the obtained data multivariate splines were used. As the density of data points along the angles of attack were lower than the density of the data points along the advance ratio the data along constant advance ratio values were fitted with 1<sup>st</sup> order polynomials to counter the behaviour of multivariate splines along low data density points.

As the centre of the dataset had more dynamics, different triangulation densities were tested. The final triangulation was made with 1-simplices on a constant field of 10 points along the angle of attack, each corresponding to 10 degrees. Along  $J$  a different triangulation was used where the advance ratio was split into three sections, with two, eight and two simplices each. Thus in total creating 216 simplices. In Figure 7.4 the triangulation can be seen, with the final thrust model, which used 5<sup>th</sup> order polynomials over each simplex with 0<sup>th</sup> order continuity ( $S_0^5$ ).

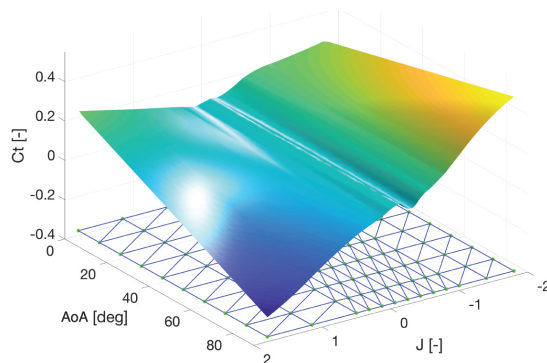


Figure 7.4: Multivariate Splines Triangulation and Thrust Model

### 7.2.3. Validation of Data Fit

To validate the fit of the thrust model the variance of the B-coefficients was examined, furthermore a residual quality analysis was performed. Firstly the dataset was split in two separate data sets: the identification dataset and the validation dataset. Every other data point was assigned to the other dataset such that both contained 50 % of the data points, note that every 10 points the order was switched. The identification dataset was then used to identify the model and this model was then tested with the validation dataset.

In Table 7.1 one can see the effects on model quality based on different amounts and distributions of simplices, polynomial orders ( $d$ ) and continuity orders ( $r$ ). The measures used to indicate the quality of the model are the Root Mean Square (RMS) error, the relative RMS error, and the B-Coefficient variance, where the relative RMS error and B-Coefficient variance are defined as:

$$RMS_{rel}(\epsilon) = \frac{RMS(\epsilon)}{RMS(Y)} \quad (7.6)$$

$$B_{var} = Cov(\hat{c}) \quad (7.7)$$

Where  $\epsilon$  is the error,  $\hat{c}$  is the Ordinary Least Squares (OLS) estimator of the B-coefficients and  $Y$  is the validation model.

$S_r^d$	$n_{simp.}$	$n_{J_{dist}}$	$RMS(\epsilon)$	$RMS_{rel}(\epsilon)$	Average $B_{var}$
$S_0^1$	108	[1 4 1]	0.0054	2.86 %	0.0034
$S_0^3$	108	[1 4 1]	0.0008	0.42 %	0.0014
$S_0^5$	108	[1 4 1]	0.0004	0.19 %	0.0011
$S_0^7$	108	[1 4 1]	0.0002	0.10 %	0.0020
$S_1^2$	144	[2 4 2]	0.1024	53.70%	0.0097
$S_1^3$	144	[2 4 2]	0.0062	3.24 %	0.0012
$S_1^4$	144	[2 4 2]	0.0033	1.74 %	0.0010
$S_1^5$	144	[2 4 2]	0.0014	0.74 %	0.0010
$S_1^6$	144	[2 4 2]	0.0009	0.46 %	0.0011
$S_1^7$	144	[2 4 2]	0.0005	0.25 %	0.0039
$S_0^1$	216	[2 8 2]	0.0023	1.22 %	0.0010
$S_0^3$	216	[2 8 2]	0.0003	0.16 %	0.0004
$S_0^5$	216	[2 8 2]	0.0001	0.06 %	0.0003
$S_0^7$	216	[2 8 2]	0.0000	0.02 %	0.0138

Table 7.1: Model Quality Results

### 7.2.4. Validation of the Model

To validate the model, it was compared to flight data. An external motion capture system (Optitrack), was used to obtain the velocity of the quadrotor. The velocity per rotor was determined through Eq. 7.8, where  $\vec{\Omega}$  is the rotation velocity vector consistent of p, q and r,  $\vec{r}_i$  indicates the location of the  $i^{th}$  rotor w.r.t. the centre of gravity and  $\vec{V}_{tot}$  is the total velocity of the quadrotor.

$$\vec{V}_i = \vec{\Omega} \times \vec{r}_i + \vec{V} \quad (7.8)$$

The thrust coefficient, advance ratio and angle of attack were determined through their definitions given in Sub-Section 7.1.1 (Eqs. 7.1 and 7.2). Where the thrust was determined through Newton's first law and the local velocity and rotor speeds were used to determine the  $C_t$  values per rotor.

In Figure 7.5 the comparison between the flight data and the model data can be seen, where the dataset is split up in four manoeuvres : (1) vertical manoeuver, (2) transverse manoeuver, (3) longitudinal manoeuver and (4) yaw changes while holding position. Where manoeuvres (1) & (2) were performed at yaw angles of 0 to 90 degrees. To compare the  $C_t$  value of the whole quadrotor to the data obtained from the model both sets were z-normalised, thus the datasets indicate the standard deviations with respect to the mean of the respective set. Note that the model data was multiplied by 1.3 to obtain the result seen in the figure.

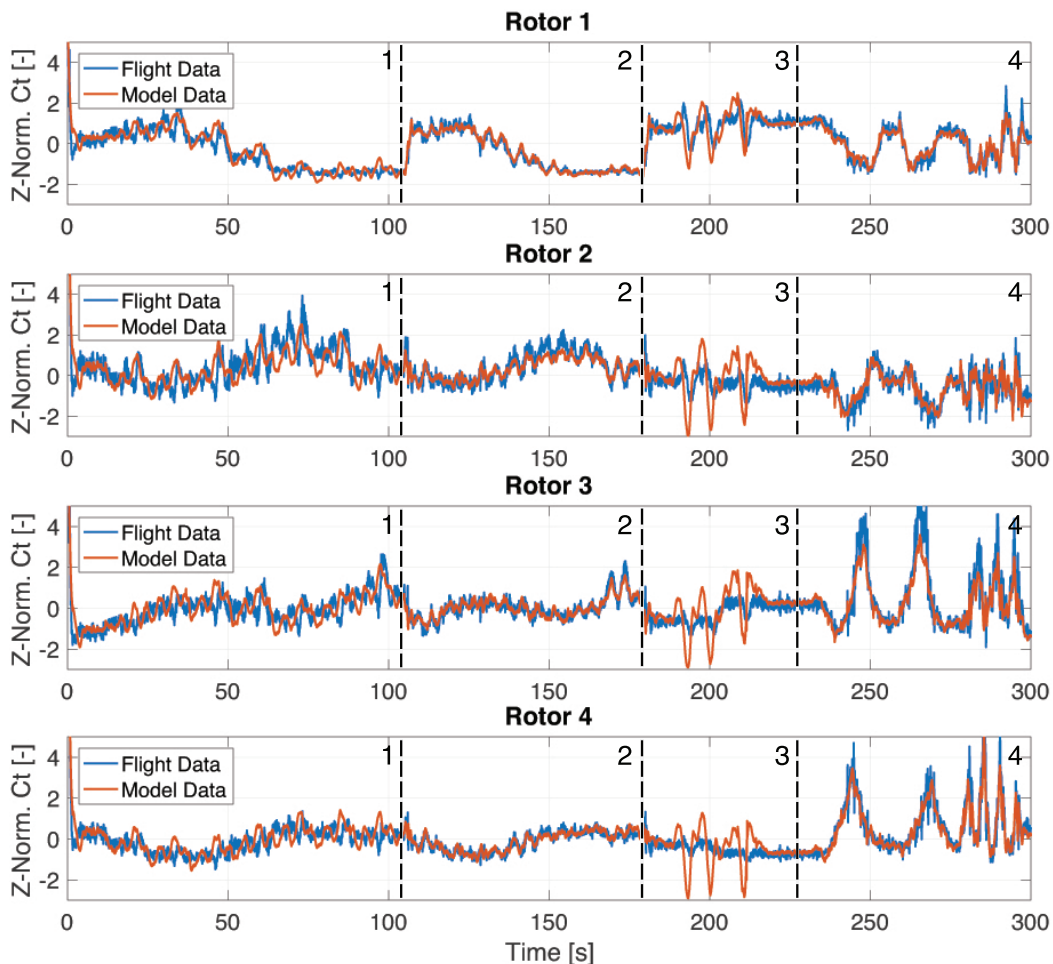


Figure 7.5: Z-Normalised Nominal Configuration Flight Data & Model Data,  $V = 8$  m/s

### 7.3. Discussion

From the model quality results, see Table 7.1, the  $S_0^5$  model was chosen because of its lowest average B-coefficient variance. With lower average b-coefficients variance there are less inadequate local data coverages/conditionings and/or incorrect model structures. From the comparison, Figure 7.5, it can be seen that the dynamics of the model are similar to those of the flight data, except for dynamics in the longitudinal manoeuvre. This difference is theorized to be caused by rotor speed and velocity inaccuracies during forward flight. Furthermore the thrust magnitude was not similar as the model data was multiplied by 1.3. This thrust difference is theorized to come from several factors:

- **The lift produced from the body of the quadrotor**

The lift was not taken into account in the model. It was separately tested through strapping the quadrotor to the thrust stand. As this experiment was not prepared before hand and involved improvisation of tools at hand, it was not added to the model. What was however seen is that the body of the quadrotor did indeed produce lift.

– **The actuator being directly attached to the thrust stand**

The small rotor was in close proximity to the thrust stand, thus the output was affected by the thrust stand. A difference in thrust output was observed for tests in ascending and descending flights in zero wind speed conditions.

– **The quality of the rotor**

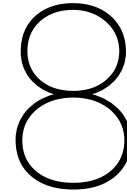
New rotors from the same batch, which were expected to be the same, produced different thrust values for the same commands and flight conditions.

– **A bias in the accelerometer data**

A bias in the accelerometer data could cause a constant offset.

As the thrust model was meant to be used as an indication for Loss-Of-Control (LOC) areas in the flight regime of a quadrotor, validation of the dynamics of the model were considered to be sufficient. The validation results showed that the dynamics of the model showed similarities to those of the quadrotor, therefore the model was considered to be validated. With the dynamics validated the model could be used to find and validate the (un)stable areas in the flight regime of the quadrotor.

For use of thrust model in for example Safe Flight Envelopes (SFEs) or simulation, the thrust difference should be identified. Thus more experiments should be performed to quantify this difference. One could for example design an experiment to measure the forces and moments of a rotor in the same flight regime as the experiments that were performed. This data could also be used to quantify the effect of blade flapping and the aerodynamics caused by the offset of the rotor plane and the centre of gravity plane.



# Theory Validation

In this chapter the primary causes for Loss-Of-Control (LOC) events and precursors as seen in Chapter 6 are validated through confirming their influence over the thrust values on the single rotor thrust model. Firstly the precursors are discussed, with the Vortex Ring State (VRS) in Section 8.1 and blade flapping in 8.2. Finally the primary cause for LOC of quadrotors: rotor saturation is discussed in Section 8.3. As the model was created for a single rotor, the aerodynamic influences of rotors on each other will not be discussed.

## 8.1. Vortex Ring State

From multiple sources the VRS is seen as one of the regimes where the momentum theory fails, as it is essentially the state in the flight regime where the wind flow is reversed in direction. In this unstable flight regime, the thrust produced is expected to be fluctuating [64]. For further explanation of the VRS state one is referred to Appendix A.

### 8.1.1. Thrust Variation

To find the thrust variation over the flight regime of the actuator the 50 measurements per data point were used. The minimum and maximum values per data point were obtained and their difference was taken as variation. The variation was obtained for all the data points of the thrust model and can be seen in Figure 7.4.

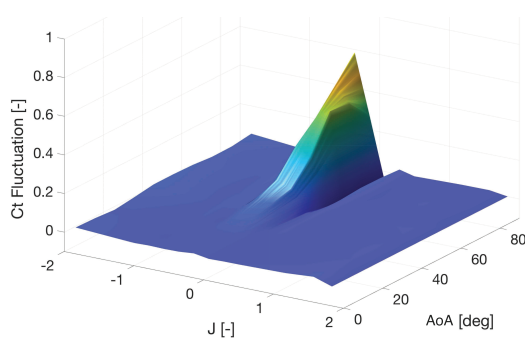


Figure 8.1: Thrust Model, Maximum  $C_t$  Fluctuation

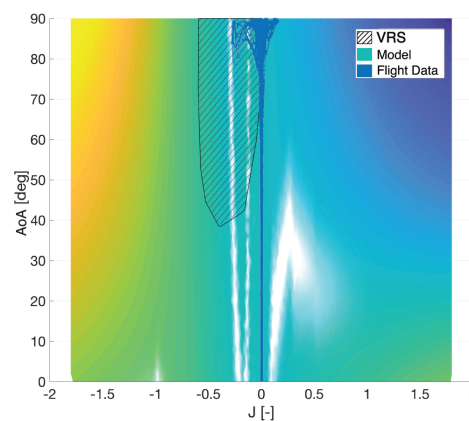


Figure 8.2: Thrust Fluctuation on Thrust Model

One can see that the thrust only fluctuates in a single area in the flight regime. The thrust fluctuations experienced in that area are in the range of  $\pm 20\%$  of the average thrust experienced in the model. Furthermore it can be seen that for higher angles of attack the fluctuation is highest. When the area is plotted over the thrust model, see Figure 8.2, one can see that this area actually corresponds to the dip in thrust coefficient that is observed around an advance ratio of  $-0.3$ , see Figure 7.4. Note that the indicated area shows the area of the flight regime that sees fluctuations of more than 3% thrust fluctuation.

As the location of the dip in thrust, with respect to the thrust model, and the observed fluctuation of thrust values were what was expected from literature, this area is seen as the area of the flight regime where one encounters the Vortex Ring State. Thus one can conclude from the Figure 8.2, that when descending it is best to have some translational velocity, to minimize thrust fluctuation. In amateur flight, translational movement is also known as a way to counter the "Wobble of Death".

### 8.1.2. A Flight in the Vortex Ring State

A single flight, in nominal configuration, was flown with the intention to maximize descent velocity with minimum forward speed. During the experiment the only indication of the expected instability that was seen, was a slight wobble when stabilizing after dropping from maximum height. Therefore the assumption was made that the descent velocity was not high enough to reach the VRS.

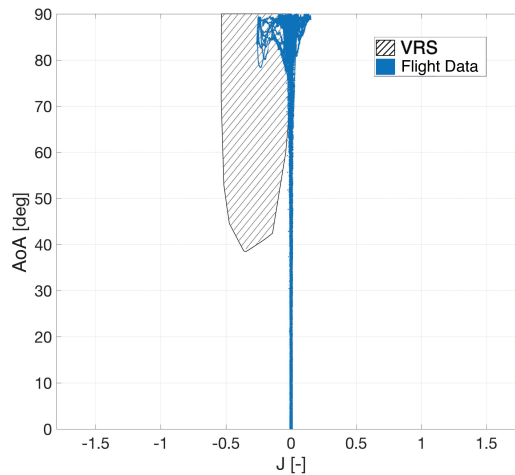


Figure 8.3: A Flight in the Vortex Ring State

The flight of the quadrotor in VRS was projected over the thrust model, see Figure 8.3. From the figure one can see that according to the model the VRS was reached. Contrary to the assumption made, the descent velocity was high enough. The area with the highest thrust fluctuation was even reached, which corresponds to  $\pm 20\%$ . However, when looking at the time history of the manoeuvre that reached the highest thrust fluctuation area, Figure 8.4, a thrust reference error of 1.5 % was reached, where overall in the flight the reference error fluctuated between  $\pm 0.25\%$ . The thrust error was observed in the VRS area, though a more significant thrust fluctuation was expected. This could be caused by various factors such as time in descent, influence of the control system and sudden side winds, which are frequently discussed in the amateur scene. For further validation, more experiments should be performed in the heart of the VRS area, possibly from higher heights.

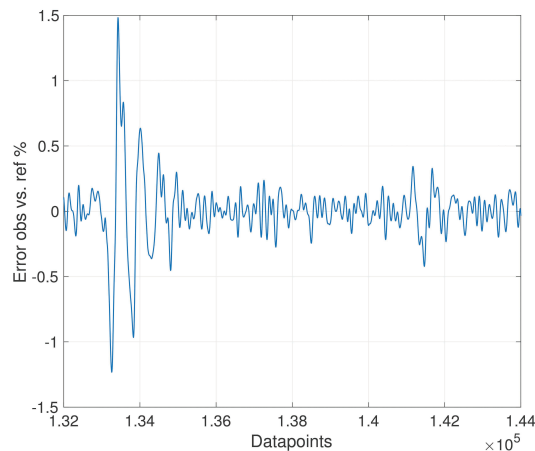


Figure 8.4: Percentage Thrust Reference Error, Rotor One

## 8.2. Blade Flapping

As there were no sensors to measure the moment around the actuator hub or the longitudinal thrust, it was not possible to directly extract the flapping angles through direct measurements. In order to investigate the effect of blade flapping on the quadrotor performance, a model was used to estimate the blade flapping angle. The hinged blade model suggested in [61] was used, shown in Equation 8.1:

$$\alpha_{fl} = \frac{1}{1 + \frac{\mu_{lon}^2}{2}} \frac{4}{3} \left( \frac{C_t}{\sigma} \frac{2}{3} \frac{\mu_{lon} \gamma}{a_0} + \mu_{lon} \right) \quad (8.1)$$

Where  $a_0$  is the lift curve per radian, which is approximately equal to 6.0 for conventional airfoils at low Mach numbers [59].  $\mu_{lon}$  is defined as the longitudinal velocity to tip speed ratio, see Equation 8.2,  $\sigma$  is defined as the solidity ratio, which is essentially the area of the rotor surface covered by rotor blades, see Equation 8.3 and  $\gamma$  is the non-dimensional Lock number, which gives the ratio between aerodynamic and centrifugal forces and can be seen in Equation 8.4, where  $I_b$  is the moment of inertia of the blade about the hinge and  $c$  is the chord of a blade.

$$\mu_{lon} = \frac{v_{lon}}{v_t} \quad (8.2)$$

$$\sigma = \frac{A_b}{A} \quad (8.3)$$

$$\gamma = \frac{\rho a_0 c R^4}{I_b} \quad (8.4)$$

The flapping angle is then used to determine the percentage of lost thrust due to flapping, see Equation 8.5 and Figure 5.4, where  $F_{meas}$  is the force perpendicular to the original blade.

$$T_{loss} = \left(1 - \frac{T_{meas}}{T}\right) \cdot 100 = (1 - \cos \alpha_{fl}) \cdot 100 \quad (8.5)$$

The results of the hinged blade model can be seen in Figures 8.5 and 8.6, where one can see the flapping angle with respect to the angle of attack and the advance ratio and the percentage of thrust lost due to blade flapping. What can be seen is that the flapping angle goes up to  $\pm 40$  degrees and the percentage of thrust loss reaches a maximum of 25 %. Though the maximum values only occur for the maximum values of  $J$ , which only occur at high velocities with low rotor rotation rates. Normal flights occur between  $\pm 0.8J$  (Appendix C), which show more plausible values, flapping angles between  $\pm 20$  and thrust losses up to 8%. To make up for such a significant loss of thrust, the rotor speeds need to be increased significantly, thus causing a higher probability of rotor saturation. As the results are from a model and very sensitive to the estimation of the moment of inertia of the blade around the hinge, it is recommended that an experiment be performed to validate the results of the model.

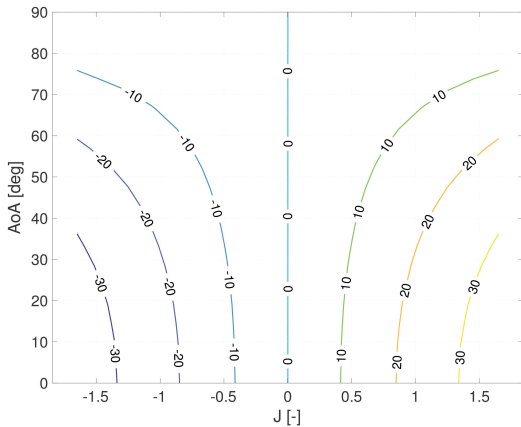


Figure 8.5: Flapping Angle (in deg)

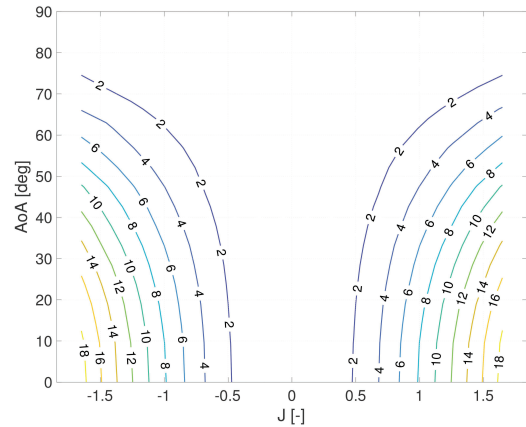


Figure 8.6: Thrust Loss due to Blade Flapping (in percent)

### 8.3. Rotor Saturation

The limitations of the actuators of the Bebop 2 are 3000 and  $\pm 11000$  Rotations Per Minute (rpm). Where the minimum limit is caused by the inbuilt hardware, and the maximum limit was found through experiments. Through analysis of the advance ratio it was found that rotor saturation is not immediately visible, like the VRS, or expected to be omnipresent, like the loss in thrust due to blade flapping. In Figure 8.7 one can see the distribution of the advance ratio with the minimum and maximum limits saturation limits and the advance ratio indicated in steps of  $0.1J$ , where the red lines indicate steps of  $0.5J$ .

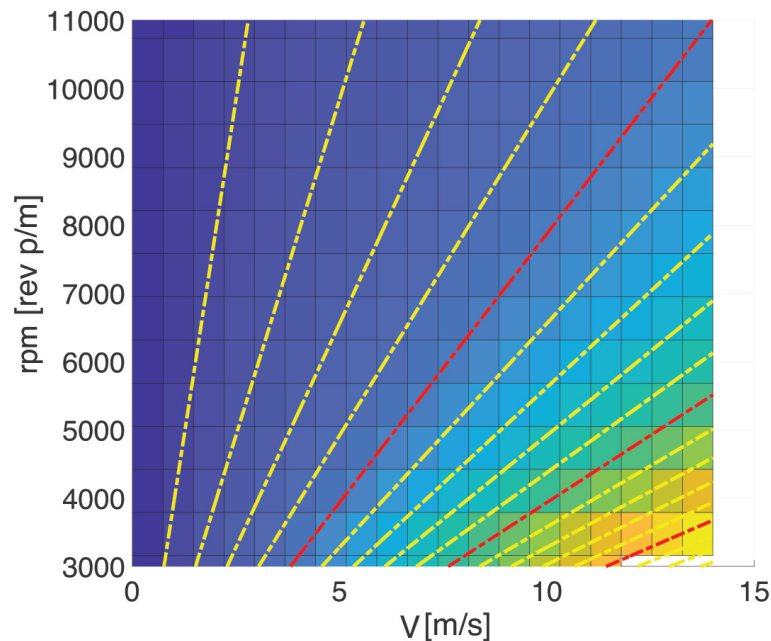


Figure 8.7: Advance Ratio Distribution

From the figure a general feeling as to what advance ratios can be expected at which velocities and vice versa. Take for example a flight at 14 m/s, through the maximum actuator saturation one can see that the advance ratio range is from  $0.5J$  till  $1.8J$ . However the advance ratio was determined through an equation, thus trying to reach a theoretical advance ratio of  $1.8J$  at 14 m/s would be implausible as the rotors would not produce enough thrust to prevent a crash.

To show the the limiting factor of the quadrotor that is rotor saturation, flights in both the nominal and Single-Rotor Failure (SRF) configuration are projected over the flight regime that was tested in the rotor thrust experiment. They will be discussed in respective order in Sub-sections 8.3.1 and 8.3.2.

#### 8.3.1. Nominal Quadrotor Rotor Saturation

In Appendix C data of the flights that were flown in both the nominal and SRF configuration are projected on the flight regime, that was used for the thrust model, to give an indication of the range the quadrotor can reach in different configurations and under various circumstances. Note that these projections are the data sets of the first rotor, where in the nominal case the other rotors show similar behaviours. Also note that the advance ratio per rotor was determined through the same method as in the Model Validation (Sub-Section 7.2.4).

From the nominal flights it can be seen that the advance ratio varied between  $\pm 0.8J$ , where, in combination with Figure 8.7, it can be seen that the limit of  $0.8J$  at 14 m/s is a lower limit of 7000 rpm. From the advance ratio ranges observed for the other velocities in Figure C.1, it can be seen that the maximum advance ratio flown in each flight speed is limited by the minimum rpm and that consequently the minimum advance ratio is limited by the maximum rpm. Thus the maximum attainable advance ratio for nominal quadrotors is dependent on the minimum rpm that can stabilize the quadrotor at a given velocity. This minimum value increases with the velocity, which in turn also increases the angle of attack and also the flapping angle. This eventually leads to the minimum rpm exceeding the maximum rpm, thus one can conclude that the nominal configuration is indeed limited by rotor saturation.

### 8.3.2. SRF Quadrotor Rotor Saturation

The quadrotor flights in SRF configuration can be found in Appendix C.2. As with the nominal configuration flights only the first rotor datasets were projected on the flight regime used for the thrust model. However, contrary to the rotors of the nominal configuration, the rotors of the SRF configuration did not show similar behaviour, see Figure 8.8. As the SRF uses the primary-axis theorem [17], this was to be expected. Note that the flights in the SRF configuration do not include a legend, as the pattern of the SRF configuration flights is more dependent on the wobbling angle than the wind speed.

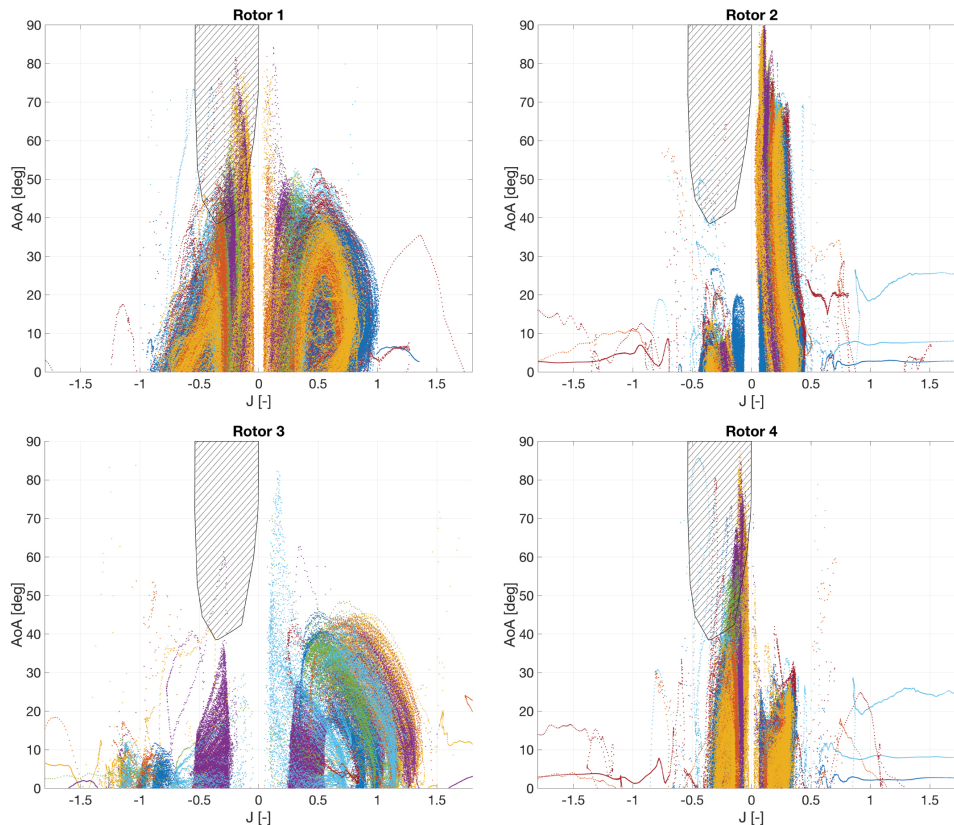


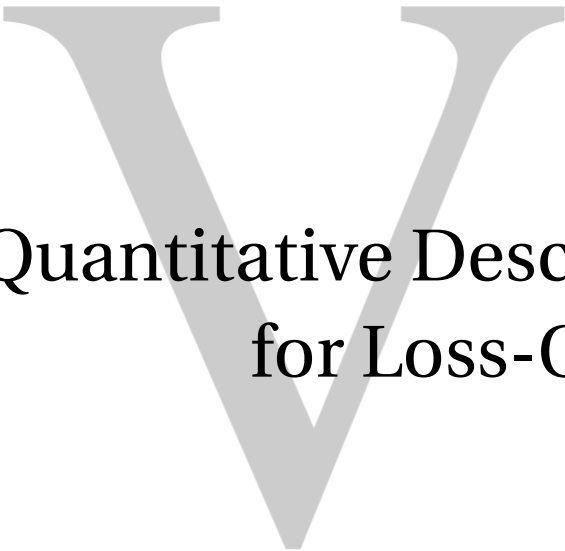
Figure 8.8: Vertical Flights of Quadrotors in SRF Configuration (All Rotors, Right Back (3) Removed)

In comparison to the nominal configuration the SRF configuration reaches higher angles of attack and higher advance ratio values in the rotor opposite to the failed rotor. The increased angles of attack are caused by the wobbling angle that increases with the tilt of the primary-axis. Increasing the tilt of the primary-axis in the direction of the rotor opposite to the failed rotor also lowers the total energy needed to keep wobbling and consequently the rpm of the remaining rotors (two and four) are lowered. Note that there is an optimum in trading rpm speeds between the rotors.

It can be observed that the higher advance ratio values seen in the SRF configuration all occur in the rotor opposite to the failed rotor. Furthermore the remaining rotors have similar, but mirrored patterns. This pattern was also seen in the discussion on the Double Blade Flapping (DBF) phenomenon (Sub-Section 5.4.1). Due to the increased effective velocity on the advancing side and the lowered effective velocity on the retreating side the rotor opposite to the failed rotor sees a greater fluctuation in rotor rpm, where the minimum rpm is the cause of the increased advance ratio. Thus as with the nominal configuration, the maximum advance ratio of the SRF configuration is determined by the minimum rpm needed to stabilize at a given velocity and therefore it is also limited by rotor saturation.

Finally the vertical flights in the SRF configuration also touched upon the VRS domain. As 80% of the SRF configuration test flights showed crashes during descending vertical flight, this could likely be due to the thrust variation in the VRS. Where the prime suspect for rotor saturation is the first rotor as it sees higher rotation speeds than the other rotors (two & four). Note that this assumption changes when the quadrotor rotates in the opposite direction and/or a different rotor fails.





A Quantitative Description  
for Loss-Of-Control



# Defining Loss-Of-Control of Quadrotor Quantitatively

In the Section 9.1, the generated theory that was validated will be worked into the final quantitative Loss-Of-Control (LOC) definition, then an augmentation for increased reliability is suggested in Section 9.2.

## 9.1. The Quantitative Loss-Of-Control Definition for Quadrotors

The Quantitative Loss-Of-Control Definition (QLD) for quadrotors is similar to the definition given to LOC of Commercial Air Transport (CAT), but where the CAT have multiple upset conditions, the quadrotor only has one: actuator saturation. Furthermore a difference is seen in the dynamic and equipment failure precursors to the primary causes. The final definition of the QLD can be found in Figure 9.1, where the precursors are further specified in Table 9.1. Note that though hazards, which are currently unlikely to occur, such as the hazards under the "Atmospheric Disturbances", were also added as they are likely to occur when quadrotors will eventually be used for longer flights over greater distances.

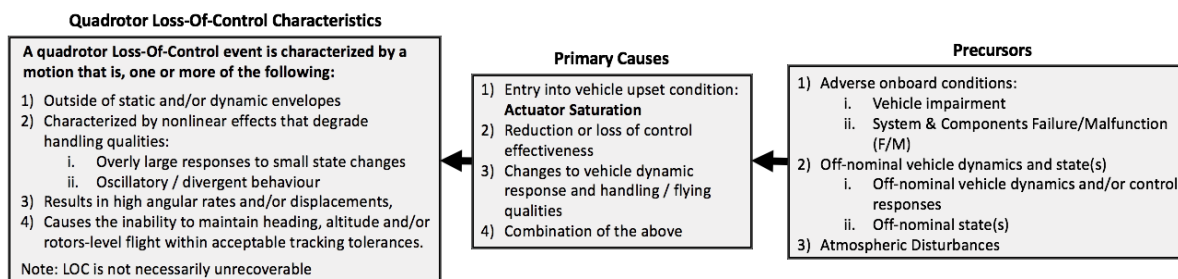


Figure 9.1: Quantitative LOC Definition (QLD) for quadrotors, Primary Causes and Precursors, Adapted from CAT LOC [31]

As the two major sub-systems of the Active Fault Tolerant Control System (AFTCS), the Fault Tolerant Control (FTC) and Fault Detection and Diagnosis (FDD), are often researched separately in literature and have not been successfully unified, actuator failure has not been added to the primary causes. Once the AFTCS has been completed and actuator failures have become survivable, it should be added. In case the QLD is adapted to multicopters it could be immediately added, as multicopters that have more rotors than the quadrotor have inbuilt redundancy and are therefore resistant to actuator failure.

With the QLD for quadrotors defined, investigators of LOC events of quadrotors have a valuable tool to be able to label and group events and thus are able to systematically seek viable safety intervention strategies to reduce the occurrence of LOC.

Precursors	Sub-Categories	Hazards
Adverse Onboard Conditions	Vehicle Impairment	Improper Maintenance Improper Loading: Weight/Balance CG Airframe, Actuator and/or Rotor Damage
	System & Components Failure/Malfunction (F/M)	Control Component Failure/Inadequacy System Software Failure/Inadequacy <sup>1</sup>
Off-Nominal Vehicle Dynamics & State(s)	Off-Nominal Vehicle Dynamics and/or Control Responses	Aerodynamic Interaction of Rotors Vortex Ring State (VRS) (Double) Blade Flapping (DBF) <sup>2</sup> Oscillatory Response Asymmetric Vehicle
	Off-Nominal State(s)	Off-Nominal Attitude and/or Angular Rates Off-Nominal Wind Speed Abrupt Disproportionate Response Flight Trajectory Not Within Tolerances
Atmospheric Disturbances	Atmospheric Disturbances	Wake Vortex Wind/Turbulence Thunderstorms/Rain <sup>1</sup>

<sup>1</sup> To be investigated, but is expected to be a precursor

<sup>2</sup> DBF will only occur in rotor failure flights that use the primary axis control scheme

Table 9.1: Quadrotor LOC Precursors and Accompanying Hazards, Adapted From Aircraft LOC Precursors [31]

## 9.2. Variable-Pitch Rotors for Increased Reliability

There are not many quadrotors which have variable-pitch rotors [7]. Most quadrotors have fixed pitch blades for weight considerations and simplicity, as variable-pitch rotors include complex linkages and a swash plate that are usually used in pod-and-boom style helicopters. This simplicity also increases the robustness against damage.

Although fixed pitch rotors have advantages over variable-pitch rotors, they also have disadvantages, such as the limitation of only being able to produce thrust in one direction and the control bandwidth, which is limited by the inertia of the motors and the propellers. While the above disadvantages do not have a big impact on for example delivery drones, the more important feature that fixed pitch rotors miss, does. The ability that is lost by using fixed pitch blades is the ability to autorotate, see Appendix A.

Currently quadrotors are limited to height limitations due to other air traffic and privacy issues, therefore having the ability to autorotate is not necessarily needed. However when quadrotors become reliable enough for autonomous package delivery, they will most definitely fly at higher heights thus having the ability to autorotate would be advantageous. The reliability of quadrotor would increase with the ability to land with broken actuators.

# 10

## Conclusions & Recommendations

The final chapter of this thesis includes the conclusions and recommendations, which are presented in that respective order.

### 10.1. Conclusions

Currently the main method to increase reliability of quadrotors is to complete the Active Fault Tolerant Control System (AFTCS). Though what is seen in current research is that the sub-systems of the AFTCS, the Fault Tolerant Control (FTC) and the Fault Detection and Diagnosis (FDD), are mostly designed for singular problems. As it is very challenging to be able to combine these systems in a real time fashion, it is not strange that they are often researched separately. Though recent research has been moving towards a more unified system, such as the control system that is able to deal with two challenging tasks [16], and the Fault Detection and Accommodation (FDA) system with experimental results [28], there is still considerably more research and experimentation needed for a fully functioning AFTCS.

To push for a more holistic view on preventing Loss-Of-Control (LOC) of quadrotors and to give more insight on such situations, the Quantitative Loss-Of-Control Definition (QLD) for quadrotors has been defined through a comparative data analysis, which was based on the grounded theory. Data from test flights under various conditions were analysed and compared to generate categories of failures, which were thought to be related to LOC. These were then delimited and combined with observations, from the experiments performed, into a theory on the primary causes and precursors of LOC of quadrotors.

To validate the developed theory an experiment was performed for the analysis of a single rotor of a quadrotor. The rotor was placed on a test stand and tested for the flight regime covering the expected flight range. The thrust data over the flight regime was fit with multivariate splines, which was then validated by examining the variance of the B-coefficients used and through a residual quality analysis. The final thrust model was then compared to flight data of a nominal quadrotor for validation. The conclusion of the validation was that the dynamics of the model were similar to the real data, but the thrust scale was not the same. As the thrust model was created to validate the various dynamics in suspected LOC cases, the thrust model was considered to be validated. The thrust deficiency that was observed was theorized to come from the influence the body had on the lift of the quadrotor, the influence of the thrust stand on the experiment, the quality of the rotor and a possible bias in the accelerometer of the quadrotor.

To validate the theory developed through the comparative data analysis, the precursor events and the primary causes of LOC were tested against the thrust model. The Vortex Ring State (VRS) area in the flight regime was found through analysis of the thrust variance over the flight regime. The area where thrust loss was observed in the thrust model matched with the area which showed up to  $\pm 20\%$  thrust fluctuation, thus the VRS area on the thrust model was considered validated. A single nominal configuration flight, which was designed to enter the VRS, was projected on the thrust model. The data indicated that the quadrotor entered the highest thrust fluctuation area of the VRS, though only showed a 1.5 % thrust offset. This unexpected outcome was theorized to be caused by the time spent in the VRS, influence of the control system and the lack of side winds, which in the amateur scene are most frequently discussed. To investigate these theorized factors, more experiments, if possible from higher heights, should be performed in the heart of the VRS.

As there were no sensors to measure the moment around the actuator hub or the longitudinal thrust, it was not possible to directly validate the influence of blade flapping on the thrust of the actuator. Therefore a hinged blade model was used to show the theoretical influence of blade flapping on the thrust model. Flapping angles up to  $\pm 20$  degrees were seen for general flight ranges ( $\pm 0.8J$ ), which translated to a maximum thrust offset of 8 %. The significant values seen were however not validated. The theoretical flapping angle was, as expected, very dependent on the moment of inertia of the rotor blade about the hinge.

The aerodynamic interactions of the rotors of the quadrotors were also not validateable, as the thrust model was made without the influence of other rotors. Recently in literature however various researchers have researched this topic and have come to the conclusion that there is indeed a significant difference in the rotor speeds between the front and back rotors. This was also seen in longitudinal flights flown in the Open Jet Facility (OJF).

Rotor saturation was validated through analysis of the advance ratio of the nominal and Single-Rotor Failure (SRF) configuration flights. The maximum attainable advance ratio, for both configurations, was limited by the minimum rpm needed to stabilize at a given velocity and vice versa. In the SRF configuration, a higher advance ratio was observed on the advancing side of the rotation plane, due to the DBF phenomena. Furthermore higher angles of attack were observed, which were caused by the primary axis control scheme. By tilting the primary axis towards the rotor opposite to the failed rotor, the rotor speeds needed in the remaining rotors could be lowered. Finally the 1<sup>st</sup> actuator was concluded to be the first to saturate, with the 3<sup>rd</sup> rotor failed, as it showed a higher average rotor speed.

Thus through the thrust model the theory on primary causes and precursors of LOC for quadrotors was partly validated. Through the validation the QLD for quadrotors was defined. Where actuator saturation was defined as the primary cause for LOC events of quadrotors. Rotor failure was not added to the primary causes of LOC as it is not possible to recover from such a failure, though this is expected to be possible in the future. VRS, blade flapping, aerodynamic interactions of rotors and equipment failures are seen as the precursors to LOC of quadrotors. Under rotor failure conditions Double Blade Flapping (DBF) is added to the precursors. Furthermore the QLD of quadrotors is theorized to be able to be adapted to bigger multicopters by adding rotor failure to the primary causes to LOC.

## 10.2. Recommendations

To give a clear overview of the recommendations that were found through the duration of this thesis a separate section was created for the summation of the recommendations. Thus the author recommends:

- that the time needed for a SRF recovery be quantified;
- that the thrust model be improved through quantification/validation of the thrust deficiency, through an experiment that measures all forces and moments in the same flight regime with minimum influence of the experimental set-up;
- that the factors of the VRS be investigated through further experimentation;
- that the influence of blade flapping be investigated through an experiment;
- that the lift capabilities of the quadrotor body be investigated;
- that research be done into the influence that the working rotors, of the SRF configuration, have on each other;
- that research be done into the influence of software errors on LOC events of quadrotors;
- that variable pitch rotors be compared to fixed pitch rotors to find their advantages/disadvantages.

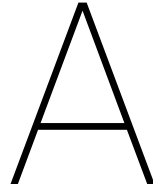
# Bibliography

- [1] Belcastro, C., Foster, J., Shah, G., Gregory, I., Cox, D., Crider, D., Groff, L., Newman, R., and Klyde, D., "Aircraft Loss of Control Problem Analysis and Research Toward a Holistic Solution," *Journal of Guidance, Control, and Dynamics*, Vol. 40, 2017.
- [2] Boeing, "Statistical Summary of Commercial Jet Airplane Accidents Worldwide Operations 1959-2016," Technical report, Aviation Safety Boeing Commercial Airplanes, Seattle, Washington, USA, 2017.
- [3] Belcastro, C., Newman, R., Evans, J., Klyde, D., Barr, L., and Ancel, E., "Hazards Identification and Analysis for Unmanned Aircraft System Operations," *17th AIAA Aviation Technology, Integration, and Operations Conference*, Denver, Colorado, USA, 2017.
- [4] Federal Aviation Administration, "FAA Small Drone Rule Lets Unmanned Aircraft Soar," [https://www.faa.gov/news/updates/?newsId=88748&omniRss=news\\_updatesAoc&cid=101\\_N\\_U](https://www.faa.gov/news/updates/?newsId=88748&omniRss=news_updatesAoc&cid=101_N_U), 2017, [Online; accessed 07-march-2018].
- [5] Jiang, T., Geller, J., Ni, D., and Collura, J., "Unmanned Aircraft System Traffic Management: Concept of Operation and System Architecture," *International Journal of Transportation Science and Technology*, Vol. 5, 2016.
- [6] Sun, S., Schilder, R., and de Visser, C., "Identification of Quadrotor Aerodynamic Model from High Speed Flight Data," *AIAA Atmospheric Flight Mechanics Conference*, Kissimmee, Florida, USA, 2018.
- [7] Cutler, M. and How, J., "Analysis and control of a Variable-Pitch Quadrotor for Agile Flight," *ASME Journal of Dynamic Systems, Measurement and Control*, Vol. 137, No. 10, 2015.
- [8] Mueller, M. and D'Andrea, R., "Relaxed Hover Solutions for Multicopters: Application to Algorithmic Redundancy and Novel Vehicles," *The International Journal of Robotics Research*, 2015.
- [9] Zhang, Y. and Jiang, J., "Bibliographical Review on Reconfigurable Fault-Tolerant Control Systems," *Annual Reviews in Control*, Vol. 32, 2008, pp. 229–252.
- [10] Zhang, Y., Chamseddine, A., Rabbath, C., Gordon, B., Su, C., Rakheja, S., Fulford, C., Apkaraian, J., and Gosselin, P., "Development of Advanced FDD and FTC Techniques with Application to an Unmanned Quadrotor Helicopter Testbed," *Journal of the Franklin Institute*, Vol. 350, 2013, pp. 2396–2422.
- [11] Smeur, E. J., Chu, Q., and de Croon, G., "Adaptive Incremental Nonlinear Dynamic Inversion for Attitude Control of Micro Air Vehicles," *Journal of Guidance, Control, and Dynamics*, Vol. 38, 2015.
- [12] Matamoros, I. and de Visser, C., "Incremental Nonlinear Control Allocation for a Tailless Aircraft with Innovative Control Effectors," *2018 AIAA Guidance, Navigation, and Control Conference*, Kissimmee, Florida, USA, 2018.
- [13] Merheb, A., Noura, H., and Bateman, F., "Design of Passive Fault-Tolerant Controllers of a Quadrotor Based on Sliding Mode Theory," *International Journal of Applied Mathematics and Computer Science*, 2015.
- [14] Slegers, N., Kyle, J., and Costello, M., "Nonlinear Model Predictive Control Technique for Unmanned Air Vehicles," *Journal of Guidance, Control, and Dynamics*, Vol. 29, No. 5, 2006, pp. 1179–1188.
- [15] Raffo, G., Ortega, M., and Rubio, E., "An Integral Predictive/Nonlinear Hinf Control Structure for a Quadrotor Helicopter," *Automatica*, Vol. 46, No. 1, 2010, pp. 29–39.
- [16] de Crousaz, C., Farshidian, F., Neunert, M., and Buchli, J., "Unified Motion Control for Dynamic Quadrotor Maneuvers Demonstrated on Slung Load and Rotor Failure Tasks," *IEEE International Conference on Robotics and Automation (ICRA)*, 2015.

- [17] Mueller, M. and D'Andrea, R., "Stability and Control of a Quadcopter Despite the Complete Loss of One, Two, or Three Propellers," *IEEE International Conference on Robotics and Automation (ICRA)*, Hong Kong, China, 2014.
- [18] Peng, L. and van Kampen, E.-J., "Active Fault-Tolerant Control for Quadrotors Subjected to a Complete Rotor Failure," *IEEE/RSJ International Conference on Intelligent Robots and Systems (IROS)*, 2015.
- [19] Sun, S., Sijbers, L., Wang, X., and de Visser, C., "High-Speed Flight of Quadrotor Despite Loss of Single Rotor," *IEEE Robotics and Automation Letters*, Vol. 3, No. 4, 2018.
- [20] Mellinger, D., Michael, N., and Kumar, V., "Trajectory Generation and Control for Precise Aggressive Maneuvers with Quadrotors," *The International Journal of Robotics Research*, Vol. 31, No. 5, 2012.
- [21] Brescianini, D., Hehn, M., and D'Andrea, R., "Quadcopter Pole Acrobatics," *IEEE/RSJ International Conference on Intelligent Robots and Systems (IROS)*, Tokyo, Japan, 2013.
- [22] Freddi, A., Longhi, S., and Monteriu, A., "A Model-Based Fault Diagnosis System for a Mini-Quadrotor," *Workshop on Advanced Control and Diagnosis*, Zielona Gora, Poland, 2009.
- [23] Freddi, A., Longhi, S., and Monteriu, A., "Actuator Fault Detection System for a Mini-Quadrotor," *IEEE International Symposium on Industrial Electronics*, Bari, Italy, 2010.
- [24] Chandra, K., Alwi, H., and Edwards, C., "Fault Reconstruction for a Quadrotor using an LPV Sliding Mode Observer," *Proc. 9th IFAC Symp. Fault Detection, Supervision Safety Tech. Processes SAFEPROCESS*, Paris, France, 2015.
- [25] Zhang, N., Doncescu, A., and Mora-camino, F., "Discrete Flatness for Non Linear Systems FDI," *International Conference on Broadband, Wireless Computing, Communication and Applications*, Fukuoka, Japan, 2010.
- [26] Amoozgar, M., Chamseddine, A., and Zhang, Y., "Experimental Test of a Two-Stage Kalman Filter for Actuator Fault Detection and Diagnosis of an Unmanned Quadrotor Helicopter," *Journal of Intelligent & Robotic Systems*, Vol. 70, No. 1, 2013.
- [27] Avram, R., Zhang, X., and Muse, J., "Quadrotor Sensor Fault Diagnosis with Experimental Results," *Journal of Intelligent and Robotic Systems*, Vol. 86, No. 1, 2017, pp. 115–137.
- [28] R.C. Avram, Zhang, X., and Muse, J., "Quadrotor Actuator Fault Diagnosis and Accommodation Using Nonlinear Adaptive Estimators," *IEEE Transactions on Control Systems Technology*, Vol. 25, No. 6, 2017.
- [29] Pardee, J. and Russell, P., "Final Report - Loss of Control JSAT: Results and Analysis," Technical report, Federal Aviation Administration (FAA), Washington D.C., USA, 2000.
- [30] Wilborn, J. and Foster, J., "Defining Commercial Aircraft Loss-of-Control: A Quantitative Approach," *AIAA Atmospheric Flight Mechanics Conference and Exhibit*, 2004.
- [31] Belcastro, C., Newman, R., Crider, D., Klyde, D., Foster, J., and Groff, L., "Aircraft Loss of Control: Problem Analysis for the Development and Validation of Technology Solutions," *AIAA Guidance, Navigation, and Control Conference*, San Diego, California, USA, 2016.
- [32] Belcastro, C. and Jacobson, S., "Future Integrated Systems Concept for Preventing Aircraft Loss-of-Control Accidents," *AIAA Guidance, Navigation, and Control Conference*, Toronto, Ontario, Canada, 2010.
- [33] Belcastro, C., "Loss of Control Prevention and Recovery Onboard Guidance, Control, and Systems Technologies," *AIAA Guidance, Navigation, and Control Conference*, Minneapolis, Minnesota, USA, 2012.
- [34] Belcastro, C., Groff, L., Newman, R., Foster, J., Crider, D., Klyde, D., and Huston, A., "Preliminary Analysis of Aircraft Loss of Control Accidents: Worst Case Precursor Combinations and Temporal Sequencing," *AIAA Guidance, Navigation, and Control Conference*, National Harbor, Maryland, USA, 2014.

- [35] Tekles, N., Chongvisal, J., Xargay, E., Choe, R., Talleur, D., Hovakimyan, N., and Belcastro, C., "Design of a Flight Envelope Protection System for NASA's Transport Class Model," *Journal of Guidance, Control, and Dynamics*, Vol. 40, 2017.
- [36] Pfifer, H., Venkataraman, R., and Seiler, P., "Quantifying Loss-of-Control Envelopes via Robust Tracking," *Journal of Guidance, Control, and Dynamics*, Vol. 40, 2017.
- [37] Schuet, S., Lombaerts, T., Aeosta, D., Kaneshige, J., Wheeler, K., and Shish, K., "Autonomous Flight Envelope Estimation for Loss-of-Control Prevention," *Journal of Guidance, Control, and Dynamics*, Vol. 40, No. 4, 2017.
- [38] Barr, L., Newman, R., Ancel, E., Belcastro, C., Foster, J., Evans, J., and Klyde, D., "Preliminary Risk Assessment for Small Unmanned Aircraft Systems," *AIAA Aviation Technology, Integration, and Operations conference*, Denver, Colorado, USA, 2017.
- [39] Foster, J. and Hartman, D., "High-Fidelity Multirotor Unmanned Aircraft System Simulation Development for Trajectory Prediction Under Off-Nominal Flight Dynamics," *17th AIAA Aviation Technology, Integration, and Operations Conference*, Denver, Colorado, USA, 2017.
- [40] Olson, I. and Atkins, E., "Qualitative Failure Analysis for a Small Quadrotor Unmanned Aircraft System," *AIAA Guidance, Navigation, and Control (GNC) Conference*, Boston, MA, USA, 2013.
- [41] Wild, G., Murray, J., and Baxter, G., "Exploring Civil Drone Accidents and Incidents to Help Prevent Potential Air Disasters," *Aerospace*, Vol. 3, No. 3, 2016.
- [42] Tvaryanas, A., Thompson, W., and Constable, S., "Human Factors in Remotely Piloted Aircraft Operations: HFACS Analysis of 221 mishaps over 10 Years," *Aviat. Space Environ. Med.*, Vol. 77, No. 7, 2006, pp. 724–732.
- [43] Federal Aviation Administration, *Helicopter Flying Handbook*, chap. Helicopter Emergencies and Hazards, Oklahoma City, USA, 2012, pp. 11–1 – 11–24.
- [44] Textron, B. H., *Bell, Model 204B: Flight Manual*, Bell Helicopter Company.
- [45] European Aviation Safety Agency (EASA), *Certification Specifications for Normal, Utility, Aerobatic, and Commuter Category Aeroplanes CS-23, Amendment 3*, 2012.
- [46] Oort, E. V., *Adaptive Backstepping Control and Safety Analysis for Modern Fighter Aircraft*, Dissertation, Delft University of Technology, 2011.
- [47] Stapel, J., de Visser, C., Kampen, E.-J. V., and Chu, Q., "Efficient Methods for Flight Envelope Estimation through Reachability Analysis," *AIAA Guidance, Navigation, and Control Conference*, 2016.
- [48] van Oort, E., Chu, Q., and Mulder, J., "Maneuver Envelope Determination through Reachability Analysis," *Advances in Aerospace Guidance, Navigation and Control*, edited by F. Holzapfel and S. Theil, Springer, 2011.
- [49] Zhang, Y., de Visser, C., and Chu, Q., "Database Building and Interpolation for a Safe Flight Envelope Prediction System," *2018 AIAA Information Systems-AIAA Infotech @ Aerospace*, Kissimmee, Florida, USA, 2018.
- [50] McDonough, K. and Kolmanovsky, I., "Computable Recoverable Sets and Their Use for Aircraft Loss-of-Control Handling," *Journal of Guidance, Control, and Dynamics*, Vol. 40, No. 4, 2017.
- [51] Mitchell, I., Yeh, J., Laine, F., and Tomlin, C., "Ensuring Safety for Sampled Data Systems: An Efficient Algorithm for Filtering Potentially Unsafe Input Signals," *IEEE 55th Conference on Decision and Control (CDC)*, Las Vegas, USA, 2016.
- [52] Zhang, Y., de Visser, C., and Chu, Q., "Online Safe Flight Envelope Prediction for Damaged Aircraft: A Database-driven Approach," *AIAA Modelling and Simulation Technologies Conference*, San Diego, California, USA, 2016.

- [53] Zhang, Y., de Visser, C., and Chu, Q., "Online Aircraft Damage Case Identification and Classification for Database Information Retrieval," *2018 AIAA Atmospheric Flight Mechanics Conference*, Kissimmee, Florida, USA, 2018.
- [54] Zhang, Y., de Visser, C., and Chu, Q., "Aircraft Damage Identification and Classification for Database-Driven Online Flight-Envelope Prediction," *Journal of Guidance, Control and Dynamics*, Vol. 41, No. 2, 2018.
- [55] Bansal, S., Chen, M., Herbert, S., and Tomlin, C., "Hamilton-Jacobi Reachability A Brief Overview and Recent Advances," *CDC '17: Proceedings of 56th IEEE Conference on Decision and Control*, 2017.
- [56] Chen, M., Herbert, S., and Tomlin, C., "Exact and Efficient Hamilton-Jacobi Guaranteed Safety Analysis via System Decomposition," *IEEE International Conference on Robotics and Automation (ICRA)*, Singapore, 2017.
- [57] Nabi, H., Lombaerts, T., Zhang, Y., van Kampen, E., Chu, Q., and de Visser, C., "Effects of Structural Failure on the Safe Flight Envelope of Aircraft," *Journal of Guidance, Control, and Dynamics*, Vol. 41, No. 6, 2018.
- [58] Chen, M., Hu, Q., Fisac, J., Akametalu, K., Mackin, C., and Tomlin, C., "Reachability-based Safety and Goal Satisfaction of Unmanned Aerial Platoons on Air Highways," *Journal of Guidance, Control, and Dynamics*, Vol. 40, No. 6, 2017.
- [59] Prouty, R., *Helicopter Performance, Stability, and Control*, Prindle, Weber and Schmidt (PWS Publishers), 1986.
- [60] Huang, H., Hoffmann, G., Waslander, S., and Tomlin, C., "Quadrotor Helicopter Flight Dynamics and Control: Theory and Experiment," *AIAA Guidance, Navigation and Control Conference and Exhibit*, South Carolina, USA, 2007.
- [61] Pounds, P., Mahony, R., and Corke, P., "Modelling and Control of a Quad-Rotor Robot," *Proceedings of the Australasian Conference on Robotics and Automation*, 2006.
- [62] Barcelos, D., Kolaei, A., and Bramesfeld, G., "Performance Predictions of Multirotor Vehicles Using A Higher-Order Potential Flow Method," *2018 AIAA Aerospace Sciences Meeting*, Kissimmee, Florida, 2018.
- [63] Glaser, B. and Strauss, A., *The Discovery of Grounded Theory: Strategies for Qualitative Research*, Aldine, 1967.
- [64] Shetty, O. R. and Selig, M. S., "Small-Scale Propellers Operating in the Vortex Ring State," *49th AIAA Aerospace Sciences Meeting AIAA*, 2011.
- [65] RcBenchmark.com, *Manual Series 1580*, 2012.
- [66] Leishman, J., *Principles of Helicopter Aerodynamics*, Cambridge University Press, 2006.
- [67] Huang, H., Hoffmann, G., Waslander, S., and Tomlin, C., "Aerodynamics and Control of Autonomous Quadrotor Helicopters in Aggressive Maneuvering," *2009 IEEE International Conference on Robotics and Automation*, Kobe, Japan, 2009.



# Loss-Of-Control of Aircraft

The comparable Loss-Of-Control (LOC) theories appendix is used for more in-depth explanations about LOC of aircraft, specifically airplanes and helicopters. This appendix is structured as follows: the LOC events of airplanes are discussed in Section A.1, followed by the LOC event of helicopters in Section A.2.

## A.1. Airplanes

The primary causes of LOC events of airplanes [30] are the following:

- **Stall**  
Stall is the reduction of lift that is generated by an airfoil as the angle of attack increases. Once the critical angle of attack is reached stall starts to occur. Typically the critical angle of attack is  $\pm 15$  degrees, though it is affected by the type of airfoil in question and the Reynolds number. A stall is usually experienced as a sudden drop in lift as, the pilot tries to increase the angle of attack past the critical point. Stall is recoverable and therefore a perfect example of LOC of airplanes.
- **(Sideslip-Induced) Rolls**  
Rolls are rotations about the x-axis. Sideslip-induced rolls are rolls caused by sideslip which was induced by the airplane through yawing with respect to the airflow. As most commercial airplanes have a bit of sweep, this sideslip with respect to the airflow will cause the wing that moves further into the flow to create more lift and conversely the wing that moves down the flow will create less lift, thus causing a rolling moment.
- **Pilot Induced Oscillation (PIO)**  
Pilot Induced Oscillation is caused by the attempts of the pilot to control the airplane. When the pilot tries to commands the aircraft in the opposite direction of movement, the aircraft does not react as expected and the pilot tries to correct the first mistake. This repeats with increasing overcorrections in the wrong direction causing oscillations. This is usually caused by the lag of the pilot's response.
- **Yaw**  
Rotation about the z-axis of an aircraft, which changes the direction the nose of the aircraft is pointing in (left and right). Increasing the yaw angle with respect to the incoming flow increases the sideslip angle and thus could cause sideslip-induced rolls.

## A.2. Helicopters

As mentioned in Chapter 4, LOC is not officially quantified for helicopters, though emergencies and hazards affecting helicopters have been thoroughly researched [43], these emergencies and hazards are similar to the definition for LOC and can be seen below:

### – Autorotation

A power-off manoeuvre in which the engine of the helicopter is disengaged from the rotor system. Thus the rotor system is only driven by the upwards flow that is created by falling. It is possible to land a helicopter with just autorotation, gliding forwards and using a flare to reduce forward airspeed and a decrease of descent rate before landing.

### – Height/Velocity Diagram

Also known as the dead man's curve, the H/V curve is a graph that shows the safe/unsafe flight profiles for a specific helicopter. In the unsafe area of the curve there may not be sufficient time to stabilize from a failure. Usually used to indicate where it should theoretically be possible to do an autorotation. This curve is comparable to the flight envelope of an airplane.

### – Vortex Ring State (VRS)

The VRS for helicopters has been thoroughly investigated and discussed [66] [59]. It is the part of the flight regime where air is recirculated randomly, thus causing the induced velocity to vary greatly and making it such that momentum theory can not be applied. An empirical model for the induced velocity, in VRS, was given in [66], this model however fails to capture the periodic nature of the vortex entrapment [60]. In Figure A.1 one can see the different flight states in vertical flight, where the turbulent wake state is seen as a transition between the VRS and the windmill brake state, which occurs at even higher descent speeds but is predictable with momentum theory.

VRS for quadrotors has not been investigated as thoroughly as for helicopters, though the trend of the loss of thrust in VRS experienced in [64] was similar to results obtained in studies for normal rotors. In [67] theory for the vertical flight states was tested against thrust stand data which also showed a trend of losing thrust in VRS. These results show that VRS does have a significant effect on the flight capabilities of a quadrotor, so much so that it has been renamed as the 'wobble of death' in the hobby scene, therefore it is surprising that this phenomenon has not been studied and possibly modeled more. In Figure A.1 the flight states of a rotor in descent can be seen, where the instabilities in the VRS wake can be visually seen. Other than a prototype VRS model that was discussed recently in off-nominal modelling [39], where improvements to the VRS model were seen as a future plan, the author has not seen any discussion regarding VRS for quadrotors in literature.

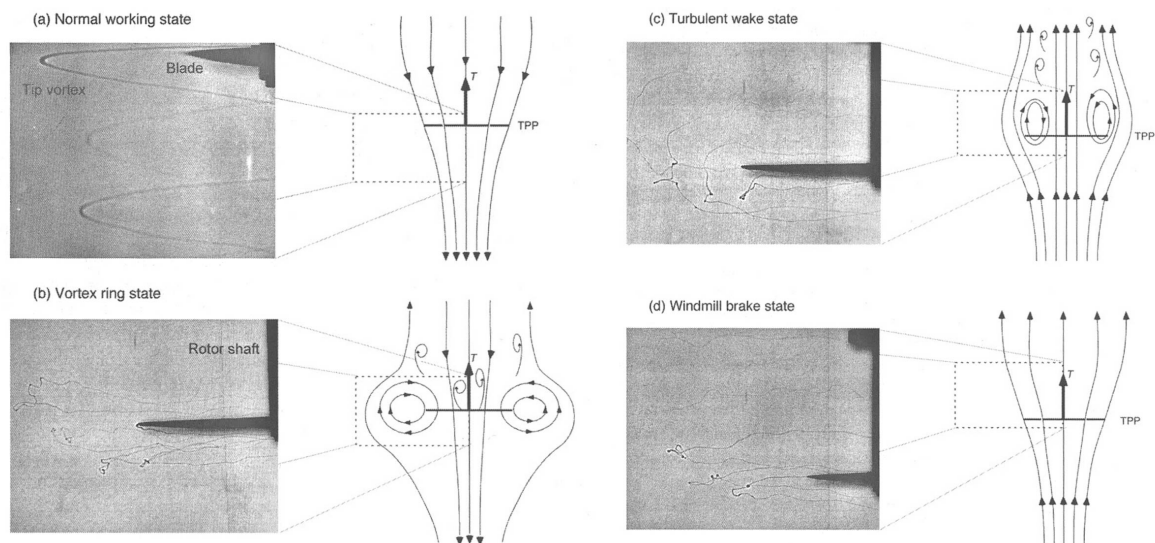


Figure A.1: Rotor Flight States in Vertical Flight [66]

– **Retreating Blade Stall**

Relative airspeed through the main rotor plane is different for the advancing side and retreating side of the disk. The advancing side sees an increased airspeed due to the forward speed of the helicopter, conversely the other side has a lower airspeed, thus the lift is unequally distributed.

To generate equal lift over the rotor disk, helicopters flap the advancing blades up and the retreating blades down, these rotor blades are known as variable-pitch rotors. Thus creating less lift on the advancing blades and increasing lift on the retreating blades. The retreating blade will eventually cause a stall and loss of lift due to its high angle of attack and low blade speed.

– **Ground Resonance**

A destructive vibration that occurs when the an out of balance rotor increases the natural frequency and thus vibrate the entire helicopter as the engine is providing power to the vibrations. The helicopter can then destroy itself within seconds.

– **Dynamic Rollover**

A helicopter can do a dynamic rollover due to a lateral rolling tendency if a certain critical rollover angle is reached. For it to occur the helicopter first needs to pivot around landing gear to a critical rollover angle then the cyclic cannot eliminate the thrust component, thus the helicopter rolls over.

– **Low G Conditions and Mast Bumping**

The helicopter reaches a state where the gravity pulling down on the fuselage and the rotor lift keeping it up do not act in their usual plane. This happens for example when an helicopter prepares for a steep dive, the fuselage is then not supported by the rotor, in this state the rotor system could hit the mast (mast bumping) which usually leads to a fatal ending.

– **Low Rotor rpm and Blade Stall**

Not having enough rotations per minute to keep up with the lift needed for the helicopter. Losing lift would lead to a descent. The relative wind changes and thus the angle of attack increases, at some point the blades stall and could break due to the forces present.



# B

## The Grounded Theory Approach

The grounded theory is described by Glaser and Strauss, in [63], as '*The discovery of theory from data*'. Originally this theory was used in sociology, but the ideas presented are applicable to this research. The name comes from the fact that this theory is based on '*hard study of much data*' and is therefore well grounded in contrast to other theories based on logic with ungrounded assumptions (in sociology).

### B.1. Comparative Analysis

The grounded theory approach generates theory through the process of comparative analysis. As the name suggests, it uses the logic of comparison. The purpose of using the comparative analysis in the grounded theory is due to the following points [63]:

– **Accurate Evidence**

In comparative analysis evidence which was initially found is compared to evidence found in groups that are comparable. So the evidence is replicated using comparison. In general if research is replicable it can be used as a means for validation.

– **Empirical Generalizations**

Comparative analysis is also used to create generality of a fact or in other words making the fact generally applicable. Thus a more generalized theory can be used for better predictions. By comparison one can also find boundaries/limits of a theory.

– **Specifying a Concept**

Using comparative data to find a specific unit of analysis, this is done by clearly demarcating a specific unit and comparing it to similar units. These units might be in the same category, but have different natures. Thus all cases can be found and clearly identified.

– **Verifying Theory**

Comparative data is the best data for verification of theory. If one formulates a hypothesis on a singular case and then tries to verify it through comparative data, the hypothesis can then be modified to fit both sets. Once this cycle is continued a more general theory emerges from the data.

– **Generating Theory**

The main goal of the grounded theory. It is very much like verification, as modifying theory can be seen as theory generation. One should however keep an open and inquisitive mind for generation of new theory.

### The Elements of Theory

Theory that was generated through comparative analysis has elements. Firstly conceptual categories exist within the theory, these are then complemented with conceptual properties and finally a hypotheses or generalized relationship within those categories and properties exist [63].

## B.2. The Constant Comparative Method of Qualitative Analysis

Glaser and Strauss suggest a comparative method for qualitative analysis for the systematic generation of theory, called the constant comparative method, which is built up out of four stages [63], which are firstly run in serial and once completed in parallel with the current step:

### 1. Comparison of Incidents Applicable to Each Category

As many categories of analysis as possible should be derived from each single incident. In such a way one will see new categories appear and incidents added to already existing categories. Glaser and Strauss set up the first rule for the constant comparative method: *'while coding an incident for a category, compare it with the previous incidents in the same and different groups coded in the same category'* [63]. Using this rule each category will form its own dimensions, conditions, relations to other categories and other properties. It might also be possible that after adding incidents to a category, conflicts might appear in the theoretical notion of the researcher about that category. For this situation Glaser and Strauss define the second rule of the constant comparative method: *'stop coding and record a memo on your own ideas'* [63], this rule was designed for the initial freshness of the thoughts and to relieve conflict.

### 2. The Integration of Categories and Accompanying Properties

This stage should emerge by itself. Once one starts to move from comparing incidents to comparing the incident with the properties of the category that came from the original comparison of incidents. The most important properties of the categories become apparent and the relations with other properties within the category become apparent. In doing so the properties become more integrated to form a whole category.

### 3. Delimitation of the Theory

What is meant by delimitation of the theory is that the theory becomes more streamlined as the researcher progresses. The delimitation of the theory can be split into two levels: the theory and the categories. Firstly when the theory becomes more apparent it delimits itself e.g. removal of non-relevant properties and modifications happen less frequently and are mainly used for the clarification of the theory, thus becoming more streamlined. Secondly once one comes to a saturation point of the theory, one can start to cut down on the original list of categories. The relations between categories become apparent and a smaller set of categories is also sufficient to explain the theory.

### 4. Writing of the Theory

Once the researcher reaches a point where he/she thinks the generated theory is an accurate statement of what was studied and is useful to the field of study, the theory can be finalized. The categories become the major themes of the theory and one can point out the weak/strong points of the generated theory. Furthermore the researcher can continue towards publication of the theory.

### Conveying Credibility

In the field of Sociology it is harder to convey credibility of a research than within an exact field, such as engineering. This is due to the fact that the main sources of information are individuals. Although the information can be found relatively fast and information is in general diverse, it might also be subjective. Therefore Glaser and Strauss suggest several methods to convey the credibility within Sociology. As this research is within the field of engineering, Glaser and Strauss's suggestions are not applicable. Therefore to add credibility experiments can be designed to validate generated theory and thus conveying credibility.

# C

## Quadrotor Flights

In this appendix datasets of flown flights are projected over the thrust model to give an indication of the flight regime that the quadrotor operates in, note that the data of the first rotor is used in all cases. The flights have been split in two main sections: the flights in nominal configuration, which can be found in Section C.1 and the flights in SRF configuration, which can be found in Section C.2.

### C.1. Nominal Quadrotor Flights

The flights in nominal configuration were split into two different sets: the flights which covered the movements in vertical and longitudinal directions under all wind conditions, which can be seen in Fig. C.1 and flights in which only longitudinal movements were flown, in Fig. C.2.

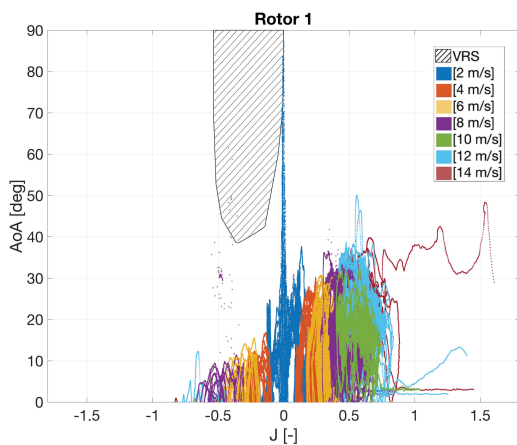


Figure C.1: Vertical/Longitudinal Flights, Nominal Configuration

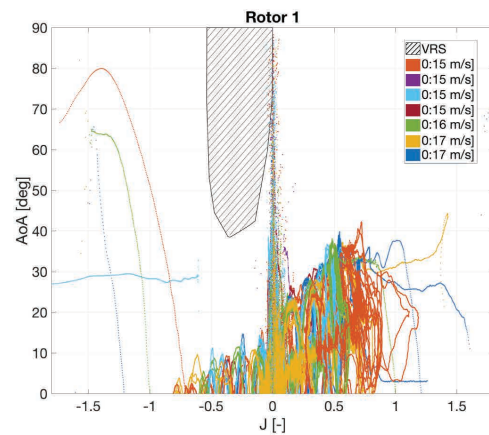


Figure C.2: Longitudinal Flights, Nominal Configuration

## C.2. Single Rotor Failure Quadrotor Flights

The flights in SRF configuration were flown in two different sets: the longitudinal flights, seen in Fig. C.3 and the vertical flights, which can be seen in Fig. C.4.

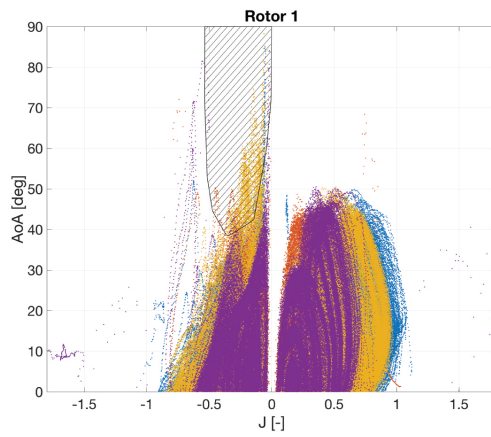


Figure C.3: Longitudinal Movement, SRF Configuration

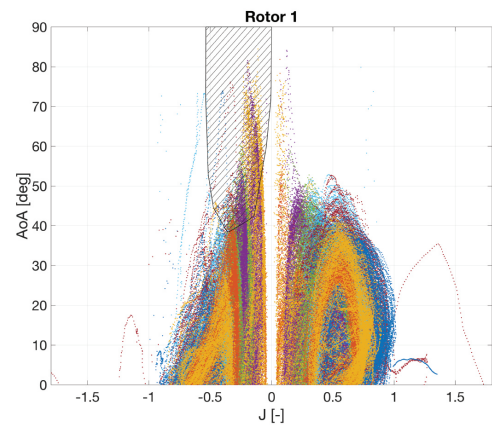


Figure C.4: Vertical Movement, SRF Configuration